

AD-A092 369

TRW DEFENSE AND SPACE SYSTEMS GROUP REDONDO BEACH CA --ETC F/8 3/2  
A STUDY OF THE ASSOCIATION OF PC 3, 4 MICROPULSATIONS WITH INTE--ETC(U)  
NOV 77 E W GREENSTADT F49620-77-C-0018

UNCLASSIFIED

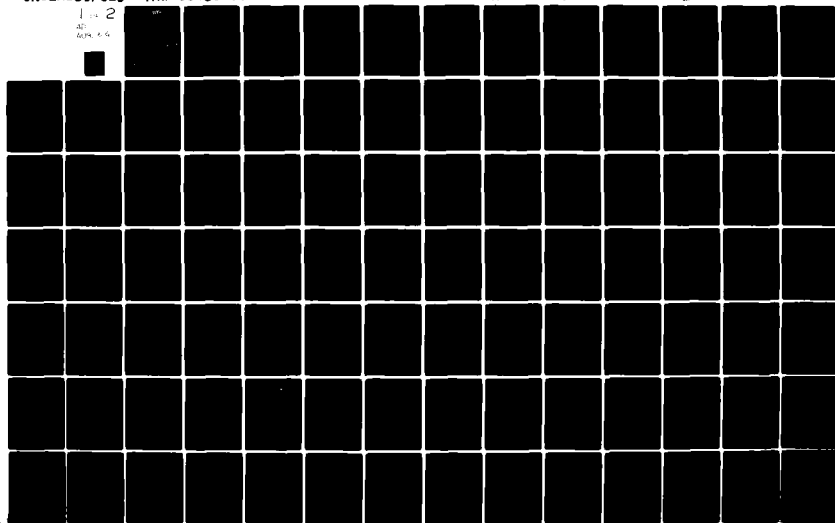
TRW-30435-6007-RU-00

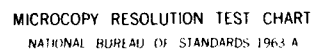
AFOSR-TR-80-1161

NL

1 2

AD-A092 369





MICROCOPY RESOLUTION TEST CHART  
NATIONAL BUREAU OF STANDARDS 1963 A

AD A092369

BDC FILE COPY

UNCLASSIFIED		LEVEL II		12	
SECURITY CLASSIFICATION OF THIS PAGE (When Data Entered)				READ INSTRUCTIONS BEFORE COMPLETING FORM	
17 REPORT DOCUMENTATION PAGE		AC		3. RECIPIENT'S CATALOG NUMBER	
18 AFOSR/TR-80-1161		AD-4092369		5. TYPE OF REPORT & PERIOD COVERED Final 9-30-77 thru 9-30-79	
4. TITLE (and Subtitle) 4 Micropulsations with Interplanetary Magnetic Field Orientation & Other Solar Wind Parameters.		6. PERFORMING ORG. REPORT NUMBER		8. CONTRACT OR GRANT NUMBER(s) F49620-77-C-0018	
7. AUTHOR(s) 10 Eugene W. Greenstadt		14 TRW-30435-6907-RU-90		10. PROGRAM ELEMENT, PROJECT, TASK AREA & WORK UNIT NUMBERS 16 2311/A1 61162 F	
9. PERFORMING ORGANIZATION NAME AND ADDRESS TRW Defense & Space Systems Group One Space Park Redondo Beach, California 90278		11. CONTROLLING OFFICE NAME AND ADDRESS Air Force Office of Scientific Research/INP Building 410 Bolling AFB, Washington, D.C. 20332		12. REPORT DATE 13 November 1977	
14. MONITORING AGENCY NAME & ADDRESS (if different from Controlling Office) 9		13. NUMBER OF PAGES 122		15. SECURITY CLASS. (of this report) Unclassified	
16. DISTRIBUTION STATEMENT (of this Report) Approved for public release; distribution unlimited.		17. DISTRIBUTION STATEMENT (of the abstract entered in Block 20, if different from Report)		15a. DECLASSIFICATION/DOWNGRADING SCHEDULE	
18. SUPPLEMENTARY NOTES					
19. KEY WORDS (Continue on reverse side if necessary and identify by block number) Micropulsations Pc 3 Pc 4 Solar Wind Interaction					
20. ABSTRACT (Continue on reverse side if necessary and identify by block number) This report describes the results of a research program extending from 1 Dec 1977 to 30 Sept 1979. The objectives of the program have been to study the relationships between geomagnetic pulsation activity in the period range 10 to 300 sec (Pc 3, 4, and 5 by traditional classification) and solar wind parameters. The study has centered on two particular parameters, solar wind speed $V_{SW}$ and interplanetary magnetic field (IMF) cone angle $\theta_{XB}$ (the angle between the IMF and the sun-earth line) as representing the critical quantities in two models of pulsation origin.					

DD FORM 1 JAN 73 1473

EDITION OF 1 NOV 65 IS OBSOLETE

UNCLASSIFIED

412 069

**AFOSR-TR- 80 - 1161**

**30435-6007-RU-00**

**FINAL REPORT**

**A STUDY OF THE ASSOCIATION OF PC 3,4  
MICROPULSATIONS WITH INTERPLANETARY  
MAGNETIC FIELD ORIENTATION & OTHER  
SOLAR WIND PARAMETERS**

**for**

**Air Force Office of Scientific Research  
Contract F49620-77-C-0018**

**Principal Investigator: E. W. Greenstadt**

**13 November 1979**

<b>Accession For</b>	
NTIS GRA&I	<input checked="checked" type="checkbox"/>
DDC TAB	<input type="checkbox"/>
Unannounced	<input type="checkbox"/>
Justification	
<b>By</b>	
<b>Distribution/</b>	
<b>Availability Codes</b>	
<b>Dist</b>	<b>Avail and/or special</b>
<b>A</b>	

**Space Sciences Department  
TRW Defense & Space Systems Group  
One Space Park  
Redondo Beach, California 90278**

**Approved for public release;  
distribution unlimited.**

**80 12 01 201**

## TABLE OF CONTENTS

	<u>Page</u>
INTRODUCTION	1
RESULTS	3
<u>Statement of Work</u>	3
<u>Specific Accomplishments</u>	4
SUMMARY AND RECOMMENDATIONS	9
FIGURES	12 - 14
APPENDICES	
Appendix A. Evidence for the Control of PC 3,4 Magnetic Pulsations by the Solar Wind Velocity	
Appendix B. Geomagnetic Pulsation Signals and Hourly Distributions of IMF Orientation	
Appendix C. IMF Orientation, Solar Wind Velocity, and PC 3-4 Signals: A Joint Distribution	
Appendix D. The Solar Wind and Magnetospheric Waves	
Appendix E. Correlation of Pc 3, 4, and 5 Activity with Solar Wind Speed	
Appendix F. Association of Low-Frequency Waves with Suprathermal Ions in the Upstream Solar Wind	
Appendix G. Magnetic Field Orientation and Suprathermal Ion Streams in the Earth's Foreshock	
Appendix H. Current Investigation of the Mid-Period Geomagnetic Pulsations and Potential Use of the AFGL Network	
Appendix I. Letters to Dr. Sagalyn	

AIR FORCE OFFICE OF SCIENTIFIC RESEARCH (AFSC)  
 NOTICE OF TRANSMITTAL TO DDC  
 This document has been reviewed and is  
 approved for public release IAW AFR 190-12 (7b).  
 Distribution is unlimited.  
 A. D. BLUSH  
 Technical Information Officer

## INTRODUCTION

This report describes the results of a research program extending from 1 December 1977 to 30 September 1979. The objectives of the program have been to study the relationships between geomagnetic pulsation activity in the period range 10 to 300 seconds (Pc 3,4, and 5 by traditional classification) and solar wind parameters. The study has centered on two particular parameters, solar wind speed  $V_{SW}$  and interplanetary magnetic field (IMF) cone angle  $\theta_{XB}$  (the angle between the IMF and the sun-earth line) as representing the critical quantities in two models of pulsation origin.

According to the first model the properties of the bow shock, and in particular, turbulence in the downstream magnetosheath, are controlled by the solar wind velocity and field direction. As these waves are swept around the magnetosphere they penetrate or stimulate the boundary and excite internal resonant field line oscillations. These are observed at the ends of the resonant field lines as ground magnetic pulsations.

In the second proposed mechanism, magnetosheath flow along the magnetopause excites the Kelvin-Helmholtz instability producing surface waves. These evanescent waves couple internally to resonant field lines and produce ground pulsations. In this mechanism the instability criterion is a function of solar wind velocity and field orientation.

In this program statistical correlations between solar wind parameters at Explorer 35 and two ground observatories reached fruition. The amplitude of ground pulsation increased as the velocity increased, and was larger when

the field was aligned with the earth-sun line. These results have been confirmed in several ways by researchers at other institutions as well.

The ultimate purpose of the investigation is to attain the capacity to use micropulsation records acquired from surface magnetometers to infer certain key parameters of the solar wind, such as field magnitude, field direction, wind velocity, and of the magnetosphere, such as magnetopause distance and subauroral plasma density. The present investigation has suggested this is a realizable goal.

The following pages discuss the results in a general way in terms of activities carried out under the initial work statement and specific scientific findings. Technical descriptions of results appear as Appendices consisting of copies of published or submitted papers. Additional results, pending, but incomplete or undocumented, are described briefly and the status of the project is summarized and recommendations offered.

## RESULTS

Statement of Work. The following statements summarize the activities of this program in terms of the work statement in the proposal of August 1977.

- a. Study the relationship of solar wind parameters and wave propagation and fluid flow in the magnetosheath to micropulsation excitation.

Theoretical computations of plasma parameters in the magnetosheath were examined as a guide to the locations and local times the magnetopause is most likely to be affected by convection and propagation of large amplitude oscillations from the shock. Also, the literature on Kelvin-Helmholtz excitation of the magnetopause was reviewed to clarify whether that phenomenon constitutes a competing or a complementary source of geomagnetic pulsations, and to determine the extent to which the K-H mechanism has been tested by observation. Factors governing the resonance of waves in the magnetosphere were reviewed to assess the possible effects on ground station data. Finally, upstream wave and energetic particle components of the quasi-parallel (pulsation) shock structure were studied in relationship to the IMF.

- b. Improve the methodology employed in handling surface and satellite data appropriate to the Study.

The use of hourly distributions of interplanetary field data was developed and applied; joint distributions of pulsation amplitude, solar wind velocity, and IMF cone angle were studied; the representation of the cone angle by its cosine was explored and found to improve the organization of the data; an approach to normalizing ground station data to produce a global measure of pulsation activity independent of local time, latitude, and spectral distortions was designed and proposed for future study.



- c. Exploit the schedules and formats of the available surface and satellite data for further correlational analysis.

Correlations between solar wind speed were expanded to include a second data interval, a second ground station, and a range of longer period pulsations (Pc 5) than had previously been investigated.

- d. Assess the prospects for initiating an operational system using ground station micropulsation records to estimate selected solar wind parameters.

Evaluations were made of the methods necessary to turn data into an operational index (see b. above) of the AFGL network's potential contributions to an operational system and its relationship to other networks, of the state of knowledge of the sources of daytime pulsations, and of the prospects for employing pulsations as event predictors.

- e. Publish significant results in the scientific literature as they are developed.

Six reports were published, completed, or submitted for publication during the performance interval. Three international meetings and workshops were attended and results presented at each.

Specific Accomplishments. It was established that a definite, strong correlation prevails between pulsation amplitude and solar wind speed  $V_{SW}$  for Pc 3 and 4 (Appendix A).

The velocity correlation also applies to Pc 5 (Appendix E).

The correlation between IMF cone angle  $\theta_{XB}$  and pulsation amplitude is strongly dependent on transient excitation of pulsation signals, so that in dealing with data in, say, hourly units of time, the distribution of  $\theta_{XB}$  within

the hour, rather than its average, should be taken into account for best results (Appendix B).

Pulsation amplitude is jointly dependent on both  $\theta_{XB}$  and  $V_{SW}$ ; maximal activity occurs when both  $\theta_{XB}$  is small and  $V_{SW}$  is large (Appendix C).

The observations supporting either the direct excitation of pulsations by waves in the magnetosheath or the stimulation of pulsations by surface wave instability (Kelvin-Helmholtz) are incomplete at best, leaving appreciable gaps in models attempting to connect signals at the magnetopause with signals at the ground (Appendix D).

The quasi-parallel portion of the bow shock is intimately associated with hydromagnetic waves and suprathermal particles in the solar wind outside as well as *inside the shock*. This association will have to be taken into account in application of pulsation measurements as diagnostics of plasma properties outside the magnetopause (Appendices F,G).

The AFGL magnetic observatory system may, by virtue of site locations and data handling capability, have the virtue of recording measurements ideally suited to investigating and monitoring a part of the pulsation band diagnostic of magnetospheric and solar wind conditions, but considerable improvement in the data processing and distribution will be required (Appendix H).

#### PENDING RESULTS

Several incipient or incomplete investigations bear on the objectives of this study. Two results drawn from these investigations are sufficiently advanced to be described here.

Magnetosheath Wave Patterns. Figure 1 illustrates the relative influence of two principal factors governing the delivery of large amplitude, quasi-parallel shock-structured waves to the magnetopause. These factors are: solar wind velocity (speed and direction) and Alfvén wave velocity. As the streamlines in the figure show, only solar wind passing through the subsolar region of the shock impinges directly on, or comes very close to, the magnetopause.

Waves convected with the wind on the flank of the shock can reach the dayside magnetopause only if they cross the sheath in less time than the plasma carrying them takes to sweep them downstream. The small pairs of arrows indicate, at the intersection of each pair, the relative velocities of the solar wind in its local direction of flow, and the Alfvén wave velocity toward the magnetopause. The flow and wave velocities have been estimated from the computations of Spreiter and Alksne (1969) for the IMF in the ecliptic (the plane of the figure) at  $45^\circ$  to the sun-earth line. The small, circled numbers in the magnetosheath in the figure indicate approximately the local ratio  $c_A/V_{SW}$  (i.e.,  $M_A^{-1}$ ) where  $c_A$  is the Alfvén speed ( $M_A$  is the Alfvén Mach number).

It is clear in Figure 1 that not only does plasma entering the flank of the magnetosheath avoid the magnetopause, but waves originating in the flank plasma are so slow relative to  $V_{SW}$  that they are unlikely to propagate to the magnetopause until far downstream. In contrast, subsolar plasma not only streams toward the magnetopause, but its parametric properties support faster wave propagation than at the flank, making delivery of waves to the magnetopause highly probable. The figure suggests that up to some angle from the subsolar point, quasi-parallel waves could cross layers of solar wind and

reach the dayside magnetopause, while beyond that angle they could not. The numbers on the streamlines just inside the nominal shock outline are rough estimates of the length of the corresponding streamline segment up to the terminator (the -Y axis) divided by the shortest distance from the streamline to the magnetopause. These numbers are a crude guide to the ratio of  $V_{SW}$  to  $C_A$  needed to pass shock oscillations to the magnetopause. If the distance ratio is greater than the velocity ratio (the inverse of the circled numbers), the waves may reach the magnetopause; otherwise they will not. The figure suggests, then, that waves reaching the magnetopause must originate in the shock no more than about  $45^\circ$  or so from the subsolar point, when the IMF is at  $45^\circ$ . Such a requirement is compatible with the model of shock origin, since a  $45^\circ$  IMF will cause quasi-parallel structure to prevail in the subsolar region.

Further evaluation of Figure 1 and its implications for other directions of the IMF are in progress as this report is being prepared and will be released and discussed in coming months.

Correlations at Synchronous Elevations. All the published correlations of this study so far have compared interplanetary with ground station data. The phenomena of interest, however, are magnetospheric waves, of which traditional micropulsations at the earth's surface are only one manifestation. An additional approach to tying the magnetosphere's oscillations to the solar wind is through satellite measurements, of which those made in geosynchronous orbit constitute a readily available data set. Two preliminary results follow.

Figure 2 shows clearly that the signal power in the Pc 3 frequency range at ATS-6 increased with  $V_{SW}$ , just as the hourly maximal amplitude does

on the ground. The data base for Figure 2, and Figure 3 below, is some 3000 two-hour intervals of ATS-6 magnetometer recordings between June and September 1974.

The inserts in Figure 3 reproduce the three-dimensional summary diagrams from Appendix C, showing the general trend of the joint distribution of hourly pulsation maximum with hourly average  $V_{SW}$  and the cosine  $\theta_{XB}$ , when 20-percent of the hourly cone angles of the IMF were below  $\theta_{XB}$ . The large central diagram in Figure 3 summarizes the data from ATS 6 in the same format as the inserts. In this case, two-hour averages of  $V_{SW}$  and  $\theta_{XB}$  were used and the vertical scale represents the probability of occurrence of Pc 3, based on the appearance of definable power peaks in the magnetic field spectra.

We see that one result of the ATS study has been a remarkable verification of the joint dependence of pulsation activity on  $V_{SW}$  and  $\theta_{XB}$ . The same pattern of pulsation activity rising with solar wind speed and cosine of the cone angle appears at synchronous orbit as on the ground, despite the somewhat different means of processing the data. The dependence of  $\delta B$  on  $V_{SW}$  is much steeper, and its occurrence much higher at low angle than high, and the dependence of  $\delta B$  on  $\cos \theta_{XB}$  is more pronounced, and the occurrence much higher at high velocity than at low. There is a hint in the ATS diagram that Pc 3 occurrence peaks or levels off at  $V_{SW} \approx 600-700$  Km/sec, but a data set containing many more of the rather unusual speeds above 700 Km/sec will be necessary to sustain such an inference.

The entire ATS 6 study will be the subject of a report in preparation.

In addition to the studies of the foregoing paragraphs, two other investigations have been initiated, although neither has advanced enough to provide results for this report. The first will attempt to find correlations of pulsations at the ground with identified surface wave events recorded at the magnetopause by ISEE 1. The second will attempt to define, develop and test a composite index of worldwide pulsation activity.

#### SUMMARY AND RECOMMENDATIONS

This project has, within its own activities, demonstrated the control of daytime, midperiod pulsation activity by the joint influence of the solar wind velocity and the IMF direction. In addition, the project has, through the effect of its publications, stimulated parallel results by other investigators which have, except for some details still to be reviewed, corroborated our findings.

Much of what has been done has established qualitative relationships between  $V_{SW}$  and cone angle  $\theta_{XB}$ , and pulsation signals represented in several guises: hourly average, hourly maximum, two-hourly power peak, or probability of occurrence above background. The major thrust of these qualitative results, aside from mere proof of their existence, has been to focus attention on general signal amplitude rather than sporadic appearance of visually defined "wavetrain" events. Thus, the magnetosphere must be thought of as a system responding to solar influences in a wholly general way and not just resonating on occasion at certain periods or transferring wavetrains to the ground only at special times. The system contains resonant responses, and the propagation of quasi-sinusoidal waves to any particular point at any particular time is

enhanced according to prevailing parameters of the system, but it appears that at any time the solar wind is delivering stimulus to the magnetopause, the effect can probably be detected in the magnetosphere at some level by "listening" to signal strength over most of the midperiod band.

This project has also produced some quantitative results. Indeed, one of its contributions has been to de-emphasize the event-approach to pulsations that has been customary by operating on signal level rather than on selected sets of "continuous pulsations." We have determined that the distinction in period between Pc 3 and Pc 4 is of little, if any, value when correlating signal level with solar wind parameters, and that the distinction between Pc 4 and Pc 5 is probably no better; that pulsation signals should be treated in terms of transient amplitude (or power) enhancement and that correlations should be expected over intervals of ten minutes or longer, depending on period; that thresholds of about 250 Km/sec and  $55^\circ$  exist, such that pulsation activity is negligible when  $V_{SW}$  and  $\theta_{XB}$  are jointly below and above their respective thresholds.

It is recommended as an outcome of this program's findings and review of the results of other concurrent investigations that future effort move to:

- a. Investigate direct observations of wave transfer into and through the magnetosphere,
- b. Develop an index or measure of global geomagnetic pulsation activity,
- c. Quantify the relationship between global activity and solar wind properties.

REFERENCES

Spreiter, J. R., and A. Y. Alksne, Plasma flow around the magnetosphere, Magnetospheric Physics, ed. D. J. Williams and G. D. Mead, William Byrd Press, Inc., Richmond, Virginia, 11-50, 1969; Rev. of Geophys., 1, 11, 1969.



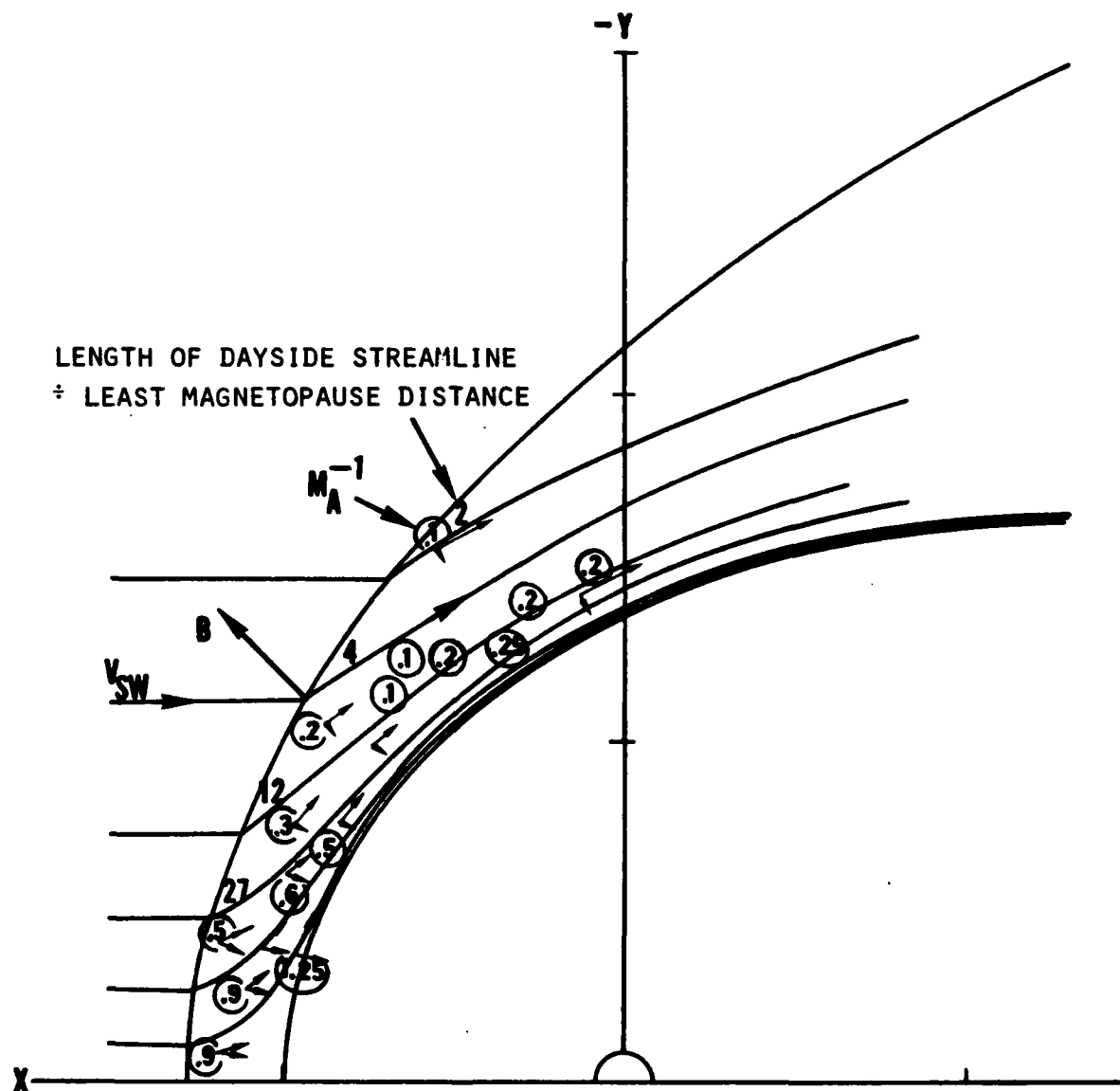


Figure 1. Solar wind streamlines in the magnetosheath and wind-wave speed parameters for  $45^\circ$  IMF.

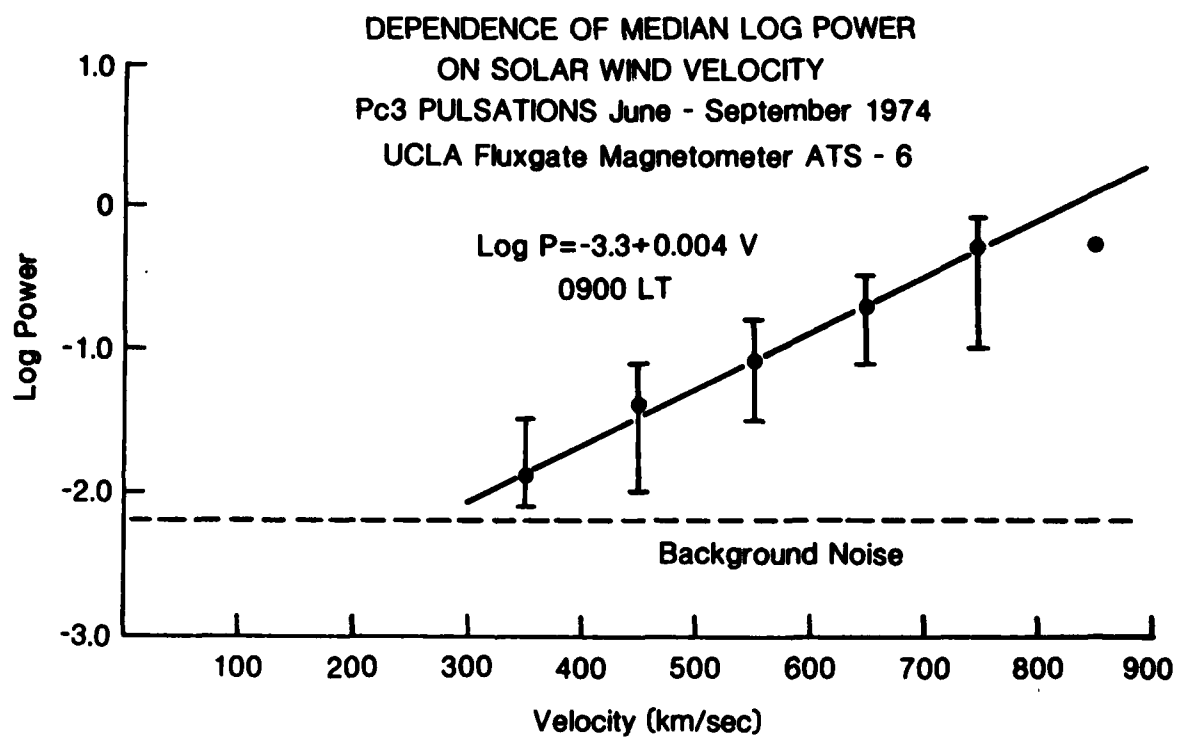


Figure 2

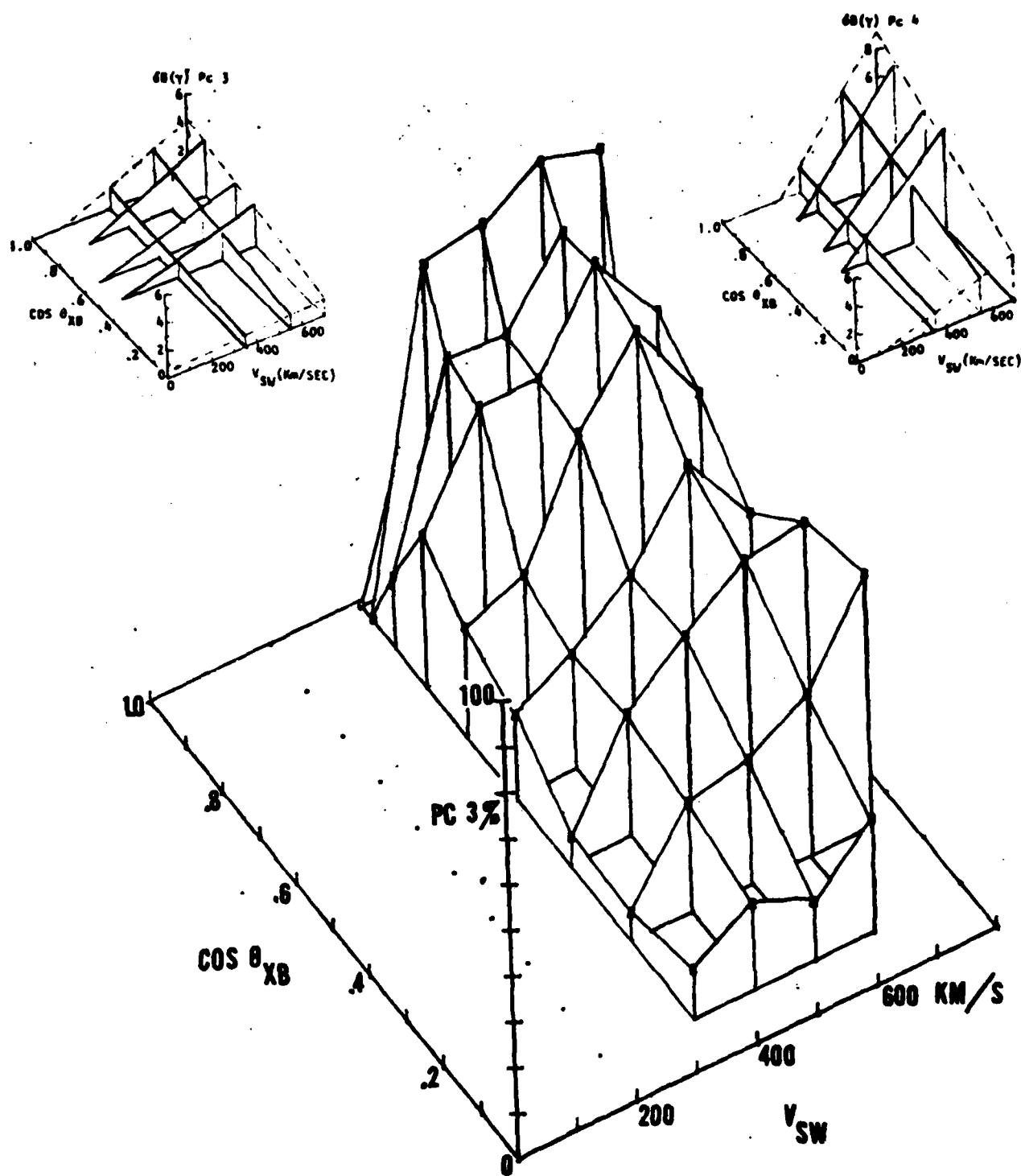


Figure 3

**APPENDIX A**

**EVIDENCE FOR THE CONTROL OF PC 3,4 MAGNETIC PULSATIONS  
BY THE SOLAR WIND VELOCITY**

EVIDENCE FOR THE CONTROL OF Pc 3,4 MAGNETIC PULSATIONS  
BY THE SOLAR WIND VELOCITY

H.J. Singer, C.T. Russell, and M.G. Kivelson

Institute of Geophysics and Planetary Physics  
University of California, Los Angeles, California 90024

E.W. Greenstadt

Space Sciences Department, TRW Defense and Space Systems  
Redondo Beach, California 90278

J.V. Olson

Institute of Earth and Planetary Physics, University of Alberta,  
Edmonton, Alberta, Canada

**Abstract.** The amplitude of Pc 3,4 magnetic pulsations at Calgary is shown to increase as the solar wind velocity increases. The pulsation amplitude dependence on solar wind velocity can be understood in terms of the Kelvin-Helmholtz instability at the magnetopause boundary.

## Introduction

Any method for monitoring the properties of the solar wind and magnetosphere using ground-based rather than satellite records would decrease the cost of obtaining this much needed information about the space environment. Consequently, correlations between solar wind properties and features of ground magnetic records have long been sought (cf. Jacobs, 1970). In particular, it has been suggested that the amplitudes of Pc 3 (10-45 sec) and Pc 4 (45-150 sec) magnetic pulsations at the earth's surface are highly correlated with such solar wind parameters as the interplanetary magnetic field (IMF) orientation (Bol'shakova and Troitskaya, 1968; Greenstadt and Olson, 1976, 1977; Webb and Orr, 1976), Alfvén waves in the solar wind, and solar wind velocity (Vinogradov and Parkhomov, 1974). Furthermore, the periods of the pulsations have been correlated with solar wind velocity (Troitskaya and Gul'yel'mi, 1967), IMF magnitude (Troitskaya et al., 1971; Gul'yel'mi and Bol'shakova, 1973; Gul'yel'mi et al., 1973; Russell and Fleming, 1976) and solar wind density (Gringauz et al., 1971). Each correlation developed by the studies cited above has been somewhat ambiguous because of compounded physical effects, methodological imperfections, or both. In particular, the recent work by Greenstadt and Olson (1976, 1977 referred to as G and O) identified correlations of IMF direction with Pc 3,4 noise, despite wide scatter of individual data points. In the work to be described in this paper we used the G and O data set of hourly Pc 3 and 4 amplitudes, plus plasma measurements from two satellites to demonstrate that solar wind velocity was also correlated with the amplitude of Pc 3 and Pc 4 activity.

## Pc 3,4 Pulsation Amplitude vs. IMF Orientation

Greenstadt and Olson examined the relationship between the amplitude of dayside magnetic activity

in the Pc 3 and 4 frequency range and  $\theta_{XB}$ , the angle that the interplanetary magnetic field makes with the sun-earth line. They found that large amplitude activity was associated with small  $\theta_{XB}$ , i.e. when the solar wind and IMF are nearly aligned. Their results were consistent with Greenstadt's previous work (Greenstadt, 1972a and b) regarding the propagation and convection of large amplitude quasi-parallel shock oscillations through the magnetosheath to the magnetopause.

Using data from Calgary during September through November 1969, G and O displayed Pc 3 and Pc 4 hourly maximal noise amplitude vs. hourly minimal angle  $\theta_{XB}$ . This display illustrated that larger amplitudes are associated with smaller  $\theta_{XB}$  min; however, the large scatter in the data which contained many large amplitude events at relatively large  $\theta_{XB}$  min, suggested that other parameters may have a significant influence on the pulsation amplitude.

## Pc 3,4 Pulsation Amplitude vs. Solar Wind Velocity

A plot of hourly Pc 3 activity amplitude vs. solar wind velocity using the G and O data is shown in Figure 1. The solar wind velocities are hourly averages from Explorer 33 and HEOS 1 [normalized to Explorer 33 values (Moreno and Signorini, 1973)] from the composite Solar Wind Plasma Data Set compiled by J.H. King (personal communication 1976). The median amplitudes are shown in 50 km/sec bins, and the amplitude increases with increasing velocity. The amplitude in the 500-600 km/sec range is nearly twice (1.8) the amplitude in the 300-400 km/sec range, and 67% of the high amplitude points ( $>2\sigma$ ) have velocities  $>500$  km/sec.

The trend for larger amplitude ground activity to be associated with large velocities is also demonstrated in Figure 2 illustrating hourly maximum amplitude of Pc 4 activity as a function of solar wind velocity. Again, the median amplitudes clearly demonstrate that large amplitudes were associated with larger velocities, and 73% of the high amplitude points ( $>4\sigma$ ) were associated with velocities  $>500$  km/sec.

There are clearly exceptions to the general trends of the dependence of pulsation amplitude on  $\theta_{XB}$  min and on solar wind velocity. At times of small  $\theta_{XB}$  or large solar wind velocity, the

Copyright 1977 by the American Geophysical Union.

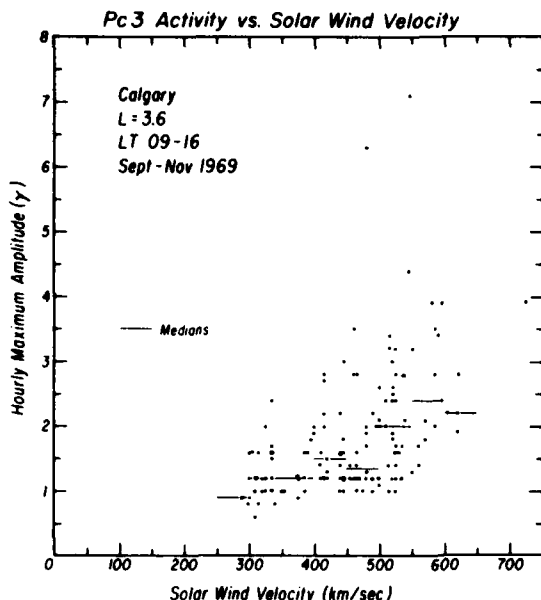


Figure 1. Hourly maximum amplitude of Pc 3 waves (10-45 sec) measured at Calgary, Alberta for local times from 0900 to 1600 as a function of solar wind velocity.

expected large amplitude pulsation activity is not always observed. However, the use of the minimum value of  $\theta_{XB}$  during a one hour interval may be misleading, for  $\theta_{XB}$  may attain its minimum value only briefly during the hour interval. One would not necessarily expect to see large amplitude activity for hours during which  $\theta_{XB}$  min was small for short intervals. Moreover, large amplitude activity may not have been observed if the conditions for resonance in the magnetosphere were not attained at these times, or our observation point may not have been near the resonance region.

Other exceptions to the general trend of dependence on solar wind velocity occurred during times of small solar wind velocities when large amplitude pulsation activity was observed. For example, in Figure 2 there are 11 points in this class, if the cutoffs are chosen for amplitudes  $>4\gamma$  and velocities  $<500$  km/sec. We examined the few large amplitude points that occurred at low velocities to see if they might be occurring at times of small  $\theta_{XB}$  min. Small  $\theta_{XB}$  min should be associated with large amplitudes according to Greenstadt and Olson, but these large amplitude values were not well ordered by  $\theta_{XB}$  min. However, 7 of 11 of these hours of large amplitude at low velocity were found to occur on the leading edge of a high velocity stream. The leading edge of a high velocity stream is often associated with the highest level of Alfvénic wave activity according to Belcher and Davis (1971), and the solar wind wave amplitude may be related to the increased pulsation activity amplitude at Calgary (Vinogradov and Parkhomov, 1974). Geomagnetic activity was moderately high ( $2 < K_p < 4$ ) during the seven hours associated with the leading edge of the high velocity stream, as expected (Sawyer and Haurwitz, 1976). Therefore,

another possible explanation for these exceptions is that they are generated within the magnetosphere, not without.

Finally, we examined the exceptions to the general  $\theta_{XB}$  min trend where large amplitude activity was associated with large  $\theta_{XB}$  min. The purpose was to test whether large solar wind velocity could account for these large amplitude events. We chose the class of Pc 4 events with amplitudes  $>4\gamma$  and  $\theta_{XB}$  min  $>30^\circ$ . The cut-offs are somewhat arbitrary; however, other values were chosen without substantially changing the results. The average velocity for the 18 events in the large amplitude, large  $\theta_{XB}$  min class is  $544 \pm 17$  km/sec. This is in contrast to the average velocity of  $449 \pm 8$  km/sec for all 134 events considered in this study. In addition the velocity distribution for the large amplitude, large  $\theta_{XB}$  min class is highly skewed towards large velocities as opposed to all cases which have a velocity distribution which is roughly a gaussian about the mean. Therefore, large solar wind velocities may account for some of the scatter in the results of G and O.

#### Discussion

We have made plots similar to Figures 1 and 2 for Pc 3 and 4 amplitudes as a function of solar wind density and dynamic pressure, as a function of IMF magnitude and as a function of geomagnetic activity as expressed by the  $K_p$  index. None of these parameters correlated with pulsation amplitude as clearly as did the solar wind velocity. The correlations that were apparent were consistent with the known correlation between the various parameters and the solar wind velocity. Thus, the amplitude of Pc 3 and 4 magnetic pulsations, at least as observed at Calgary during day time hours, appears to be controlled mainly by two external boundary conditions, the direction of the IMF and the solar wind velocity.

The dual control can be understood in a framework in which disturbances in the magnetosheath

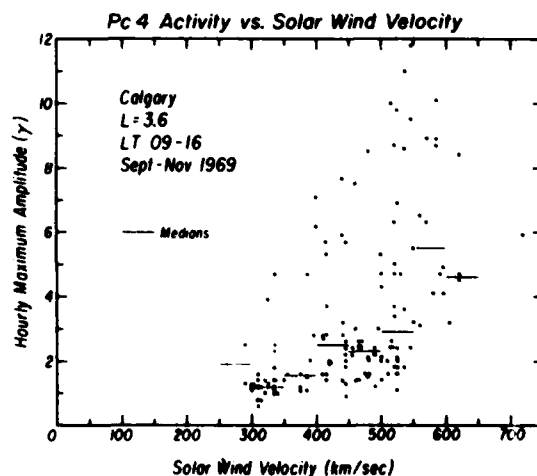


Figure 2. Hourly maximum amplitude of Pc 4 waves (45-150 sec) measured at Calgary, Alberta for local times from 0900 to 1600 as a function of solar wind velocity.

are amplified at the magnetopause by the Kelvin-Helmholtz instability (Landau and Lifshitz, 1960; Chandrasekhar, 1961; Southwood, 1968; Boller and Stolov, 1970, 1973, 1974). The larger the solar wind velocity, the more likely is wave growth at the magnetopause. The source of the magnetosheath disturbances that are amplified by this instability may be the quasi-parallel shock oscillations described by Greenstadt (1972a) or any other source of waves in the dayside magnetosheath. Thus, this mechanism is consistent with the reported control of Pc 3,4 pulsation periods by the magnitude of the interplanetary magnetic field as well as the control of amplitudes by the direction of the IMF. The Kelvin-Helmholtz instability would simply act to amplify these already existing fluctuations. These waves would then couple to resonant regions inside the magnetosphere as discussed by Southwood (1973, 1974, 1975) and by Chen and Hasegawa (1974a and b).

**Acknowledgments.** We are grateful to D.J. Southwood and W.J. Hughes for many useful discussions on the properties of and sources for Pc 3 and 4 magnetic pulsations, and to the National Space Science Data Center and J.H. King for providing the solar wind data. This work was supported at UCLA by the National Science Foundation under research grant DES 74-23464 and by the National Aeronautics and Space Administration under research grant NGR 05-007-004, at TRW by Air Force Office of Scientific Research contract F49620-77-C-0018 and at the University of Alberta by the National Research Council of Canada.

#### References

- Belcher, J.W., and L. Davis, Jr., Large-amplitude Alfvén waves in the interplanetary medium, *J. Geophys. Res.*, **76**, 3534, 1971.
- Boller, B.R., and H.L. Stolov, Kelvin-Helmholtz instability and the semiannual variation of geomagnetic activity, *J. Geophys. Res.*, **75**, 6073, 1970.
- Boller, B.R., and H.L. Stolov, Explorer 18 study of the stability of the magnetopause using a Kelvin-Helmholtz instability criterion, *J. Geophys. Res.*, **78**, 8078, 1973.
- Boller, B.R. and H.L. Stolov, Investigation of the association of magnetopause instability with interplanetary sector structure, *J. Geophys. Res.*, **79**, 673, 1974.
- Bol'shakova, O.V. and V.A. Troitskaya, Relation of the interplanetary magnetic field direction to the system of stable oscillations, *Dokl. Akad. Nauk., SSSR*, **180**, 343, 1968.
- Chandrasekhar, S., *Hydrodynamic and Hydromagnetic Stability*, p. 481-514, Oxford University Press, 1961.
- Chen, L. and A. Hasegawa, A theory of long-period magnetic pulsations, 1, Steady state excitation of field line resonance, *J. Geophys. Res.*, **79**, 1024, 1974a.
- Chen, L. and A. Hasegawa, A theory of long-period magnetic pulsations, 2, Impulse excitation of surface eigenmode, *J. Geophys. Res.*, **79**, 1033, 1974b.
- Greenstadt, E.W., Field-determined oscillations in the magnetosheath as possible sources of medium-period daytime micropulsations, in *Proceedings of the Conference on Solar Terrestrial Relations*, p. 515, University of Calgary, April 1972a.
- Greenstadt, E.W., Observations of nonuniform structure of the earth's bow shock correlated with interplanetary field orientation, *J. Geophys. Res.*, **77**, 1729, 1972b.
- Greenstadt, E.W. and J.V. Olson, Pc 3,4 activity and interplanetary field orientation, *J. Geophys. Res.*, **81**, 5911, 1976.
- Greenstadt, E.W. and J.V. Olson, A micropulsation contribution in the Pc 3-4 range correlated with IMF radial orientation, submitted to *J. Geophys. Res.*, 1977.
- Gringauz, K.I., E.K. Solomatina, V.A. Troitskaya, and R.V. Shchepetnov, Variations of solar wind flux observed by several spacecraft and related pulsations of the earth's electromagnetic field, *J. Geophys. Res.*, **76**, 1065, 1971.
- Gul'yel'mi, A.V. and O.V. Bol'shakova, Diagnostics of the interplanetary magnetic field from ground-based data on Pc 2-4 micropulsations, *Geomagn. Aeron.*, **13**, 535, 1973.
- Gul'yel'mi, A.V., T.A. Plyasova-Bakunina, and R.V. Shchepetnov, Relation between the period of geomagnetic pulsations Pc 3,4 and the parameters of the interplanetary medium at the earth's orbit, *Geomagn. Aeron.*, **13**, 331, 1973.
- Jacobs, J.A., *Geomagnetic Micropulsations*, Chapter 6, Springer-Verlag, New York, 1970.
- Landau, L.D. and E.M. Lifshitz, *Electrodynamics of continuous media*, p. 227, Pergamon Press, 1960.
- Moreno, G. and C. Signorini, Comparison of interplanetary plasma experiments, *Eldo-Cecles/Esro-Cers Scient. and Tech. Rev.*, **5**, 401-412, 1973.
- Russell, C.T. and B.K. Fleming, Magnetic pulsations as a probe of the interplanetary magnetic field: a test of the Borok B index, *J. Geophys. Res.*, **81**, 5882, 1976.
- Sawyer, C. and M. Haurwitz, Geomagnetic activity at the passage of high-speed streams in the solar wind, *J. Geophys. Res.*, **81**, 2435, 1976.
- Southwood, D.J., The hydromagnetic stability of the magnetospheric boundary, *Planet. Space Sci.*, **16**, 587, 1968.
- Southwood, D.J., The behavior of ULF waves and particles in the magnetosphere, *Planet. Space Sci.*, **21**, 53, 1973.
- Southwood, D.J., Some features of field line resonances in the magnetosphere, *Planet. Space Sci.*, **22**, 483, 1974.
- Southwood, D.J., Comments on field line resonances and micropulsations, *Geophysics J.R. Astr. Soc.*, **41**, 425, 1975.
- Troitskaya, V.A. and A.V. Gul'yel'mi, Geomagnetic micropulsations and diagnostics of the magnetosphere, *Space Sci. Rev.*, **7**, 689, 1967.
- Troitskaya, V.A., T.A. Plyasova-Bakunina, and A.V. Gul'yel'mi, Relationship between Pc 2,4 pulsations and the interplanetary magnetic field, *Dokl. Akad. Nauk., SSSR*, **197**, 1312, 1971.
- Vinogradov, P.A. and V.A. Parkhomov, MHD waves in the solar wind - a possible source of geomagnetic Pc 3 pulsations, *Geomagn. Aeron.* (English Ed.) **15**, 109, 1974.
- Webb, D. and D. Orr, Geomagnetic pulsations (5-50 mHz) and the interplanetary magnetic field, *J. Geophys. Res.*, **81**, 5941, 1976.

(Received June 27, 1977;  
accepted July 11, 1977.)

**APPENDIX B**

**GEOMAGNETIC PULSATION SIGNALS AND HOURLY  
DISTRIBUTIONS OF IMF ORIENTATION**



## Geomagnetic Pulsation Signals and Hourly Distributions of IMF Orientation

E. W. GREENSTADT

*Space Sciences Department, TRW Defense and Space Systems Group, Redondo Beach, California 90278*

J. V. OLSON

*Institute of Earth and Planetary Physics, University of Alberta, Edmonton, Alberta, Canada T6G 2J1*

Hourly distributions of the angle  $\theta_{XB} = \arccos(\mathbf{X} \cdot \mathbf{B})$ , where  $\mathbf{X}$  is the solar ecliptic earth-sun axis and  $\mathbf{B}$  is the interplanetary magnetic field (IMF), have been compared with hourly Pc 3 and Pc 4 signal activity at Calgary for 198 hours in September, October, and November 1969. Hours whose distributions were concentrated above or below  $\theta_{XB} = 50^\circ$  were correlated with a clear separation of inactive from active micropulsation intervals. The correlation was stronger for the Pc 3 than for the Pc 4 band, and hours with significant fractions, say 10–20% of their  $\theta_{XB}$  distributions below  $30^\circ$ , corresponded particularly well with high amplitudes of micropulsation signals. Signals in the Pc 3 period range on the ground can therefore be used as a crude monitor of certain extremes of IMF orientation.

### INTRODUCTION

For several years an international effort has been underway to define relationships between micropulsation properties at the earth's surface and plasma properties in the magnetosphere and solar wind with the ultimate aim of establishing reliable diagnostics of exospheric parameters obtainable from sensitive magnetometers on the ground. A number of promising correlations have been discovered, but gaps in theory and methodology still bar the way to the desired objective. This report describes an advance in data analytical methodology applied to one particular pair of correlation parameters.

One relationship long under investigation has been that between interplanetary magnetic field (IMF) orientation and micropulsation occurrence in the period ranges 10–45 s (Pc 3) and 45–150 s (Pc 4). Very briefly, the results are that micropulsation events are initiated or terminated when the IMF assumes or departs from certain preferred orientations. Statistical scatter has been large, and the exact details are not wholly confirmed from one worker to another. All seem to agree that Pc 4 events occur more or less when the IMF aligns itself with the sun-earth line. Pc 3 events, on the other hand, have been found to occur when the IMF either is along the nominal spiral angle [Bol'shakova and Troitskaya, 1968], is aligned with the sun-earth line [Greenstadt and Olson, 1976; Nourry, 1976], or possesses an enhanced radial component [Webb and Orr, 1976].

Traditionally, investigators have identified quasi-sinusoidal micropulsation 'events' at an observatory and then looked for the IMF's that correspond to them. Statistically significant accumulations of such events have demonstrated the patterns cited above, and a few striking individual events have been illustrated in the literature [Bol'shakova and Troitskaya, 1968; Nourry, 1976]. IMF orientation has been defined in terms of field vector latitude  $\lambda_B$  and longitude  $\phi_B$  separately and in combination [Troitskaya et al., 1971; Bol'shakova and Troitskaya, 1968; Gul'elmi, 1974; Greenstadt and Olson, 1976; Nourry, 1976]. Only rarely, and recently, has micropulsation activity been treated, without preselection of events, by examining broadband, mixed frequency pulsation signal level and by applying spectral analysis [Greenstadt and Olson, 1976; Webb and Orr, 1976; Barker et al., 1977; Webb et al., 1977; Arthur et al., 1977].

The ongoing study from which this report originated is an attempt to test a model according to which approximate alignment of  $\mathbf{B}$  with the solar wind permits large-amplitude, quasi-parallel bow shock waves to be delivered from the subsolar region of the shock to the subsolar region of the magnetopause, providing periodic or nearly periodic perturbations at the dayside magnetospheric boundary as a possible instigator of daytime geomagnetic pulsations. Arguments leading to the model have been given elsewhere [Greenstadt, 1972; Greenstadt and Olson, 1976] and are not central to this communication.

It is worth noting here, however, that recent results showing the global nature of pulsation enhancements have strongly reinforced the association of Pc 3–4 origin with solar wind properties, particularly changes in IMF direction [Barker et al., 1977; Webb et al., 1977].

The initial thrust of the study has aimed at a simple demonstration of whether or not field alignment, measured by  $\theta_{XB}$ , the angle between  $\mathbf{B}$  and the solar ecliptic  $\mathbf{X}$  axis (approximately the solar wind flow line), is correlated with signal level in the Pc 3 and Pc 4 bands at Calgary observatory. By signal level we mean the peak-to-peak value of the horizontal field variation in filtered Pc 3 and Pc 4 frequency ranges. Correlation was sought earlier between hourly maximal peak-to-peak Pc 3–4 signal level,  $\delta B$ , and hourly minimal  $\theta_{XB}$ , by using data from a particular 3-month interval, September–November 1969. The results were favorable but beset by so much scatter that convincing physical conclusions were impossible. Numerous potential explanations of the weak correlations, both physical and methodological, were proposed [Greenstadt and Olson, 1976; Singer et al., 1977]. The research segment covered here has attempted to reduce the scatter by attacking the most severe methodological distortion introduced earlier, namely, the misrepresentation of each hour's IMF readings by the hourly minimal  $\theta_{XB}$ . We use the same  $\delta B$  as before, which represent the hourly maximum signal level in either  $X$  or  $Y$  components, whichever was larger, at Calgary.

The method chosen for improving the data was to replace each hour's  $\theta_{XBmin}$  by an actual distribution of  $\theta_{XB}$ , of which there were nominally 44 samples, each hour. The distributions were approximated by calculating, for each hour in which at least three quarters of the data were recorded, the percent of the hour's  $\theta_{XB}$  that fell below every  $10^\circ$  increment in  $\theta_{XB}$  from  $0^\circ$  to  $90^\circ$ . The remainder of this paper describes and discusses the picture drawn by these cumulative (i.e., integral) percentile

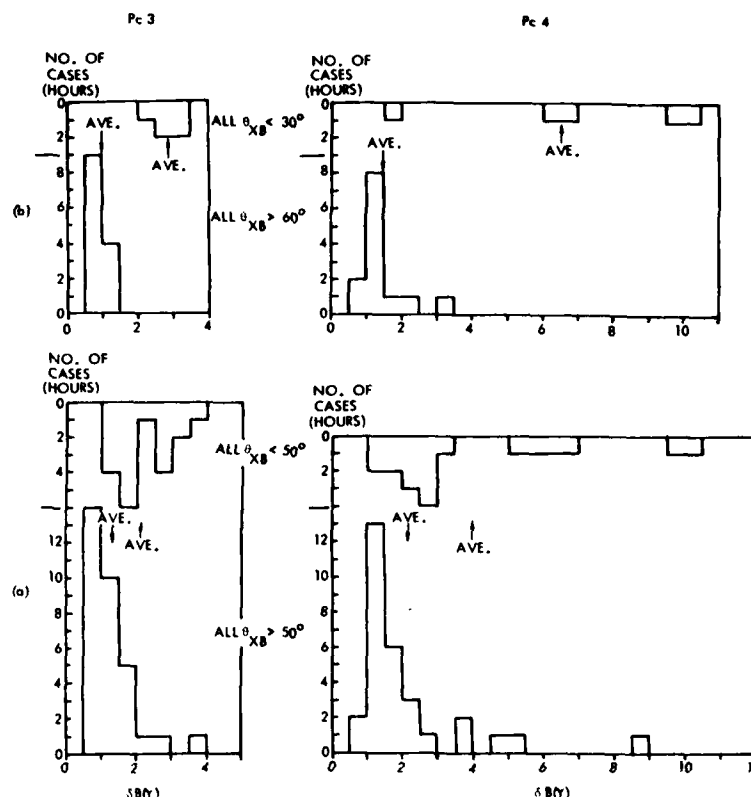


Fig. 1. Numerical histograms of micropulsation signal amplitudes  $\delta B$  corresponding to selected types of hourly distributions of  $\theta_{XB}$ . Histogram averages indicated by arrows. Results are shown for hours when (a) all  $\theta_{XB} < 50^\circ$  and all  $\theta_{XB} > 50^\circ$  and (b) all  $\theta_{XB} < 30^\circ$  and all  $\theta_{XB} > 60^\circ$ .

distributions and the differential distributions derivable from them.

#### RESULTS

**Separation of extremes.** The first and most urgent application of the percentile computation was immediately successful. Hourly distributions were found in which all  $\theta_{XB}$  were clustered near one extreme or the other of the angle scale, and the corresponding hourly amplitudes were tabulated. The results appear as histograms in Figure 1. In Figure 1a the two classes of hours all  $\theta_{XB} < 50^\circ$  and all  $\theta_{XB} > 50^\circ$  are displayed for Pc 3 and Pc 4 bands. The  $\theta_{XB} < 50^\circ$  histograms have been plotted upside down for clarity.

The dissimilarities in the distributions of amplitudes in the two classes are clear. Both the modes and the averages of the two amplitude distributions are displaced, in the predicted direction, for both micropulsation bands. The displacement is even more striking when more extreme clustering is demanded. Figure 1b shows the results for hours when all  $\theta_{XB} < 30^\circ$  and all  $\theta_{XB} > 60^\circ$ . In the case of Pc 3, not only are the averages and modes displaced, but the amplitude distributions don't even overlap on the amplitude scale. The population of the classes is admittedly small, however, since the selected cases represent relatively unusual behavior for the IMF.

The separation of hours of enlarged  $\delta B$  from hours of essen-

tially background  $\delta B$  by extreme clustering of the directional distributions of the IMF's seems to have defined necessary conditions under which Pc 3-4 were stimulated or suppressed. We wish also to examine the more difficult problem of determining sufficient conditions. Were enhanced signals produced only when the IMF was markedly aligned with the X axis or was only a temporary alignment part of each hour enough to trigger activity?

**Grouped distributions.** Figure 2 presents an overview of the 198 hourly distributions of  $\theta_{XB}$ , divided into groups according to the amplitudes of the corresponding hourly pulsation maxima. That is, all hourly distributions of  $\theta_{XB}$  corresponding to hours in which maximal Pc 3 amplitude  $\delta B$  was 0.5  $\gamma$  or less were grouped together; all distributions in which  $\delta B$  was between 0.5 and 1.0  $\gamma$  were grouped together, and so on. The range of  $\delta B$  defining each group was 0.5  $\gamma$  until  $\delta B$  became too high for 0.5  $\gamma$  to define a large enough sample of distributions; then larger increments of  $\delta B$  were used to sort the remaining distributions. The bottom value of  $\delta B$  for each group is printed in the figure.

Each small panel of Figure 2 is an overlay of all the cumulative hourly distributions of  $\theta_{XB}$  that accompanied the corresponding  $\delta B$ . The abscissa is in angular degrees; the ordinate measures the percent of  $\theta_{XB}$  recorded during a given hour below or equal to a corresponding  $\theta_{XB}$ . Accumulations were

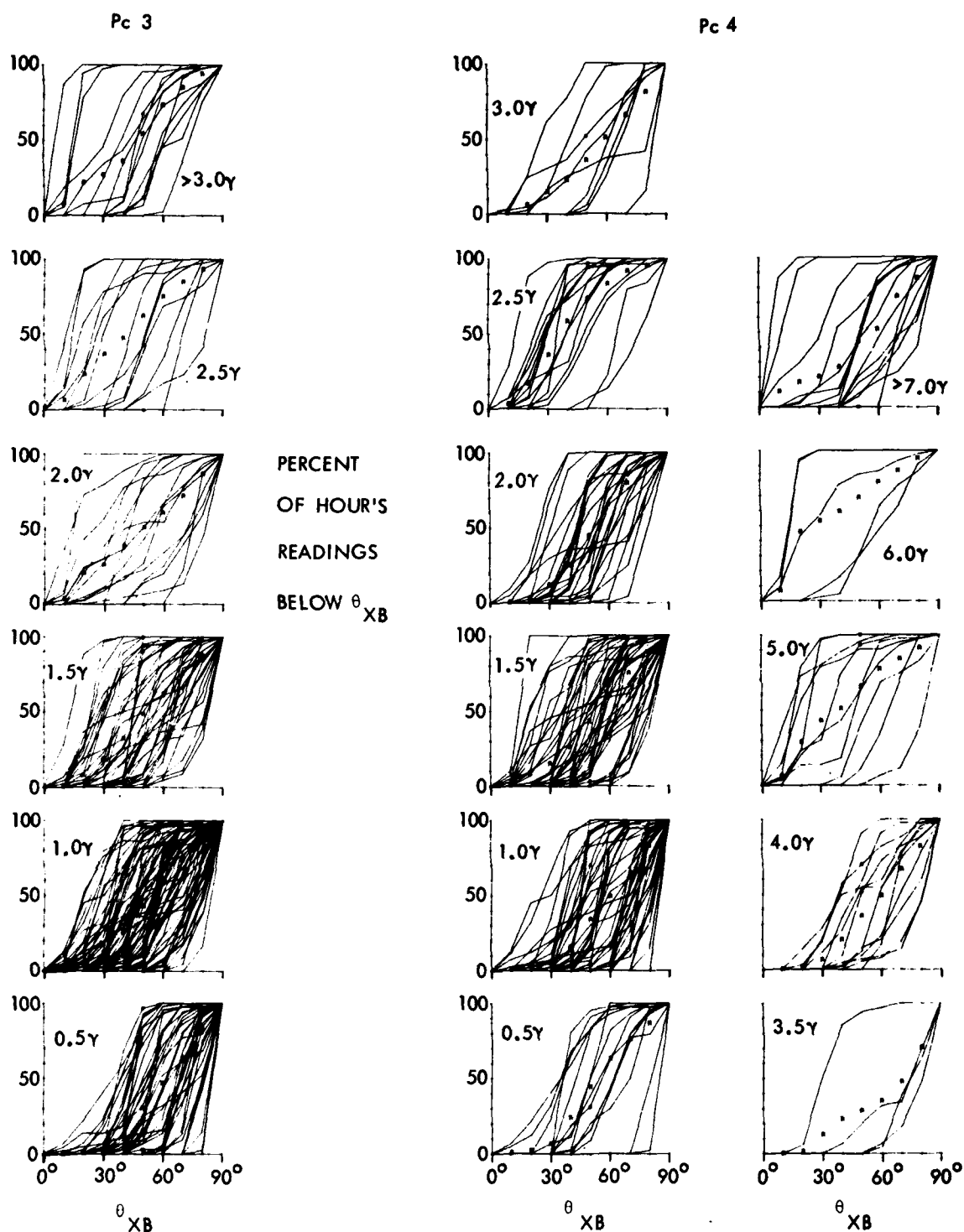


Fig. 2. Cumulative percentile distributions of hourly sets of  $\theta_{XB}$  arranged according to groups of hours whose maximal Pc 3 or Pc 4 signal amplitudes  $\delta B$  fell in selected ranges. The bottom of each amplitude range is indicated by the  $\delta B$  inserted in each small graph; e.g.,  $1.0 \gamma$  signifies the group of hours for which  $1.0 \leq \delta B \leq 1.5 \gamma$ . 'A's indicate average of the group.

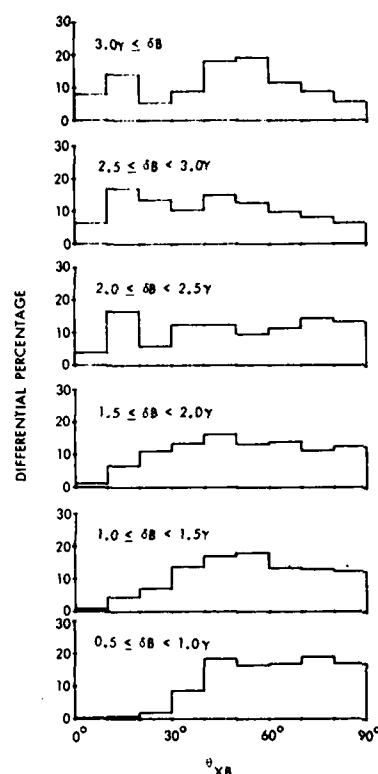


Fig. 3. Differential percentage distributions of the group distribution averages for the Pc 3 panels in Figure 2.

computed every  $10^\circ$ . An average cumulative distribution made up of the average percentile at each  $10^\circ$  point was calculated for each group and indicated in the figure by a string of A's.

The variability of the hourly distributions for a given  $\delta B$  is readily apparent, but the tendency for most  $\theta_{XB}$  to have occurred between  $30^\circ$  and  $90^\circ$  when  $\delta B$  was smallest, and between  $0^\circ$  and  $60^\circ$  when  $\delta B$  was largest, is easily discernible. The variability of the distributions in a given group made the group's average distribution (the A's) a rather poor indication of any clustering tendency among the curves. Nevertheless, the averages can be used for describing some of the statistical properties of the distributions free from the clutter in Figure 2.

**Behavior of the averages.** Figure 3 shows the histograms of the average differential percent distribution, in  $10^\circ$  intervals, for half-gamma groupings of signal amplitude. The average distributions of Pc 3 show very clearly the shift from concentration at high  $\theta_{XB}$ , with virtually no population at low  $\theta_{XB}$ , at the bottom, to a wider spread, with substantial occupation of the  $0^\circ$ - $30^\circ$  sector, at the top. The shift occurred as the hourly maximal amplitude increased. Comparable histograms for Pc 4, not shown, reflected the more erratic, less self-consistent trend visible in Figure 2's Pc 4 panels.

In another view of the same data we can clump  $10^\circ$  increments of  $\theta_{XB}$  in groups of three and examine the bottom-to-top properties of the distributions in Figure 3 in three vertical bands of  $30^\circ$  each. Figure 4 shows how the percentage of  $\theta_{XB}$  in each of three sectors,  $0^\circ$ - $30^\circ$ ,  $30^\circ$ - $60^\circ$ , and  $60^\circ$ - $90^\circ$ , varied with micropulsation signal amplitudes of corresponding hours.

The patterns of Figure 4 tell us the following:

1. Minimal micropulsation signal in both Pc 3 and Pc 4 channels was unmistakably associated with negligible hourly percentages ( $<10\%$ ) of  $\theta_{XB}$  less than  $30^\circ$ .

2. Maximal micropulsation signal in both Pc 3 and Pc 4 channels was unmistakably associated with substantial percentages (20-30%) of  $\theta_{XB}$  less than  $30^\circ$ .

3. A substantial, even predominant, percentage of  $\theta_{XB}$  between  $30^\circ$  and  $60^\circ$  was not necessarily associated with significant micropulsation signal levels. Restated from the opposite point of view, it was not necessary that  $\theta_{XB}$  be overwhelmingly concentrated near  $90^\circ$  in order to cut off Pc 3 and Pc 4 signal.

4. The trend of low-to-high amplitude with low-to-high percentages of  $\theta_{XB}$  in the  $0^\circ$ - $30^\circ$  range was more pronounced and consistent in the Pc 3 than in the Pc 4 band.

Figure 4 suggests that the extent of IMF orientation near the sun-earth line was the critical factor in influencing Pc 3-4 amplitudes. This impression is reinforced if we isolate the low-angle statistics by imagining vertical bands of  $0^\circ$ - $10^\circ$  and  $0^\circ$ - $20^\circ$  in Figure 3. Figure 5a shows the percentages of hourly  $\theta_{XB}$  less than  $20^\circ$  versus amplitude. We see that the more stringent the alignment we require, the more definite the trends of percentage versus  $\delta B$  become for both Pc 3 and Pc 4 period ranges. This tendency is consistent with the highly restrictive angle requirements and pronounced separations described earlier in Figure 1.

**Individual exceptions.** Finally, we turn from the oversimplifications represented by the averages and return again to the way in which cases were actually distributed. Figure 6

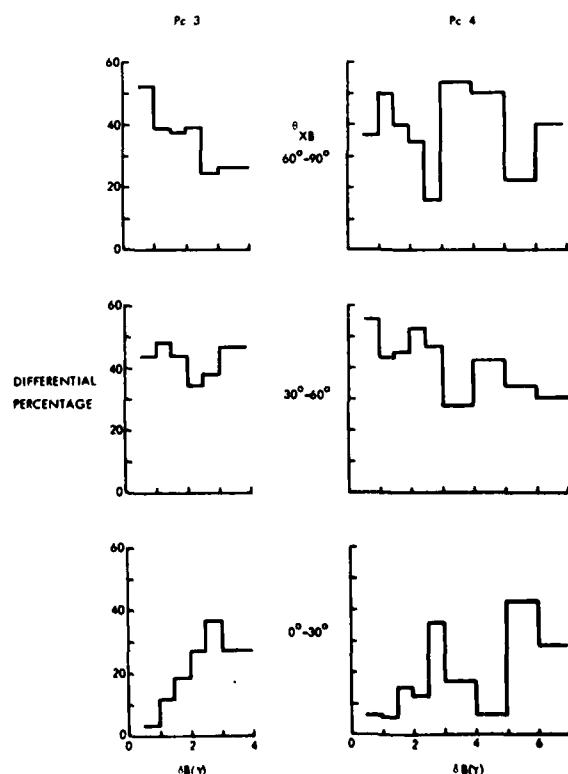


Fig. 4. Percentages of average distributions falling in three ranges of  $\theta_{XB}$ , versus  $\delta B$ .

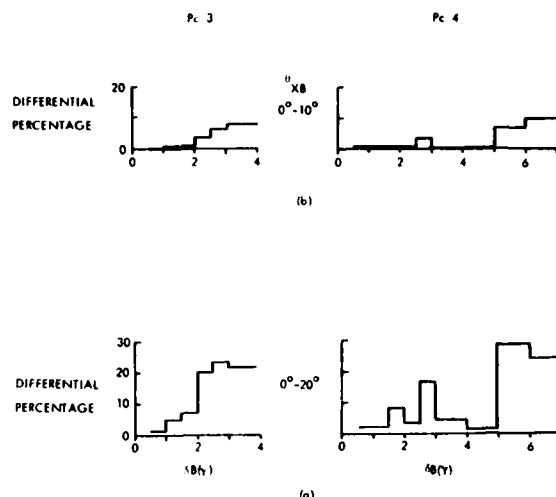


Fig. 5. Percentages of average distributions falling in the lowest ranges of  $\theta_{xB}$ , versus  $\delta B$ : (a)  $\theta_{xB} = 0^\circ$ – $20^\circ$  and (b)  $\theta_{xB} = 0^\circ$ – $10^\circ$ .

compares low-amplitude cases with high-amplitude cases for both Pc 3 and Pc 4. We are asking here a more rigorous question than heretofore, namely, how many individual (hourly) exceptions were there to the apparent correlation between pulsation amplitude and angular distribution?

We separated all essentially uneventful from all eventful hours. For Pc 3, hours when the peak amplitude was  $0.5$ – $1 \gamma$  were designated uneventful; hours when the peak amplitude was greater than  $2 \gamma$  were designated eventful in the sense that some Pc 3 signal definitely had occurred. The analogous separation for Pc 4 was for peak amplitudes of  $0.5$ – $1.5 \gamma$  (uneventful) and peak amplitudes greater than  $3 \gamma$  (eventful). These divisions correspond to separation of signals above the average peak amplitudes from signals below the average peak amplitudes as determined by averages over the whole study interval as described by Greenstadt and Olson [1977].

We want to know how many times a small percentage of  $\theta_{xB}$  readings fell at low  $\theta_{xB}$  even though there was no pulsation event and, conversely, how many times a small percentage was not accumulated until high  $\theta_{xB}$  even though there was pulsation activity during the hour. In Figure 6a the distributions are shown of the number of cases in which the 10 and 20 percentiles of the hourly angle measurements fell in each  $10^\circ$  increment of  $\theta_{xB}$  for the Pc 3 band. For example, in the bottommost graph there were 5 cases in which no more than 10% of the  $B$  field directions  $\theta_{xB}$  were below  $30^\circ$  or, conversely, 5 cases in which at least 90% of the angle measurements were above  $30^\circ$ .

The bottom pair of histograms declares that not one case in which Pc 3 activity was undetectable had as much as 10% of the corresponding  $\theta_{xB}$  below  $10^\circ$  and only 5 out of 40 cases had as much as 10% of the  $\theta_{xB}$  below  $30^\circ$ ; further, every case in which Pc 3 activity was pronounced during the hour had 10% or more of its  $\theta_{xB}$  below  $70^\circ$ , and only 4 out of 35 cases failed to have at least 10% of the  $\theta_{xB}$  below  $50^\circ$ , while over half, or 20 out of 35 cases, had 10% or more  $\theta_{xB}$  below  $30^\circ$ . Thus the trends indicated by the averages in Figures 4 and 5 were strongly reinforced by the actual distributions of cases making up the averages.

Comparable statements can be read from the other histo-

grams of Figure 6, which display the 10- and 20-percentile distributions of uneventful and eventful cases for both Pc 3 and Pc 4 bands. The total effect of Figure 6 is that the hourly distributions of  $\theta_{xB}$  for the two pulsation conditions correspond clearly to different behaviors of the IMF. The mode shifted toward  $0^\circ$  for all but one of the eventful distributions, compared to the uneventful, while the median  $\theta_{xB}$  was  $45^\circ$  or more for every uneventful distribution but  $45^\circ$  or less for every eventful distribution. The distinctions were appreciably more pronounced for Pc 3 than for Pc 4 periods.

Of great importance to this study is what Figure 6 does not show. There is no evidence in the figure that any value in the range  $\theta_{xB} = 50^\circ$ – $60^\circ$  is essential to separating active from inactive conditions, especially for Pc 4. The uneventful cases, while deficient in low  $\theta_{xB}$ , include numerous cases in which 20% or more of the measurements were below  $50^\circ$ , with the pulsation amplitude at background. Conversely, there were active cases in which all but 10% or less of the  $\theta_{xB}$  were above  $50^\circ$ . There is nothing in this form of presentation, then, that supports the shock origin model in terms of the notion of a subsolar point threshold at  $\theta_{xB} \approx 50^\circ$ . This is the nominal angle below which the subsolar point is in the quasi-parallel portion of the bow shock [Greenstadt, 1976].

There is a visually attractive demarcation in Figure 6, however. All the uneventful hours seem to have had a sharp cutoff at  $30^\circ$ , only a small fraction of cases having their 10 or 20 percentiles of  $\theta_{xB}$  below this angle. Correspondingly, all the eventful hours appear to have had a subdistribution below  $30^\circ$  that peaked in the  $10^\circ$ – $20^\circ$  interval. The striking separations of Figure 1 will be recalled. In terms of the question posed earlier, a substantial percentage (10–20%) of points below  $30^\circ$

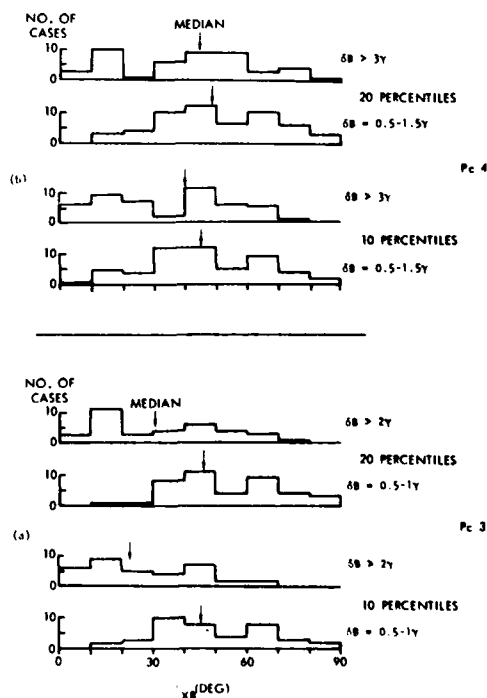


Fig. 6. Comparison of histograms of the distributions of 10 and 20 percentiles of  $\theta_{xB}$  for eventful and uneventful hours of (a) Pc 3 activity and (b) Pc 4 activity.

seemed to be sufficient to produce Pc 3, 4, but a similar percentage of  $\theta_{XB}$  below  $50^\circ$  was not sufficient for the same effect. The statistical significance of such a separation cannot be established without further data. Physically,  $\theta_{XB} = 30^\circ$  is the value below which, roughly, the 'forward cap,' i.e., the section of the bow shock corresponding to the sunward or positive  $X$  axis, rather than just the subsolar point, assumes quasi-parallel structure. This occurs because every cross section of the shock parallel to the plane containing  $B$  and  $X$  has its quasi-perpendicular section moved back behind the line  $X = 0$ . Why such a configuration should be significant for micropulsations has not been considered before, but this question will bear further investigation should the  $30^\circ$  effect be confirmed. Certainly, such a widespread production of large-amplitude noise in the shock would be compatible with the global scale of Pc 3, 4 range signals reported by Webb *et al.* [1977], but the model we are studying does not require it [Greenstadt, 1972].

#### DISCUSSION

The hourly distribution data supported the notion of  $\theta_{XB}$  as a factor correlating with the amplitude of micropulsation signal. The correlation was clearest for extreme conditions. That is, concentrations of  $\theta_{XB}$  above  $60^\circ$  were coupled with minimal pulsation signal; concentrations below  $30^\circ$  were coupled with distinctly enhanced pulsation signal. The data did not, however, indicate a straightforward connection between  $\theta_{XB}$  and  $\delta B$  in the sense of any functional relationship, since there was a wide assortment of distributions associated with any given range of amplitude. Thus it seems certain that at least one factor other than  $\theta_{XB}$  played a significant role in linking the solar wind to Pc phenomena. One such factor, solar wind velocity, has already been shown to be important [Singer *et al.*, 1977].

The evidence presented in this report does strongly support the result previously enunciated that signals of Pc 3 periods followed the same pattern as signals of Pc 4 periods, tending to be enhanced when  $\theta_{XB}$  was low, although cases of large amplitudes also occurred when the IMF was near the nominal stream angle. The distinction between Pc 3 and Pc 4 reported by some observers [Bol'shakova and Troitskaya, 1968; Kovner, 1974] was not apparent here.

The result of this study brings the advent of micropulsation diagnostics of the solar wind a little closer, albeit crudely. The following rules were implied, with reasonable confidence, by these data:

1. If in a given hour no signal is recorded above  $1.0 \gamma$  in the Pc 3 band or  $1.5 \gamma$  in the Pc 4 band peak to peak on the ground (at Calgary), it is improbable (9 cases in 94) that the IMF has been oriented within  $30^\circ$  of the solar wind flow more than 12 min out of the hour.
2. If in a given hour no (Pc 3) signal above  $1.0 \gamma$  or no (Pc 4) signal above  $1.5 \gamma$  is recorded, it is highly improbable (1 case in 94) that the IMF has been aligned within  $10^\circ$  of the solar wind flow more than 6 min out of the hour.
3. If in a given hour Pc 3 amplitude reaches above  $2 \gamma$ , and Pc 4 amplitude above  $3 \gamma$ , it is virtually assured (74 cases in 82) that the IMF has been within  $60^\circ$  of the solar wind flow for at least 12 min out of the hour.

4. If in a given hour Pc 3 amplitude reached above  $2 \gamma$  or Pc 4 amplitude above  $3 \gamma$ , there is an even chance (42 cases in 82) that the IMF has been aligned within  $30^\circ$  of the solar wind flow at least 6 min out of the hour and better than one chance in three (31 cases in 82) that the IMF has been within  $30^\circ$  of the solar wind flow at least 12 min out of the hour.

These results clearly imply that dissection of the underlying angular distributions provides a considerable improvement over hourly averages or hourly extremes of  $\theta_{XB}$  in studies of this type.

Rough as the suggested rules above may be, further quantification, finer diagnosis, generalization to other surface observation points, and clues to theoretical description of the micropulsation transfer process seem to be coming within reach.

**Acknowledgments.** This study was supported in part by AFOSR contract F 49620-77-C-0018 and the National Research Council of Canada.

The Editor thanks L. J. Lanzerotti and C. T. Russell for their assistance in evaluating this paper.

#### REFERENCES

- Arthur, C. W., R. L. McPherron, and W. J. Hughes, A statistical study of Pc 3 magnetic pulsations at synchronous orbit, *ATS 6, J. Geophys. Res.*, **82**, 1149, 1977.
- Barker, M. D., L. J. Lanzerotti, M. F. Robbins, and D. C. Webb, Azimuthal characteristics of hydromagnetic waves near  $L = 4$ , *J. Geophys. Res.*, **82**, 2879, 1977.
- Bol'shakova, O. V., and V. A. Troitskaya, Relation of the interplanetary magnetic field direction to the system of stable oscillations, *Dokl. Akad. Nauk SSSR*, **180**, 4, 1968.
- Greenstadt, E. W., Field-determined oscillations in the magnetosheath as possible source of medium-period, daytime micropulsations, in *Proceedings of the Conference on Solar Terrestrial Relations*, p. 515, University of Calgary, Calgary, Alberta, 1972.
- Greenstadt, E. W., Phenomenology of the earth's bow shock system, A summary description, in *Magnetospheric Particles and Fields*, edited by B. M. McCormac, p. 13, D. Reidel, Hingham, Mass., 1976.
- Greenstadt, E. W., and J. V. Olson, Pc 3, 4 activity and interplanetary field orientation, *J. Geophys. Res.*, **81**, 5911, 1976.
- Greenstadt, E. W., and J. V. Olson, A contribution to ULF activity in the Pc 3-4 range correlated with IMF radial orientation, *J. Geophys. Res.*, **82**, 4991, 1977.
- Gul'elmi, A. U., Diagnostics of the magnetosphere and interplanetary medium by means of pulsations, *Space Sci. Rev.*, **16**, 331, 1974.
- Kovner, M. S., Pc 2-4 pulsations and low frequency oscillations in the solar wind ahead of a shock wave front, *Geomagn. Aeron. USSR*, **XIV**, 725, 1974.
- Noury, G. R., Interplanetary magnetic field, solar wind and geomagnetic micropulsations, Ph.D. thesis, Univ. of Brit. Columbia, Vancouver, 1976.
- Singer, H. J., C. T. Russell, M. G. Kivelson, E. W. Greenstadt, and J. V. Olson, Evidence for the control of Pc 3, 4 magnetic pulsations by the solar wind velocity, *Geophys. Res. Lett.*, **4**, 377, 1977.
- Troitskaya, V. A., T. A. Plyasova-Bakunina, and A. V. Gul'elmi, Relationship between Pc 2-4 pulsations and the interplanetary magnetic field, *Dokl. Akad. Nauk SSSR*, **197**, 1312, 1971.
- Webb, D., and D. Orr, Geomagnetic pulsations (5-50 mHz) and the interplanetary magnetic field, *J. Geophys. Res.*, **81**, 5941, 1976.
- Webb, D., L. J. Lanzerotti, and D. Orr, Hydromagnetic wave observations at large longitudinal separations, *J. Geophys. Res.*, **82**, 3329, 1977.

(Received March 16, 1978;  
revised July 31, 1978;  
accepted August 7, 1978.)

**APPENDIX C**

**IMF ORIENTATION, SOLAR WIND VELOCITY, AND PC 3-4 SIGNALS:  
A JOINT DISTRIBUTION**

## IMF ORIENTATION, SOLAR WIND VELOCITY, AND Pc 3-4 SIGNALS: A JOINT DISTRIBUTION

Eugene W. Greenstadt

Space Sciences Department, TRW Defense and Space Systems Group, Redondo Beach, California 90278

Howard J. Singer and Christopher T. Russell

Institute of Geophysics and Planetary Physics, University of California, Los Angeles, California 90024

John V. Olson

Institute of Earth and Planetary Physics, University of Alberta, Edmonton, Alberta, Canada T6G2J1

**Abstract.** Separate studies using the same micropulsation data base in the period range 10-150 s have shown earlier that signal levels recorded during September, October, and November 1969 at Calgary correlated positively with both solar wind alignment of the IMF and solar wind speed, but each correlation contained enough scatter to allow for influence of the other factor. In this report, joint correlations of velocity and field direction with parameters representing hourly distributions rather than minima of IMF orientation angle display the relative effect of the two agents on magnetic pulsation signal levels. The joint correlations reduce the overall scatter and show that solar wind speeds above 200-300 km/s and angles between the IMF and the sun-earth line of less than  $50^\circ$ - $60^\circ$  are associated with enlarged magnetic pulsation amplitudes. These threshold effects tend to support both the bow shock origin and the Kelvin-Helmholtz amplification of daytime signal transients in the Pc 3, 4 period ranges.

## Introduction

In separate examinations of the same magnetic pulsation observations recorded at Calgary Observatory, Greenstadt and Olson [1976, 1977] and Singer et al. [1977] demonstrated correlations between interplanetary magnetic field (IMF) direction and the amplitude of Pc 3, 4 signals ( $\delta B$ ) and between solar wind speed ( $V_{sw}$ ) and  $\delta B$ . The IMF correlations supported some, but not all, of the same relationships reported earlier by Soviet researchers [Bol'shakova and Troitskaya, 1968; Plyasova-Bakunina, 1972], who had worked with selected Pc 3 and Pc 4 wave train events rather than unselected signal levels. More pointedly for the motivation of this study, the results of Greenstadt and Olson lent mild support to the prospect that transient enhancements of signal in the Pc 3, 4 period range were related to the transfer of large-amplitude shock pulsations from the subsolar bow shock to the midday magnetopause. Studies by Webb and Orr [1976] and Webb et al. [1977], conducted in parallel with our own, found correlations of IMF component changes with global pulsation events that were compatible, although not identical, with the statistical correlations we reported earlier.

Meanwhile, the velocity correlation of Singer et al. supported the prospect that the same Pc 3,

4 signals were related to excitation and amplification of perturbations at the magnetopause via the Kelvin-Helmholtz instability, whose influence would depend on  $V_{sw}$ .

Clearly, it is desirable to determine whether the IMF or the  $V_{sw}$  correlation is the 'true' one or whether both are before placing confidence in either. The angle  $\theta_{XB} = \arccos(\cos \lambda_B \cos \phi_B)$ , where  $\lambda_B$  and  $\phi_B$  are the solar ecliptic latitude and longitude of the IMF, respectively, was used in the cited reports as the measure of IMF orientation. Since in the solar wind,  $\tan \phi_B \propto 1/V_{sw}$ , we have  $\cos \theta_{XB} = V_{sw} \cos \lambda_B / (V_{sw}^2 + k^2)^{1/2}$ , where  $k$  is a proportionality constant, and one correlation could have been deterministically controlled by the other. Also, the scatter in either correlation was more than enough to have incorporated the effects of the other variable if two independent mechanisms were indeed present, and it would be desirable to separate the influence of both while improving the coherence of each.

In this report we show that  $\theta_{XB}$  and  $V_{sw}$  appear to have operated independently on  $\delta B$ , each in a manner consistent with the mechanism though to be responsible for its correlation. We remind the reader that the angle  $\theta_{XB}$  is thought to affect the stimulation of daytime magnetic pulsations when the IMF  $B$  is less than about  $50^\circ$ , unaberrated, or perhaps  $60^\circ$  from the sun-earth line, allowing for solar wind aberration, by providing a quasi-parallel bow shock structure in the subsolar region delivering large-amplitude magnetic oscillations directly to the magnetopause. The designation 'pulsations of shock origin' (PSO) has been suggested. The solar wind speed is thought to promote the generation of pulsations in the magnetosphere by supporting amplification of PSO's (or any other perturbations) at the magnetopause when  $V_{sw}$  is above a threshold criterion associated with the Kelvin-Helmholtz instability.

## Data

**Sources.** The data set described here was recorded in September, October, and November 1969. Magnetic pulsation data from Calgary were passed through digital filters that separated the Pc 3 ( $T = 10$ -45 s) and Pc 4 ( $T = 45$ -150 s) bands, and the maximal amplitude in X or Y in each band in each daylight hour was chosen to represent the hour's activity. IMF data were obtained from a tape recording of Explorer 35 82-s averages. Solar wind velocities were represented by hourly averages from the composite Solar Wind Plasma

Copyright 1979 by the American Geophysical Union.



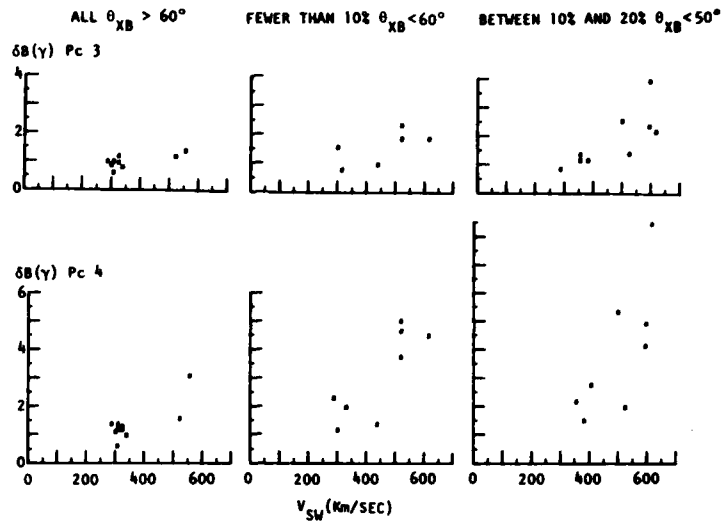


Fig. 1. Development of pulsation versus velocity correlation with small relaxation of unfavorable angular distributions. Panels show hourly maximal amplitude  $\delta B$  of pulsations versus average solar wind velocity  $V_{SW}$  for (top) Pc 3 and (bottom) Pc 4.

Data Set supplied by the National Space Science Data Center.

Additional details of the sources, processing, and characteristics of the data can be found in earlier reports cited in the introduction.

**Method.** The key to separation of velocity from field orientation effects was an improvement in methodology introduced by Greenstadt and Olson

[1978], who examined the actual distributions of  $\theta_{XB}$  within each hour's worth of data. In previous papers the hourly behavior of the IMF direction had been characterized by finding the lowest value of  $\theta_{XB}$  recorded for the hour. The idea behind this selection of 'minimal  $\theta_{XB}$ ' was that transient enhancements, and hence hourly maxima, of  $\delta B$  could have been produced by transient rota-

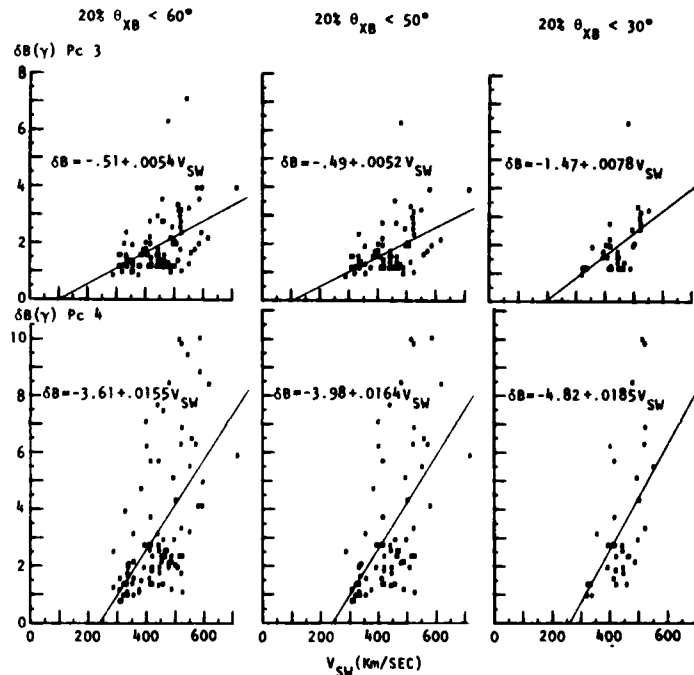


Fig. 2. Further development of pulsation versus velocity correlation with increasingly favorable angular distributions (same format as Fig. 1). Equations describe least squares straight lines.

tions of  $\delta B$  close to the solar wind flow line. However, it may be argued that the magnetosphere might require some minimal time interval to respond to a perturbation at its boundary and, moreover, that a properly filtered version of the Pc 3, 4 channels would not produce a significantly enlarged  $\delta B$  unless at least a few cycles worth of signal of the appropriate period were allowed for. It seemed reasonable that the large scatter in earlier correlations, much of which was visible as low  $\delta B$  when presumably favorable  $\theta_{XB}$  prevailed, could have resulted from hourly minima of  $\theta_{XB}$  representing only a single point or so few points that no magnetospheric response could have been registered. We therefore took advantage of the hourly distributions of  $\theta_{XB}$  computed by Greenstadt and Olson [1978] to characterize  $\theta_{XB}$  according to the percentage of values that fell below a given angle.

#### Inquiry

Did the velocity effect depend on angle? Fig. 1 shows three groups of amplitude versus velocity data, left to right, divided according to the extent of influence  $\theta_{XB}$  might be expected to have at a statistically marginal level. In progressing from left to right, cases were selected in which an increasing, but small, fraction of the hourly distributions of  $\theta_{XB}$  dropped below the postulated cutoff criterion,  $\theta_{XB} = 60^\circ$ , above which significant Pc signals are presumed to have been suppressed for any likely direction of  $V_{SW}$ .

At left, no hours are included in which any  $\theta_{XB}$  was less than  $60^\circ$  and only one point in either the Pc 3 or the Pc 4 band was significantly above background amplitude. In the center, hours when only a few, i.e., less than 10% of the  $\theta_{XB}$  were below  $60^\circ$  are included, yet the amplitude-velocity dependence has begun to emerge in both bands. At the right, hours with a similar small percentage of  $\theta_{XB}$  below  $50^\circ$  are included, and a sharp amplitude-velocity dependence has become unmistakable for both Pc 3 and Pc 4 signals.

Note that even at low velocities of about 300 km/s, only one or two points in the center and right pairs of panels were held to the low amplitudes imposed when all  $\theta_{XB} > 60^\circ$ , as at left. Thus the amplitude versus solar wind velocity correlation articulated by Singer et al. [1977] appeared to emerge when permitted to do so by marginal violation of the condition under which the IMF orientation is expected to block PSO excitation.

In Fig. 2 we look, from left to right, at the  $\delta B$ - $V_{SW}$  correlation for angle distributions increasingly encouraging to Pc 3-4 signal generation. The lines in the panels are linear least squares fits to the plotted points. As an overall generality, the more favorable the angular distribution, i.e., the lower the angle below which 20% of the hourly  $\theta_{XB}$  values fell, the less scatter and the more pronounced the correlations. This effect was largely caused by increasing reduction, left to right, in the proportion of low  $\delta B$  at high  $V_{SW}$ . Thus the more favorable the angular distribution, the more pronounced the velocity correlation, by decimation of the lower right-hand corner of the scattered points. This development is carried to its extreme in Fig. 3, where the scatter diagrams are shown for what

should have been extraordinarily favorable circumstances as far as  $\theta_{XB}$  was concerned. The dependence of  $\delta B$  on  $V_{SW}$  was at its sharpest when more than half the hourly  $\theta_{XB}$  values were less than  $30^\circ$  from alignment with the SE X axis (the solar wind).

#### Did the angular effect depend on velocity?

This question is already answered in part by Fig. 3. If under such favorable (statistical) conditions of  $\theta_{XB}$ , as were selected there, all  $\delta B$  were not well above background regardless of  $V_{SW}$ , then it is clear that it was also necessary for  $V_{SW}$  to have been favorable, that is, high, in order to produce enlarged magnetic pulsation signals at Calgary.

A more direct demonstration appears in Fig. 4, where we now look at the dependence of amplitude on angle. We have followed our own advice here for the best presentation of the angle effect [Greenstadt and Olson, 1977] and plotted  $\delta B$  versus  $\cos \theta_{XB}$  rather than  $\theta_{XB}$ . The abscissae represent the cosine of the angle below which 20% of the  $\theta_{XB}$  were recorded continuously for each hourly distribution. In this way, hours were excluded when rotations of  $B_{SW}$  toward the X axis were only momentary, even though several such rotations might have added up to 20% of the  $\theta_{XB}$  for the hour. This exclusion was made to assure that the magnetosphere had time to respond with a Pc 4 signal of, say,  $T = 150$  s, which would develop five complete cycles in a 12-min (20%) interval.

The figure shows the overall tendency, throughout the  $\cos \theta_{XB}$  scale, for points in the high-velocity plots to mark values of  $\delta B$  well above

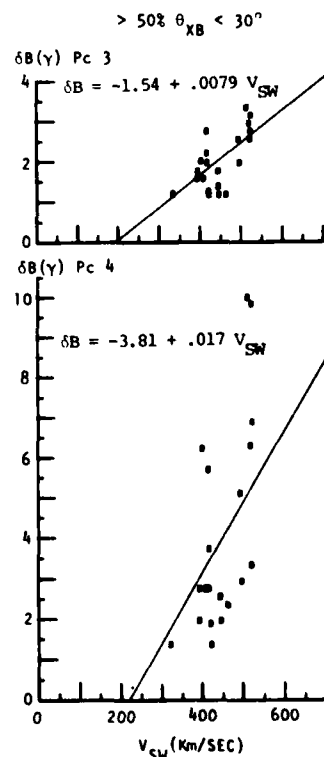


Fig. 3. Fully exposed  $\delta B$  versus  $V_{SW}$  correlations for hours of very favorable angular distributions.

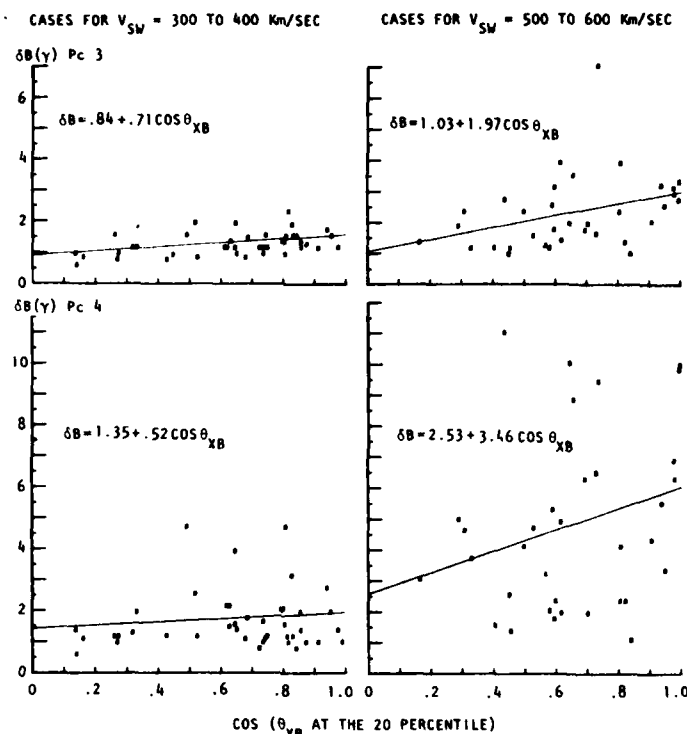


Fig. 4. Contrasting correlations of  $\delta B$  versus  $\cos \theta_{XB}$  for hours of (left) low  $V_{SW}$  and (right) high  $V_{SW}$ . (Top) Pc 3. (Bottom) Pc 4. The horizontal scales refer to the cosine of the angle below which 20% of each hour's  $\theta_{XB}$  was observed.

those at corresponding  $\theta_{XB}$  in the low-velocity plots. This general elevation of amplitudes on the right affirms the importance of solar wind velocity in the mechanism that brought Pc 3, 4 signals to the Calgary sensors. Especially significant, however, was the contrast between the slight upward trend of  $\delta B$  with  $\cos \theta_{XB}$  for cases in which  $V_{SW}$  was at the low end of its range, at left, and the more pronounced upward trend when  $V_{SW}$  was near the high end of its range, at right. It thus appears that elevated solar wind velocity was a necessary factor in enabling the amplitude-angle correlation to operate, just as the temporary rotations of  $B_{SW}$  for which a few minutes of  $\theta_{XB}$  were below  $50^\circ$  or  $60^\circ$  (Fig. 1) were necessary to expose the amplitude-velocity correlation.

Were thresholds indicated? The patterns of points in Fig.'s 1-3 and the positive horizontal intersects of the best fit lines in Fig. 2 indicate quite clearly that there was a velocity below which no significant  $\delta B$  could have been expected. The most favorable angular selections, namely, those that should have allowed the 'real' velocity correlation to appear with the least admixture of unfavorable cases, were in Fig. 3 and in the right panels of Fig. 2. These plots suggest that the minimal  $V_{SW}$  for certifiable Pc 3, 4 signals at Calgary was in the neighborhood of 250-350 km/s.

The patterns of Fig. 1 suggest, albeit weakly, that some  $\theta_{XB}$  below about  $60^\circ$  had to occur in order that significant pulsation amplitudes be recorded. Obviously, the necessity of representing hourly IMF orientations as a bivariate quantity involving both  $\theta_{XB}$  and a percentage distribu-

tion at  $\theta_{XB}$  makes detection of any single threshold level of angle rather more difficult than in the case of velocity, which tends to remain nearly constant during most hours and hence representable by one number. It is not therefore surprising that Fig. 4 fails to exhibit any clear value of  $\cos \theta_{XB}$  dividing high  $\delta B$  from low. There could conceivably be a different threshold  $\theta_{XB}$  for each percentile or for only a single, 'right' percentile or a threshold percentile for a particular  $\theta_{XB}$ , etc.

However, in Fig. 5 we follow the guidance of Fig. 1 and look again, in the same format as in Fig. 4, at the distributions of  $\delta B$  versus  $\cos \theta_{XB}$  for  $\cos \theta_{XB}$  at the 10% instead of the 20% level. Presumably, if there were a threshold, it would have been most evident under slight relaxation of the cutoff condition. There is indeed some indication, in three of the four panels of Fig. 5 (all but that at upper left), that high  $\delta B$  occurred only to the right of an imaginary vertical line at about the middle of each horizontal scale. We consider it particularly noteworthy that with the exception of a single point, every point in either right-hand panel that exceeded all points in the corresponding left-hand panel occurred when  $\cos \theta_{XB} \geq 0.62$ , or  $\theta_{XB} \leq 51^\circ$ . The dashed lines outline this behavior. It is thus suggested that truly heroic levels of  $\delta B$  were attained at high velocities only when some  $B_{SW}$  happened to rotate within about  $50^\circ$  of the solar wind flow direction. Such behavior would be entirely consistent with the postulated requirement that quasi-parallel shock pulsations in the subsolar region supply the

Pc 3-4 excitation mechanism. The subsolar point of the bow shock assumes a quasi-parallel structure when  $\theta_{XB} \leq 50^\circ$ .

#### Summary

In our view, all three issues raised in the inquiry section above were answered in the affirmative. The most self-evident correlations were in amplitude versus velocity, but the correlations were strongest for the most favorable distributions of angle and appeared to require some favorable angles to emerge at all. The correlations of amplitude versus angle were more apparent at high velocity than at low, and amplitudes in general were elevated at the highest velocities over those at the lowest velocities. Finally, there was evidence that between  $50^\circ$  and  $60^\circ$  there was a threshold above which  $\theta_{XB}$  did cut off any amplitude correlation with velocity, while it was abundantly clear that velocities below about 300 km/s would be correlated only with insignificant amplitudes regardless of angle.

Fig. 6 summarizes the overall trends in a pair of schematic three-dimensional drawings in which the various correlations are represented by the best fit straight lines, at the 20% level, of Fig.'s 2 and 4. Other combinations of percentile and velocity grouping would have produced different outlines with the same general tendencies, some weaker, some stronger, and we would not em-

phasize the quantitative content of these drawings until it is confirmed by additional data.

#### Discussion

The angle threshold of about  $50^\circ$ - $60^\circ$ , the tightened correlation of  $\delta B$  versus  $V_{SW}$  when many  $\theta_{XB} \leq 30^\circ$ , and the  $\delta B$  versus  $\cos \theta_{XB}$  correlations were consistent with the hypothesis that quasi-parallel shock oscillations in the subsolar region supply perturbations to the midday magnetopause that can be transferred to the surface as pulsations in the Pc 3, 4 period bands. At the same time the  $\delta B$  versus  $V_{SW}$  correlations, with their cutoff of significant  $\delta B$  at about 200-300 km/s, were consistent with the amplification of perturbations at the magnetopause by the Kelvin-Helmholtz mechanism: Boller and Stolov [1970, 1973] have shown that increased solar wind velocities should produce increased magnetospheric disturbance according to a Kelvin-Helmholtz stability criterion. Velocities above a threshold determined by certain MHD parameters of the plasmas on either side of the magnetopause should produce wave growth. In their investigation, Boller and Stolov [1973] found positive support for the threshold effect in satellite data, and their tables indicated a minimal solar wind velocity over many cases of about 300 km/s or a bit less.

The instability criterion they cited is independent of frequency, so it should apply equally

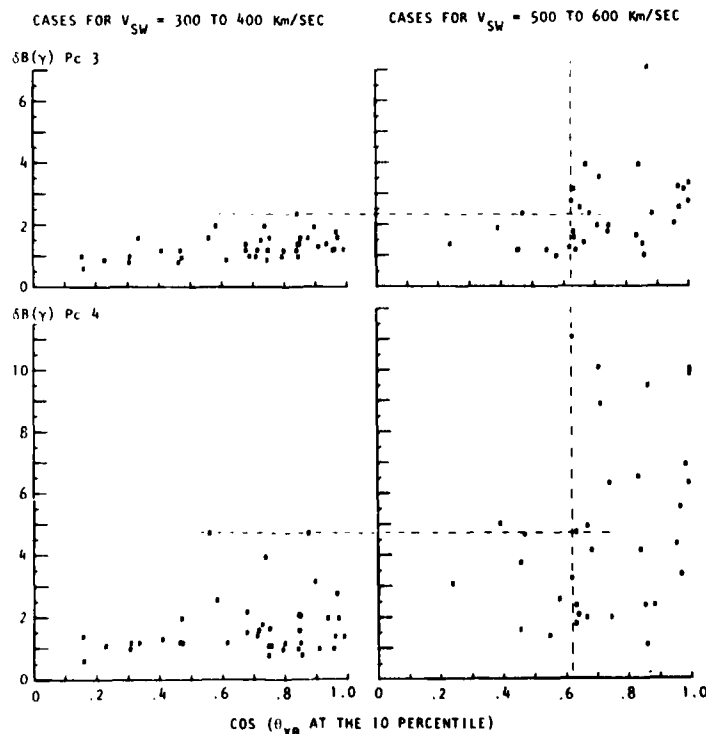


Fig. 5. Same as Fig. 4, but the horizontal scales refer to the cosine of the angle below which 10% of each hour's  $\theta_{XB}$  was observed. The horizontal dashed lines mark the highest points observed at low speed, at left. The vertical dashed lines emphasize that at high speed, at right, all values of  $\delta B$  above the horizontal line (except one) occurred for  $\cos \theta_{XB} \geq 0.61$ .

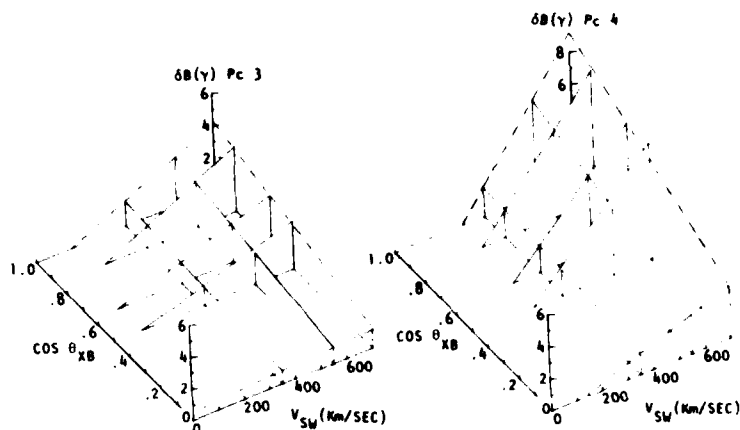


Fig. 6. Diagrammatic summary of joint  $\delta B$  versus  $\cos \theta_{XB}$  and  $V_{SW}$  correlations, represented by combining the two-dimensional straight-line fits of Fig.'s 2 and 4.

to Pc 3 and Pc 4 and, for that matter, to Pc 5 signals, if we ignore possible dispersion and resonance affecting delivery of the signals to the surface. The data of the present study therefore support the applicability of the Kelvin-Helmholtz criterion in still another way: the stronger was the  $\delta B$ - $V_{SW}$  correlation, the closer to one another were the two  $\delta B = 0$  cutoffs of the Pc 3 and Pc 4 scatter plots. The differences between the crossings of the  $\delta B = 0$  axis by the Pc 4 and Pc 3 least squares lines for  $20\% \theta_{XB} < 60^\circ$ ,  $50^\circ$ , and  $30^\circ$  (Fig. 2) and for  $50\% \theta_{XB} < 30^\circ$  (Fig. 3) were 138, 148, 72, and 27 km/s, respectively. Hence the data imply that when the angles were sufficiently favorable to expose the most reliable  $\delta B$ - $V_{SW}$  correlations, the Pc 3 and Pc 4 signal thresholds occurred close to a common minimal solar wind velocity, as the Kelvin-Helmholtz criterion would suggest. In Figure 3, incidentally, the two least squares lines would cross at  $V_{SW} = 250$  km/s, where  $\delta B = 0.44 \gamma$ , a little below the putative instrument sensitivity.

One of the main sources of weakness in the correlations shown here was the presence of too many low  $\delta B$  at both high velocity and small angle; i.e., enhanced signals often failed to appear under what should have been the most favorable circumstances. Although there was much improvement over earlier scatter diagrams, we suspect the most probable single cause of this 'non-response' was the location of Calgary Observatory under the plasmopause, where relatively small changes in magnetospheric geometry could have removed the stations from the best signal path. An expanded data set soon to be studied should resolve this issue.

For the present the data support the notion that PSO's were identifiable phenomena in the Pc 3 and 4 period ranges during the interval described in this and its preceding reports.

**Acknowledgments.** This work was supported by AFOSR contract F 49620-77-C-0018 (at TRW), NSF grant DES 74-23464, and NASA grant NGR 05-007-004 (at UCLA) and the National Research Council of Canada (at the University of Alberta). Discussions with R. L. McPherron and L. J. Lanzerotti were valuable.

The Editor thanks C. W. Arthur for her assistance in evaluating this brief report.

#### References

- Boller, B. R., and H. L. Stolor, Kelvin-Helmholtz instability and the semi-annual variation of geomagnetic activity, *J. Geophys. Res.*, **75**, 6073, 1970.
- Boller, B. R., and H. L. Stolor, Explorer 18 study of the stability of the magnetopause using a Kelvin-Helmholtz stability criterion, *J. Geophys. Res.*, **78**, 8078, 1973.
- Bol'shakova, O. V., and V. A. Troitskaya, Relation of the interplanetary magnetic field direction to the system of stable oscillations *Dokl. Akad. Nauk SSR*, **180**, 4, 1968.
- Greenstadt, E. W., and J. V. Olson, Pc 3, 4 activity and interplanetary field orientation, *J. Geophys. Res.*, **81**, 5911, 1976.
- Greenstadt, E. W., and J. V. Olson, A micropulsation contribution in the Pc 3-4 range correlated with IMF radial orientation, *J. Geophys. Res.*, **82**, 4991, 1977.
- Greenstadt, E. W., and J. V. Olson, Correlation of geomagnetic pulsation signals in the 10- to 150-s period range with concentration of IMF orientations near the sun-earth line, submitted to *J. Geophys. Res.*, 1978.
- Plyasova-Bakunina, T. A., Effect of the interplanetary magnetic field on the characteristics of Pc 3-4 pulsations, *Geomagn. Aeron.*, **12**, 675, 1972.
- Singer, H. J., C. T. Russell, M. G. Kivelson, E. W. Greenstadt, and J. V. Olson, Evidence of the control of Pc 3, 4 magnetic pulsations by the solar wind velocity, *Geophys. Res. Lett.*, **4**, 377, 1977.
- Webb, D., and D. Orr, Geomagnetic pulsations (5-50 mHz) and the interplanetary magnetic field, *J. Geophys. Res.*, **81**, 5941, 1976.
- Webb, D., L. J. Lanzerotti, and D. Orr, Hydromagnetic wave observations at large longitudinal separations, *J. Geophys. Res.*, **82**, 3329, 1977.

(Received August 17, 1978;  
revised October 2, 1978;  
accepted October 3, 1978)

**APPENDIX D**

**THE SOLAR WIND AND MAGNETOSPHERIC WAVES**

30435-6006-RU-00

THE SOLAR WIND AND MAGNETOSPHERIC WAVES

by

Eugene W. Greenstadt  
Space Sciences Department  
TRW Defense & Space Systems Group  
One Space Park  
Redondo Beach, California 90278

March 1979

Summary of Report delivered to International Workshop on  
Selected Topics of Magnetospheric Physics, Tokyo,  
March 13-16, 1979.

**TRW**  
DEFENSE AND SPACE SYSTEMS GROUP

## THE SOLAR WIND AND MAGNETOSPHERIC WAVES

## ABSTRACT

Observations have supported but not proved the postulate that the stimulation of medium-period geomagnetic pulsations occurs in the interaction between the solar wind and the geomagnetic field. Both IMF orientation and the solar wind speed have been demonstrated to correlate with the level of pulsation activity. Although the correlations are not yet free of substantial variability caused by other factors, probably both physical and methodological, they provide some insight into the shortcomings of existing theoretical formulations, the appropriate direction of further observational analysis, and the operation of magnetospheric processes.



## INTRODUCTION

In the following paragraphs, the current state of development and credibility of the principal models connecting the solar wind to midperiod ( $T = 10-300$  sec), daytime, geomagnetic pulsation signals, i.e., Pc 3,4,5, is summarized. The term signals is deliberately chosen to emphasize interest in wave energy in the bands of interest, meant to include, but not be limited to, traditional monochromatic, or quasi-periodic pulsation events. Selected, rather than exhaustive, references are given, and suggestions for future steps are enunciated.

## PULSATION MODELS

Models of midperiod, geomagnetic pulsations can be divided into two broad categories: *internal* and *external*. Internal models account for pulsations in terms of processes within the magnetosphere, where opportunities exist, for example, at the plasmapause boundary, for generating oscillations through local instabilities. External models attribute pulsations to forces outside the magnetosphere because circumstantial evidence links their habits of occurrence to properties of the solar wind.

Each model-category in turn can rest on either of two factors, or both, in making its case: stimulation or control. Oscillations may be generated in one regime, say at the magnetopause, but the ingredients required to activate the generation, or to transfer it to the earth's surface, for example, a resonant amplification, may be controlled by the other regime.

Table 1 displays the foregoing classification scheme, listing sample items in each subcategory. The crossed arrows at the center indicate the interplay between stimulation and control that may exist among various items.

Table 1. Classes of Models of Mid-Period  
(10-300 sec, Pc3-5) Geomagnetic  
Pulsations

	Internal	External
Stimulation	Gradient Instabilities Plasmopause Radiation Belt Mixed Particle Populations	Surface Waves Signals
Control	Resonance Transmission Attenuation	Injection Parametric state of solar wind

The ensuing remarks will be devoted exclusively to the external models, with the particular intent of outlining their present status and future prospects.

#### STATUS OF EXTERNAL MODELS

Figure 1 is an attempt to illustrate schematically both the conceptual logic of the two well-developed, externally-oriented models and the current state of attempts to verify them by observation. The vertical stages of the drawing, labeled from the top, Solar Wind, Foreshock, Magnetosheath, etc., represent distinct regimes forming the plasma-physical chain linking the solar wind with the earth's surface. There are others, such as ionosphere and polar cusp, omitted because they do not play a distinctly designated role in either model. The various stages are linked by lines of different types, as explained in the figure, and below.

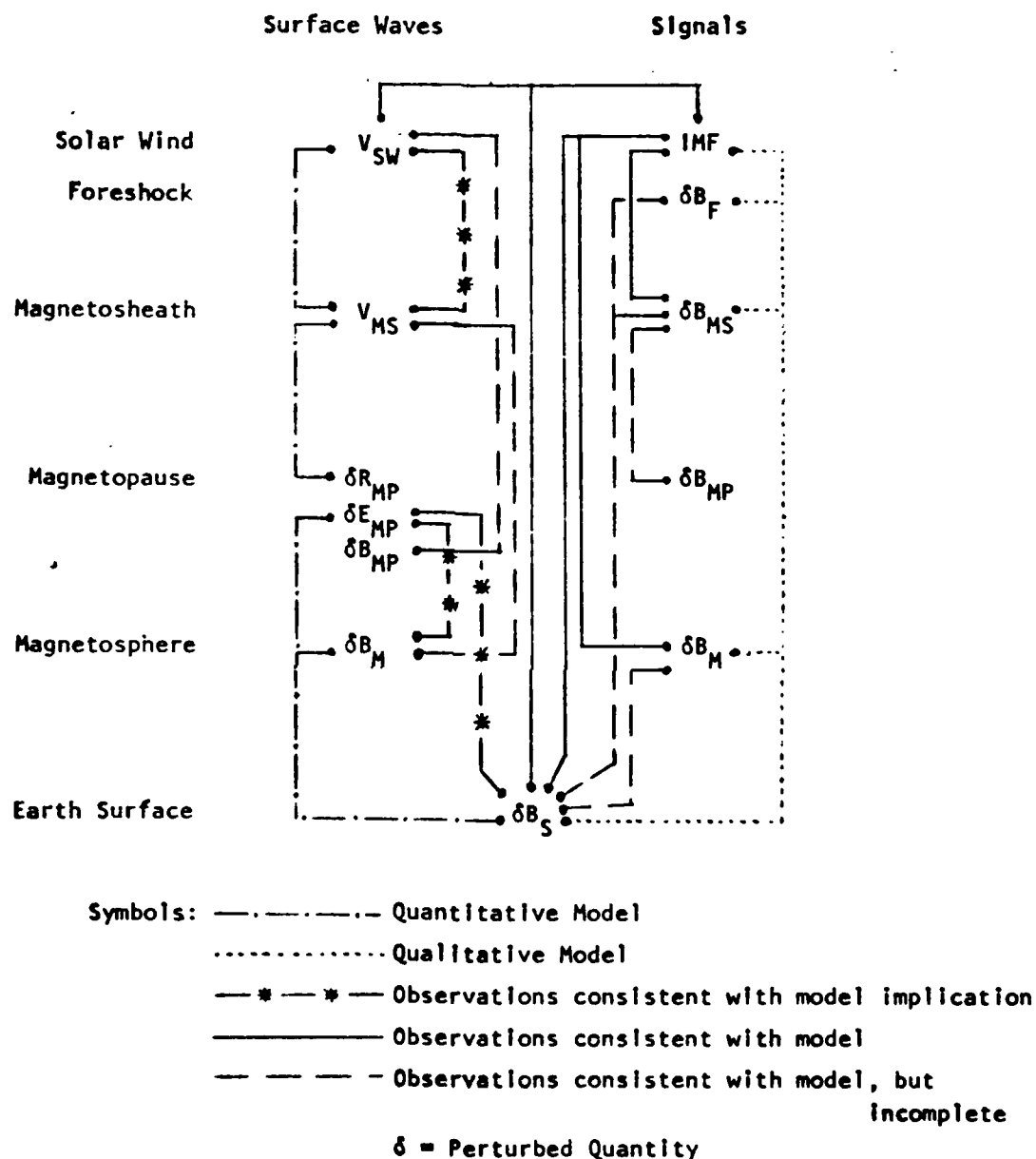


Figure 1. Status of external model verification. Symbolic connections indicate, outside the lettered columns, the physical steps making up the respective models, and, between the lettered columns, the qualities of observational evidence connecting the physical steps. Verification of either model will require solid lines in the same pattern as outside connections.

At far left and right of the diagram, the logical connections needed to operate the respective models are shown, i.e., each indicated connection or subconnection is a necessary part of its model's physical operation and must be separately verified by observation, preferably at the same time as every other, to validate the model. The central lines summarize the experimental situation that presently attends either model. In the following paragraphs, the two columns are described one-by-one.

Surface waves. The surface-wave, or Kelvin-Helmholtz model, at left, begins with fluid-like waves at the magnetopause. The waves arise because the modified solar wind in the innermost magnetosheath flows along the relatively stationary magnetopause, like wind over water. Small surface waves are amplified when the outside velocity  $V_{MS}$  exceeds a critical value, and their wave properties are transferred through the magnetosphere to the surface subject to appropriate local and global propagation laws, including not inconsiderable attenuation. Along the way, however, conditions surrounding one or another of the finite geomagnetic field lines may provoke resonance, selecting out a particular period, or band of periods, thus creating an enlarged amplitude, monochromatic oscillation that can appear at the foot of the corresponding line as a traditional geomagnetic pulsation. The locus-dependent sheath velocity (and other parameters, like density) is tied to the solar wind velocity by fluid theory (Spreiter and Alksne, 1969); the Kelvin-Helmholtz conditions, the waves' connection with the magnetosphere, and the resonances of the latter, have been developed in a large body of theoretical papers of which only a sampling is referenced here (Sen, 1965; Radoski, 1966; Atkinson and Watanabe, 1966; Southwood, 1968; Chen and Hasegawa, 1974; Lanzerotti et al., 1974).

The surface wave model has been supported experimentally, in parts, but by no means established in total: the magnetosheath's plasma flow velocities  $V_{MS}$  have been related to  $V_{SW}$  in reasonable conformity with theory in the steady state (Wolfe and McKibbin, 1968; Howe and Binsack, 1972); the solar wind velocity  $V_{SW}$  has been related to field variability at the magnetopause,  $\delta B_{MP}$ , but not necessarily to surface waves  $\delta R$ , by inference of  $V_{MS}$  and estimation of local Kelvin-Helmholtz critical velocities at the magnetopause (Boller and Stolov, 1973);  $V_{MS}$ , estimated on the basis of constant  $V_{SW}$ , has been related to  $\delta B_M$  just inside the magnetosphere through estimated Kelvin-Helmholtz critical velocities (Wolfe and Kauffman, 1975); perturbations of the magnetopause resembling surface waves propagating with  $V_{MS}$  have been identified (Aubry et al., 1971); theoretically-predicted polarization characteristics of waves propagating through the magnetosphere from waves defined at the magnetopause by their electrical perturbation  $\delta E_{MP}$  (Southwood, 1974), have been recorded at synchronous orbit (Arthur et al., 1977c; Hughes et al., 1978) and on the ground (Samson et al., 1971; Lanzerotti et al., 1972; Olson and Rostoker, 1978); and at both, simultaneously (Arthur and McPherron, 1977a); solar wind velocity has been positively correlated with ground pulsations (Saito, 1964; Singer et al., 1977). It is important to mention that most of the cases analyzed by Lanzerotti et al. (1972) gave polarization behavior contrary to that predicted by Southwood (1974), but consistent with Chen and Hasegawa (1974) (Lanzerotti et al., 1974).

Signals. The signal transfer model, at the right of Figure 1, is based on the idea that waves of tens of seconds period already present in the modified solar wind of the magnetosheath should, by driving the magnetopause, or penetrating it, make their presence known in the magnetosphere where continuing waves, or similar waves, excited at similar periods, would appear at the earth

as traditional midday geomagnetic pulsations. The notion arose from observations that, subject to local orientation of the IMF, the bow shock and magnetosheath can contain, or consist of, large amplitude magnetic pulsations of tens of seconds period that may occasionally, but not always, reach the magnetopause (Greenstadt, 1972). Since the same conditions that control the pulsation, now called quasi-parallel, shock also produce upstream waves (the foreshock) in the solar wind, it has also been suggested that these waves may simply propagate to the earth, regime by regime, in some way, left undefined, but including amplification at the bow shock (Kovner et al., 1976). Theory has provided for transfer of waves across the magnetopause, although not at very high efficiency (Wolfe and Kauffman, 1975).

The experimental situation is comparable to that of the surface wave model, namely, supportive in parts. The IMF does control the location and extent of quasi-parallel structure in the midday bow shock (Greenstadt et al., 1970), which becomes highly disturbed (Greenstadt et al., 1977); the disturbed magnetosheath can exhibit large quasi-periodic waves in the vicinity of the magnetopause (Greenstadt, 1972; Siscoe et al., 1967; Kauffman, 1970); the appropriate IMF orientation, namely  $\theta_{XB} \lesssim 50^\circ$ , where  $\theta_{XB}$  is the angle between the IMF and the X-axis (i.e., the solar wind direction), has been correlated with the occurrence of pulsation events and amplitude of signals at synchronous altitude (Arthur and McPherron, 1977b) and on the earth's surface (Troitskaya et al., 1971; Nourry, 1976; Greenstadt and Olson, 1977; Webb and Orr, 1976; Wolfe et al., 1978); specific upstream wave events have been correlated with specific pulsation events on the earth (Bol'shakova and Troitskaya, 1968; Nourry, 1976).

Note that the two external models are by no means mutually exclusive: the Kelvin-Helmholtz model requires an initial perturbation, and the signal model needs to get its perturbation across the magnetopause, preferably with amplification, or at least not too severely attenuated. Joint correlations of  $V_{SW}$  and  $\theta_{XB}$  with ground signals have suggested that both models could be operative simultaneously (Greenstadt et al., 1979; Wolfe et al., 1978).

In summary, neither of the two viable external models of geomagnetic pulsations has been verified. The best that can be said of both is that the correlations between  $V_{SW}$ ,  $\theta_{XB}$ , and  $\delta B_S$  leave no doubt that solar wind parameters play a role in control of pulsations. However, direct observations of each intermediate process will be necessary to demonstrate external stimulation of pulsations. Taken individually, the signal model has the advantage that no counterexamples have appeared, except what may be implicit in the large scatter in some of the referenced correlations. Much of the scatter was methodological and not unexpected. In the case of the surface wave model, there have been incompatible, but not contradictory, observations, depending on whether appropriate refinements of the model were employed.

#### EXTERNAL CONTROL

External control of pulsations actually generated by some internal mechanism can be just as intricate and difficult to verify as external stimulation. One example would be the possible triggering of instability in the magnetosphere by particle beams from the sheath. Quasi-parallel shock structure is accompanied by diffuse beams of suprathermal (several KeV) ions seen both in the sheath and upstream (West and Buck, 1976; Gosling et al., 1978). If

these energetic ions, under certain orientations of the IMF, have a pathway into the morning or midday magnetosphere, they might provide the means to drive an instability that would then produce waves and associated resonances in the Pc 3-5 period range.

A second example would involve a variable  $V_{SW}$ . The correlations between the IMF orientation and ground pulsations have been studied at a limited number of stations. Since Pc amplitudes tend to rise toward auroral latitude and also increase with magnetic activity and  $V_{SW}$ , and since the auroral latitude drops with activity, amplitudes at a fixed station may indeed increase statistically with  $V_{SW}$ , as observation has indicated, without implying anything about the mechanism of Pc stimulation at the magnetopause.

It may be assumed that further investigations of the external models will automatically separate the factors of stimulation and control.

#### WAVES IN THE MAGNETOSPHERE

Either of the external models is tied to questions of what the properties governing waves are in the magnetosphere, at least in the dayside. The Kelvin-Helmholtz model, for examples, has already raised some unresolved issues. Figure 2a shows an equatorial cross section of the magnetopause, with surface waves beginning about where theory predicts they should, and observation has inferred they do (Boller and Stolov, 1973; Wolfe and Kauffman, 1975), i.e., about  $40^\circ$  on either side of the sun-earth line. The surface waves presumably propagate, and grow, in the direction of  $V_{MS}$ . If waves seen to propagate in the magnetosphere and on the ground, east and west from noon, were indications of a Kelvin-Helmholtz process (Hughes et al., 1978; Olson



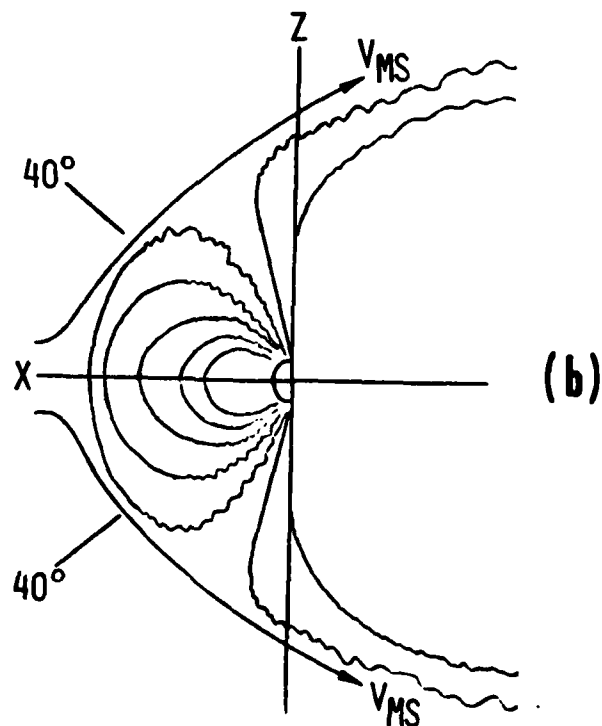
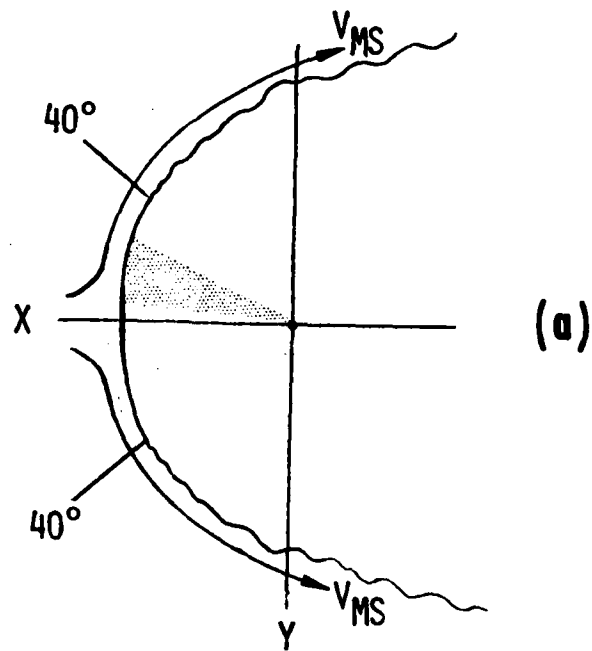


Figure 2. Magnetospheric cross sections showing hypothetical Kelvin-Helmholtz excitation of the plasmopause. (a) Equatorial, (b) Noon-midnight meridian. The shaded area in (a) represents the local time of most probably pulsation occurrence.

and Rostoker, 1978), how did these waves get from their locations on the magnetopause flanks to the noon line and then turn around again to produce the observed pattern?

One answer may be implied by Figure 2b. The modified solar wind may also reach critical velocities at about  $40^\circ$  from the subsolar (stagnation) point in the vertical, noon-midnight meridian plane. If magnetic activity conditions are such that the cusp is northward of the  $40^\circ$  point, surface waves might arise that would grow and propagate both with  $V_{MS}$  and away from the noon meridian (in and out of the plane of the picture) in conformity with observation. A northward or southward component of the IMF, or effects of seasonal geometry, might create an asymmetric response in the northern and southern hemispheres. Details of such possibilities have yet to be worked out theoretically, but it is clear that elaboration of them, and observational tests, if favorable, will advance our understanding of the way waves propagate between the magnetopause and the ground, in the east and west directions, and between the northern and southern hemispheres.

#### FUTURE EFFORTS

Theory. Two theoretical efforts are called for, one related to each external model. First, the surface wave model needs to be focussed on the operation of the Kelvin-Helmholtz instability in the noon meridian plane: wave propagation, seasonal effects, magnetic activity effects. This aspect of the problem was set aside because the theoretical requirement of a thin boundary was thought to apply best at the equator (Southwood, 1974). As Figure 2b suggests, this requirement may not be violated at higher latitudes

at noon, at least some times. Second, the signal model needs to be developed quantitatively to encourage easier testing of its operation and its credibility.

Observation. The measurements required to determine the validity of the external models can best be read directly from Figure 1. Any theoretical connection between any two or more stages needs to be matched by a corresponding solid line where there is none now, which is almost everywhere. In particular, tests of the surface wave model would benefit greatly by an effort to find simultaneous surface and ground waves which, under the influence of critical  $V_{MS}$ , appear and disappear together, while tests of the signal model should be designed around the concept of detecting the progress of signals from the sheath to the ground when the appropriate IMF conditions prevail.

The IMS data offer a bright prospect for advancing these efforts.

#### ACKNOWLEDGMENT

This report was prepared with the support of the Air Force Office of Scientific Research.

## REFERENCES

- Arthur, C. W. and R. L. McPherron, Micropulsations in the morning sector. 3. Simultaneous ground-satellite observations of 10-45 s period waves near  $L = 6.6$ , J. Geophys. Res., 82, 2859, 1977a.
- Arthur, C. W. and R. L. McPherron, Interplanetary magnetic field conditions associated with synchronous orbit observations of Pc 3 magnetic pulsations, J. Geophys. Res., 82, 5138, 1977b.
- Arthur, C. W., R. L. McPherron, and W. J. Hughes, A statistical study of Pc 3 magnetic pulsations at synchronous orbit, ATS-6, J. Geophys. Res., 82, 1149, 1977c.
- Atkinson, G., and T. Watanabe, Surface waves in the magnetospheric boundary as a possible origin of long period geomagnetic micropulsations, Earth Planet. Sci. Letter, 1, 89, 1966.
- Aubry, M. P., M. G. Kivelson, and C. T. Russell, Motion and structure of the magnetopause, J. Geophys. Res., 76, 1673, 1971.
- Boller, B. R. and H. L. Stolov, Explorer 18 study of the stability of the magnetopause using a Kelvin-Helmholtz stability criterion, J. Geophys. Res., 78, 8078, 1973.
- Bol'shakova, O. V., and V. A. Troitskaya, Relation of the interplanetary magnetic field direction to the system of stable oscillations, Dokl. Akad. Nauk SSR, 180, 4, 1968.
- Chen, L. and A. Hasegawa, A theory of long-period magnetic pulsations, steady state excitation of field line resonance, J. Geophys. Res., 79, 1024, 1974.

Gosling, J. T., J. R. Asbridge, S. J. Bame, G. Paschmann, and N. Sckopke, Observations of two distinct populations of low shock ions in the upstream solar wind, *Geophys. Res. Lett's.*, 5, 957, 1978.

Greenstadt, E. W., Field-determined oscillations in the magnetosheath as possible source of medium-period, daytime micropulsations, *Proc. of Conference on Solar Terrestrial Relations, Univ. of Calgary*, 515, April 1972.

Greenstadt, E. W., I. M. Green, G. T. Inouye, D. S. Colburn, J. H. Binsack, and E. F. Lyon, Dual satellite observation of the earth's bow shock. 3. Field-determined shock structure, *Cosmic Electrodynamics*, 1, 316, 1970.

Greenstadt, E. W. and J. V. Olson, A micropulsation contribution in the Pc 3-4 range correlated with IMF radial orientation, *J. Geophys. Res.*, 82, 4991, 1977.

Greenstadt, E. W., C. T. Russell, V. Formisano, P. C. Hedgecock, F. L. Scarf, M. Neugebauer, and R. E. Holzer, Structure of the quasi-parallel, quasi-laminar bow shock, *J. Geophys. Res.*, 82, 651, 1977.

Greenstadt, E. W., H. J. Singer, C. T. Russell, and J. V. Olson, IMF orientation, solar wind velocity, and, Pc 3-4 signals: a joint distribution, *J. Geophys. Res.*, in press, 1979.

Howe, H. C., Jr. and J. H. Binsack, Explorer 33 and 35 plasma observations of magnetosheath flow, *J. Geophys. Res.*, 77, 3334, 1972.

Hughes, W. J., R. L. McPherron, and J. N. Barfield, Geomagnetic pulsations observed simultaneously on three geostationary satellites, *J. Geophys. Res.*, 83, 1109, 1978.

- Kaufmann, R. L., J. T. Horng, and A. Wolfe, Large-amplitude hydromagnetic waves in the inner magnetosheath, *J. Geophys. Res.*, 75, 4666, 1970.
- Kovner, M. S., V. V. Lebedev, T. A. Plyasova-Bakunina, and V. A. Troitskaya, On the generation of low-frequency waves in the solar wind in the front of the bow shock, *Planet. Space Sci.*, 24, 261, 1976.
- Lanzerotti, L. J., H. Fukunishi, and L. Chen, ULF pulsation evidence of the plasmopause, 3. Interpretation of polarization and spectral amplitude studies of Pc 3 and Pc 4 pulsation near  $L = 4$ , *J. Geophys. Res.*, 79, 4648, 1974.
- Lanzerotti, L. J., A. Hasegawa, and N. A. Tartaglia, Morphology and interpretation of magnetospheric plasma waves at conjugate points during December solstice, *J. Geophys. Res.*, 77, 6731, 1972.
- Nourry, G. R., Interplanetary magnetic field, solar wind and geomagnetic micropulsation, Thesis, Univ. of British Columbia, Dept. of Geophysics and Astronomy, 1976.
- Olson, J. V. and G. Rostoker, Longitudinal phase variations of Pc 4-5 micropulsations, *J. Geophys. Res.*, 83, 2481, 1978.
- Radoski, H. R., Magnetic toroidal resonances and vibrating field lines, *J. Geophys. Res.*, 71, 1891, 1966.
- Saito, T., A new index of geomagnetic pulsation and its relation to solar M-regions, Part 1, Rept. Ions. Space Res., Japan, 18, 260, 1964.
- Samson, J. C., J. A. Jacobs, and G. Rostoker, Latitude-dependent characteristics of long-period micropulsations, *J. Geophys. Res.*, 76, 3675, 1971.

- Sen, A. K., The stability of the magnetospheric boundary, Planet. Space Sci., 13, 131, 1965.
- Singer, H. J., C. T. Russell, M. G. Kivelson, E. W. Greenstadt, and J. V. Olson, Evidence for the control of Pc 3,4 magnetic pulsations by the solar wind velocity, Geophys. Res. Lett's., 4, 377, 1977.
- Siscoe, G. L., L. Davis, Jr., P. J. Coleman, Jr., E. J. Smith, and D. E. Jones, Shock aligned magnetic oscillations in the magnetosheath: Mariner 4, J. Geophys. Res., 72, 5524, 1967.
- Southwood, D. J., The hydromagnetic stability of the magnetospheric boundary, Plan. Space Sci., 16, 587, 1968.
- Southwood, D. J., Some features of field line resonances in the magnetosphere, Planet. Space Sci., 22, 483, 1974.
- Spreiter, J. R., and A. Y. Alksne, Plasma flow around the magnetosphere, Magnetospheric Physics, ed. D. J. Williams and G. D. Mead, William Byrd Press, Inc., Richmond, Virginia, 11, 1969.
- Troitskaya, V. A., T. A. Plyasova-Bakunina, and A. V. Gul'elmi, Relationship between Pc 2-4 pulsations and the interplanetary magnetic field, Dokl. Akad. Nank. SSR, 197, 1312, 1971.
- Webb, D. and D. Orr, Geomagnetic pulsations (5-50 MHz) and the interplanetary magnetic field, J. Geophys. Res., 81, 5941, 1976.
- West, H. I. and R. M. Buck, Observations of > 100 keV protons in the earth's magnetosheath, J. Geophys. Res., 81, 569, 1976.

Wolfe, A. and R. L. Kaufmann, MHD wave transmission and production near the magnetopause, J. Geophys. Res., 80, 1764, 1975.

Wolfe, A., L. J. Lanzerotti, and C. G. MacLennan, Dependence of hydromagnetic energy spectra on interplanetary parameters (Abstract), EOS, 59, 1166, 1978.

Wolfe, J. H. and D. D. McKibbin, Pioneer 6 observations of a steady-state magnetosheath, Planet. Space Sci., 16, 953, 1968.



APPENDIX E

CORRELATION OF Pc 3, 4, AND 5 ACTIVITY  
WITH SOLAR WIND SPEED

TRW No. 30435-6005-RU-00

CORRELATION OF Pc 3, 4, AND 5 ACTIVITY  
WITH SOLAR WIND SPEED

by

E. W. Greenstadt<sup>1</sup>, J. V. Olson<sup>2</sup>, P. D. Loewen<sup>2</sup>,  
H. J. Singer<sup>3</sup>, and C. T. Russell<sup>3</sup>

<sup>1</sup>Space Sciences Department, TRW Defense & Space Systems  
Group, One Space Park, Redondo Beach, California 90278

<sup>2</sup>Institute of Earth & Planetary Physics, University of  
Alberta, Edmonton 7, Alberta, Canada

<sup>3</sup>Institute of Geophysics & Planetary Physics, University  
of California, Los Angeles, Los Angeles, California 90024

January 1979

Short Title: Pc 3-5 and  $V_{SW}$

Space Sciences Department

**TRW**  
DEFENSE AND SPACE SYSTEMS GROUP

SECURITY CLASSIFICATION OF THIS PAGE (When Data Entered)

REPORT DOCUMENTATION PAGE		READ INSTRUCTIONS BEFORE COMPLETING FORM
1. REPORT NUMBER 30435-6005-RU-00	2. GOVT ACCESSION NO.	3. RECIPIENT'S CATALOG NUMBER
4. TITLE (and Subtitle) Correlation of Pc 3, 4, and 5 Activity with Solar Wind Speed  Short Title: Pc 3-5 and V <sub>SW</sub>		5. TYPE OF REPORT & PERIOD COVERED Technical Report
7. AUTHOR(s) E. W. Greenstadt, J. V. Olson, P. D. Loewen, H. J. Singer, and C. T. Russell		6. PERFORMING ORG. REPORT NUMBER
9. PERFORMING ORGANIZATION NAME AND ADDRESS TRW Defense & Space Systems Group One Space Park, Bldg R-1, Rm 1176 Redondo Beach, California 90278		8. CONTRACT OR GRANT NUMBER(s) F 49620-77-C-0018
11. CONTROLLING OFFICE NAME AND ADDRESS Dr. Henry Radoski AFOSR/NP Bldg 410		10. PROGRAM ELEMENT, PROJECT, TASK AREA & WORK UNIT NUMBERS
14. MONITORING AGENCY NAME & ADDRESS (if different from Controlling Office)		12. REPORT DATE January 1979
		13. NUMBER OF PAGES 14
		15. SECURITY CLASS. (of this report) Unclassified
		15a. DECLASSIFICATION/DOWNGRADING SCHEDULE
16. DISTRIBUTION STATEMENT (of this Report)  Approved for public release.		
17. DISTRIBUTION STATEMENT (of the abstract entered in Block 20, if different from Report)  Distribution unlimited.		
18. SUPPLEMENTARY NOTES  Submitted to Journal of Geophysical Research		
19. KEY WORDS (Continue on reverse side if necessary and identify by block number)  Geomagnetic pulsations  V <sub>SW</sub> -magnetosphere interaction		
20. ABSTRACT (Continue on reverse side if necessary and identify by block number) Positive correlations of magnetic pulsation amplitude with solar wind speed are found for Pc 3, 4, and 5 at both Calgary and Leduc. The data, obtained in September and October 1970, confirm and extend similar results found in an earlier interval for Pc 3,4 at Calgary alone, thus adding further evidence for a velocity-controlled contribution, such as the Kelvin-Helmholtz instability, to pulsation activity.		

# ABSTRACT

Positive correlations of magnetic pulsation amplitude with solar wind speed are found for Pc 3, 4, and 5 at both Calgary and Leduc. The data, obtained in September and October 1970, confirm and extend similar results found in an earlier interval for Pc 3,4 at Calgary alone, thus adding further evidence for a velocity-controlled contribution, such as the Kelvin-Helmholtz instability, to pulsation activity.

## INTRODUCTION

Observations have linked occurrence and intensity of medium-period geomagnetic pulsations ( $T = 10$  to  $300$  sec) to Interplanetary magnetic field (IMF) orientation and solar wind speed ( $V_{SW}$ ). The motivation for these observations is the belief that magnetospheric pulsations are excited by perturbations brought by the solar wind to the dayside magnetopause where they may be amplified by the Kelvin-Helmholtz instability. Data supporting these notions is not easily obtained, so new cases, augmented statistics, and fresh approaches are being actively sought. The purpose of this letter is to show that earlier results on the velocity correlation are confirmed when the same analysis technique is extended to a new data interval, a second station, and a third band of pulsation periods.

IMF orientation has been represented by latitude and longitude angles of the IMF,  $\lambda_B$ ,  $\phi_B$ , in the solar ecliptic (SE) system, and by angle  $\theta_{XB}$  between the IMF and  $V_{SW}$  or between the IMF and SE X-axis as an approximation to the solar wind flow direction ( $\cos \theta_{XB} = \cos \lambda_B \cos \phi_B$ ). Pulsations appear when  $\lambda_B \approx 0^\circ$ ;  $\phi_B \approx 0^\circ, 180^\circ$ ;  $\theta_{XB} \lesssim 50^\circ$  (Gul'elmi, 1974, and references therein; Nourry and Watanabe, 1973; Nourry, 1976; Webb and Orr, 1976; Greenstadt and Olson, 1977), and correlated positively with  $V_{SW}$  (Singer et al., 1977). Most recently, effort has focused on examining  $\theta_{XB}$  and  $V_{SW}$  together (Greenstadt et al., 1979; Wolfe et al., 1979).

Various techniques for defining pulsation activity and solar wind parameters have been employed, from isolating individual events to comparing power spectra and hourly averages. Our present study has examined correlations of

Pc 3 and 4 at Calgary observatory with both  $\theta_{XB}$  and  $V_{SW}$ , separately and jointly, as already cited. The study has also developed the application of hourly distributions of  $\theta_{XB}$  (Greenstadt and Olson, 1979), using satellite and ground data from September, October, and November 1969.

The new data interval was September, October 1970, which satisfied the criterion that recordings were still available from Calgary, permitting a cross-check for replication of previous results. The second station was Leduc Observatory, which was recording simultaneously slightly farther north (corrected geomagnetic latitude  $61.2^\circ$ ;  $L = 4.2$ ) than Calgary ( $58.7^\circ$ ;  $L = 3.7$ ). The third band of periods was 150 to 300 seconds, corresponding to Pc 5 pulsations. It had originally been intended to enlarge the correlations of  $\theta_{XB}$  as well as  $V_{SW}$  using the new data, but the natural behavior of the IMF didn't support the effort, as explained below.

#### DATA

Measurements of horizontal and vertical field variations made at Calgary and Leduc stations were passed through digital filters separating Pc 3, 4, and 5 frequency bands, and the maximal amplitude  $\delta B$ , peak-to-peak, for each hour was used to represent the level of occurrence of magnetic pulsation activity during the hour. The hourly  $\delta B$ 's from the two stations were inter-compared, axis by axis, for the entire data interval, to test whether activity at the two stations was comparable.

The solar wind velocity data used in this study consisted of three-hour averages from a merged Vela data set, including Vela's 2-6, which is described by King (1977a,b).

For comparison of pulsation activity with solar wind parameters, the largest  $\delta B$  in either X or Y component each hour was used. Contributions of vertical (Z) components were always smaller and were not used. Corresponding IMF data registered by Explorer 35, in lunar orbit, were analyzed to find the percentile distributions of  $\theta_{XB}$  between  $0^\circ$  and  $90^\circ$  each hour. The distributions were used to separate groups of "IMF-favorable" hours; i.e., most  $\theta_{XB}$  near  $0^\circ$ , from "IMF-unfavorable" hours; i.e., most  $\theta_{XB}$  near  $90^\circ$ , for various percentile criteria. Only two really unfavorable hours were found in which all  $\theta_{XB} > 60^\circ$ , and both were at low velocity, so favorable and unfavorable IMF orientation effects on the velocity dependence of  $\delta B$  could not be contrasted. Relaxation of the criterion of unfavorable conditions failed to improve these statistics in any useful way. Similarly, no dependence of  $\delta B$  on  $\theta_{XB}$  could be developed for either high or low velocities since the unfavorable ends of the scale had no populations. Readers interested in further details of instrumentation or data handling procedures are referred to Greenstadt and Olson (1976, 1977, 1979), Singer et al. (1977), and Greenstadt et al. (1979).

## RESULTS

Station Correlations. The correlations of hourly peak amplitudes of X-components in Pc 3 and Pc 4 bands at Leduc and Calgary are displayed in Figure 1. Correlation coefficients were .498 and .79 respectively. Similar or better results were obtained for the other components and for Pc 5. The Y-components of Pc 3 and Pc 4 gave correlation coefficients of .679 and .865 respectively; the X and Z components of Pc 5 gave coefficients of .942 and .912 respectively. Hourly averages, rather than peaks, also yielded similar correlations.

Note that the slope of the Pc 4 plot in Figure 1 is  $> 1.0$ . This was true also for the Y axis of Pc 4 and for both Y and Z axes of Pc 5. Slopes of all component correlations of Pc 3 were  $< 1.0$ .

Velocity Correlations. We present the data in the same 'most favorable' format used by Greenstadt et al. (1979, Figure 3). Scatter plots of  $\delta B$  vs  $V_{SW}$  are displayed for hours in which 50 percent or more of the  $\theta_{XB}$  were within  $30^\circ$  of the X axis. Figure 2 shows the scatter plots and least-square lines for hourly maximal pulsation amplitudes vs hourly average  $V_{SW}$  in Pc 3 and Pc 4 period ranges at both Calgary and Leduc Observatories. The dashed lines are the linear least square best fits found for the earlier data from September-November 1969 (Greenstadt et al., 1978, Figure 3). The correlations were weaker at Calgary in the 1970 interval than in the 1969 interval, although stronger for Pc 4 than for Pc 3, just as in the earlier study. The correlations at Leduc were as strong (Pc 4) or stronger (Pc 3) than at Calgary. In fact, the present Pc 3 correlation at Leduc was stronger than the Pc 3 correlation at Calgary for the 1969 interval.

Scatter diagrams for Pc 5 are shown in Figure 3. Correlations of amplitude with velocity were clearly strong at both stations.

#### DISCUSSION

Both Calgary and Leduc stations are at magnetic latitudes corresponding, on average and depending on the signal period, to a strong latitude gradient in pulsation amplitude, with the maximum somewhere northward of both observatories (Samson et al., 1971; Wertz and Campbell, 1976). Our best fit lines having slopes  $> 1$  for Pc 4 and 5 were consistent with this latitude effect. The original choice of Calgary, the southernmost of the University of Alberta chain of stations, as the surface instrument for our earlier analysis, was based on a desire to depart no more than necessary from the latitude of Borok ( $53^\circ$ ), the station used for similar analyses by Soviet workers (Greenstadt and Olson, 1976; 1977, and references therein). We also desired to avoid possible confusion introduced by highly geomagnetically-active auroral phenomena. The rather clean results obtained



here from Leduc plus the well-known increase in Pc 3, 4 amplitudes with approach to auroral latitudes, suggest that stronger correlations with solar wind parameters of the type we are studying might be obtained by using data from stations still further north than Leduc, bearing in mind that the best station at any particular time might depend on local time (Samson et al., 1971) and overall geomagnetic activity. The data used in this report all came from relatively inactive conditions, i.e.,  $1 \leq A_p \leq 19$ . In fact, seven out of 18 hours in Figures 2 and 3 were designated Q or QQ (NOAA, Solar Geophysical Data). The position of Leduc, incidentally, is comparable to the northernmost observatory utilized by Webb and Orr (1976).

It is important to note that Pc 3 correlations of Calgary and Leduc did not show the same, let alone a more pronounced, slope effect, particularly in view of the report by Fukunishi and Lanzerotti (1974) who found Pc 3 larger than Pc 4 when  $L \geq 4$ . Also, the correlation of Pc 3 amplitudes with velocity was much poorer than those found for the earlier data interval or for the other bands in this data interval. The limited range of Pc 3 and the smaller population of points may have combined to obscure the velocity dependence for these relatively small pulsations. However, these deficiencies and inconsistencies in the Pc 3 results probably underscore an inherent methodological difficulty in pulsation analysis: there can be multiple resonances at separate latitudes in the plasmopause-plasmatrough region for any given Pc period range, and any particular resonance will appear at different latitudes at different times, depending on magnetic activity (Orr & Webb, 1975) and local time (Orr, 1979). Figures 1 and 3 of Orr (op cit.) illustrate these problems clearly. It may be necessary to extract a Pc 3 "index" from recordings at several stations to obtain a quantifiable measure of signal activity comparable with itself on the same baseline from one day to the next.

Certainly for the Pc 4 band the earlier  $B$  vs  $V_{SW}$  results are confirmed here, as they have also been by Wolfe et al. (1979) who analyzed data from a station at Pittsburg, New Hampshire ( $L = 3.5$ ). Thus, the contribution of the velocity-dependent, Kelvin-Helmholtz mechanism to pulsation generation remains consistent with measurement, on application of the previous analytic technique to a new data interval. This consistency adds to the persuasiveness of the Kelvin-Helmholtz model, at least under favorable conditions of IMF orientation, and is reinforced by the correlations obtained here in the Pc 5 band, which encompassed the periods expected from this model (Atkinson and Watanabe, 1966; Southwood, 1968; Chen and Hasegawa, 1974). However, alternative models, less developed quantitatively than Kelvin-Helmholtz, are by no means ruled out. Russell and Elphic (1979) have proposed a dayside flux transfer process as a possible source of pulsations at the magnetopause, and of course the perverse possibility persists that elevated  $V_{SW}$  is so correlated with reduced latitudes of the auroral edge of the closed part of the dayside magnetosphere that at any fixed station  $\delta B$  rises with  $V_{SW}$  regardless of pulsation origin, simply because of increased sensitivity of the station. Confirmation, and further study, of the dependence of  $\delta B$  on IMF orientation will have to await a more extensive and varied data population than was provided by the September-October 1970 interval.

#### ACKNOWLEDGMENTS

Discussions with J. C. Samson, A. Wolfe, and R. L. McPherron, and important comments by the reviewer, have been helpful. This study is sponsored by AFOSR Contract F 49620-77-C-0018 (at TRW), the National Research Council of Canada (at the University of Alberta), and NSF Grant ATM74-23464 (at the University of California, Los Angeles).

## REFERENCES

- Atkinson, G., and Watanabe, T., Surface waves in the magnetospheric boundary as a possible origin of long period geomagnetic micropulsations, *Earth Planet. Sci. Lett.*, 1, 89, 1966.
- Chen, L., and Hasegawa, A., A theory of long-period magnetic pulsations, steady state excitation of field line resonance, *J. Geophys. Res.*, 79, 1024, 1974.
- Fukunishi, H., and Lanzerotti, L. J., ULF pulsation evidence of the plasmopause. 1. Spectral studies of Pc 3 and Pc 4 pulsations near  $L = 4$ , *J. Geophys. Res.*, 79, 142, 1974.
- Greenstadt, E. W., and Olson, J. V., Pc 3,4 activity and interplanetary field orientation, *J. Geophys. Res.*, 81, 5911, 1976.
- Greenstadt, E. W., and Olson, J. V., A micropulsation contribution in the Pc 3-4 range correlated with IMF radial orientation, *J. Geophys. Res.*, 82, 4991, 1977.
- Greenstadt, E. W., and Olson, J. V., Correlation of geomagnetic pulsation signals in the 10- to 15-second period range with concentration of IMF orientations near the Sun-Earth line, *J. Geophys. Res.*, 84, 1493, 1979.
- Greenstadt, E. W., Singer, H. J., Russell, C. T., and Olson, J. V., IMF orientation, solar wind velocity, and Pc 3-4 signals: A joint distribution, *J. Geophys. Res.*, 84, 527, 1979.
- Gul'elmi, A. V., Diagnostics of the magnetosphere and interplanetary medium by means of pulsations, *Space Sci. Rev.*, 16, 331, 1974.

- King, J. H., Interplanetary Medium Date Book, NSSDC/WDC-A-R&S, 77-04, 1977a.
- King, J. H., Interplanetary Medium Date Book-Appendix, NSSDC/WDC-A-R&S, 77-04a, 1977b.
- Nourry, G. R., Interplanetary magnetic field, solar wind and geomagnetic micropulsation, Thesis, Univ. of British Columbia, Department of Geophysics and Astronomy, 1976.
- Nourry, G. R., and Watanabe, T., Geomagnetic micropulsations and interplanetary magnetic field (Abstract), EOS, 54, 1179, 1973.
- Orr, D., Geomagnetic pulsations and their relationship to structure within the magnetosphere, Magnetospheric Study 1979, Proc. Int'l Workshop on Selected Topics of Magnetospheric Physics, Tokyo, 124, Japanese IMS Committee, 1979.
- Orr, D. and D. C. Webb, Statistical studies of geomagnetic pulsations with periods between 10 and 70 sec and their relationship to the plasmopause region, Planet. Space Sci., 23, 1169, 1975.
- Russell, C. T., and Elphic, R. C., ISEE observations of flux transfer events at the dayside magnetopause, Geophys. Res. Lett., 6, 33, 1979.
- Samson, J. C., Jacobs, J. A., and Rostoker, G., Latitude-dependent characteristics of long-period micropulsations, J. Geophys. Res., 76, 3675, 1971.
- Singer, H. J., Russell, C. T., Kivelson, M. G., Greenstadt, E. W., and Olson, J. V., Evidence for the control of Pc 3,4 magnetic pulsations by the solar wind velocity, Geophys. Res. Lett., 4, 377, 1977.
- Southwood, D. J., The hydromagnetic stability of the magnetospheric boundary, Plan. Space Sci., 16, 587, 1968.
- Webb, D. and Orr, D., Geomagnetic pulsations (5-50 MHz) and the interplanetary magnetic field, J. Geophys. Res., 81, 5941, 1976.
- Wertz, R., and Campbell, W. H., Integrated power spectra of geomagnetic field variations with periods of .3-300 s, J. Geophys. Res., 81, 5131, 1976.
- Wolfe, A., Lanzerotti, L. J., and MacLennan, C. G., Dependence of hydromagnetic energy spectra on interplanetary parameters, J. Geophys. Res., in press, 1979.

# FIGURE CAPTIONS

Figure 1. Comparisons of hourly maximal pulsation amplitudes  $\delta B$  (X-axis) at Leduc and Calgary Observatories for September, October 1970; Pc 3 at left, Pc 4 at right. Note that the Pc 4 amplitudes tended to be larger at Leduc than at Calgary.

Figure 2. Correlations of hourly  $\delta B$  with  $V_{SW}$  at Calgary (left) and Leduc (right) for Pc 3 (upper panels) and Pc 4 (lower panels). Each point represents an hour in which 50 percent or more of the  $\theta_{XB}$ 's were less than  $30^\circ$ .

Figure 3. Correlations of  $\delta B$  with  $V_{SW}$  for the Pc 5 band, for hours in which  $\geq 50$  percent of  $\theta_{XB} < 30^\circ$ .

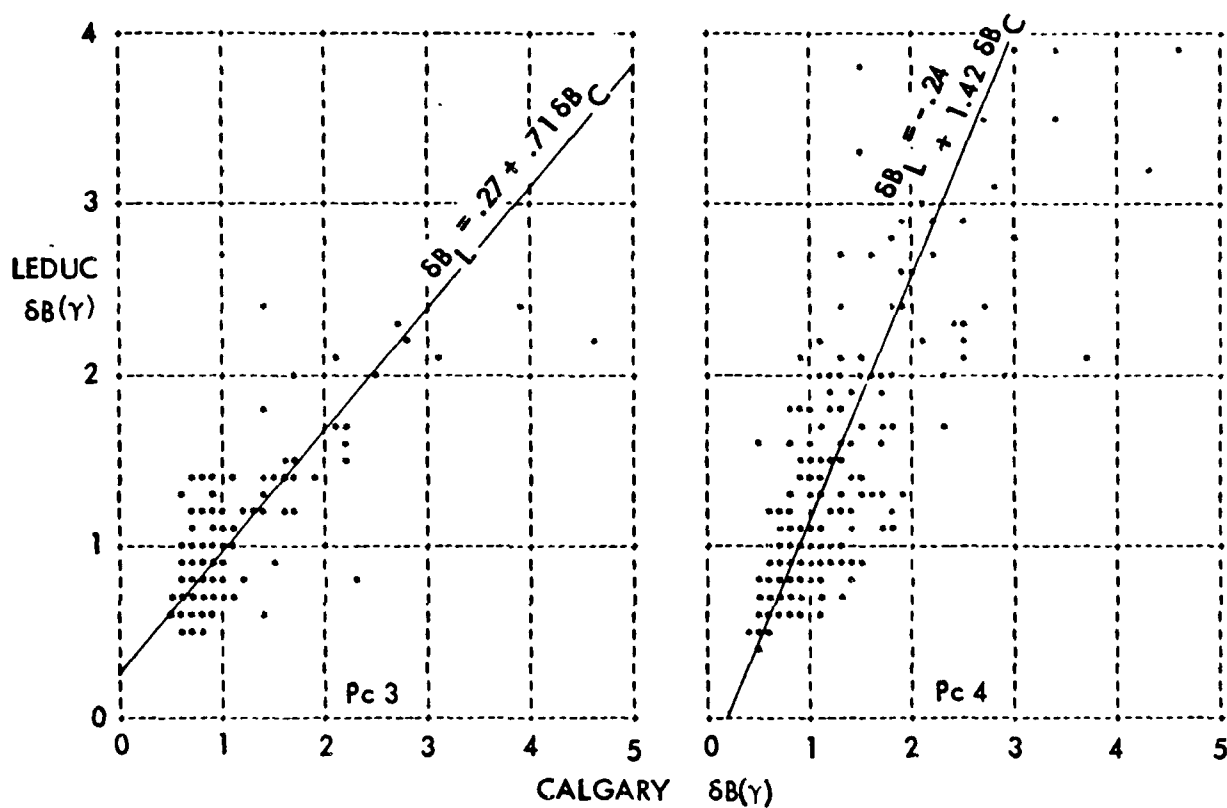


Figure 1. Comparisons of hourly maximal pulsation amplitudes  $\delta B$  (X-axis) at Leduc and Calgary Observatories for September, October 1970; Pc 3 at left, Pc 4 at right. Note that the Pc 4 amplitudes tended to be larger at Leduc than at Calgary.

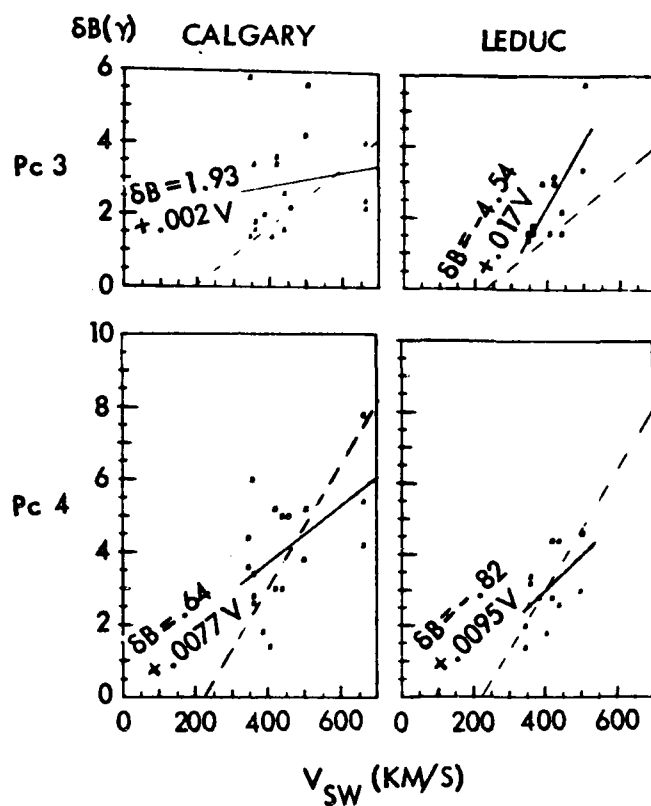


Figure 2. Correlations of hourly  $\delta B$  with  $V_{SW}$  at Calgary (left) and Leduc (right) for Pc 3 (upper panels) and Pc 4 (lower panels). Each point represents an hour in which 50 percent or more of the  $\theta_{XB}$ 's were less than  $30^\circ$ .

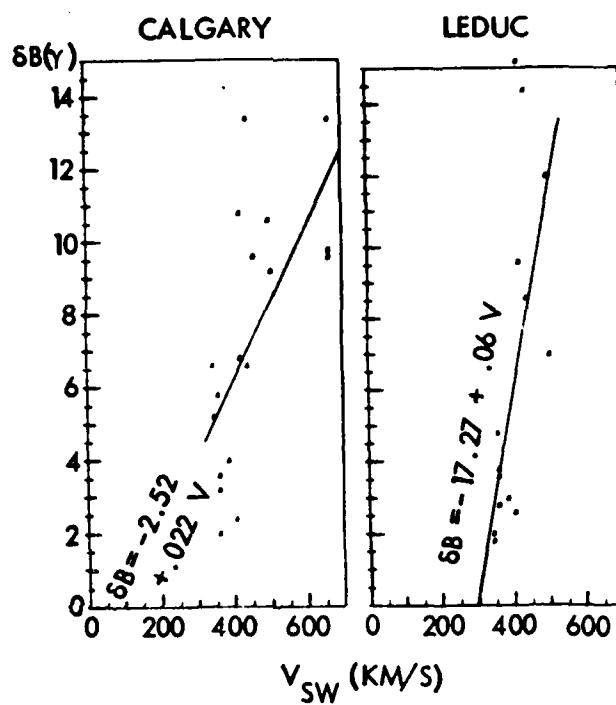


Figure 3. Correlations of  $\delta B$  with  $V_{SW}$  for the Pc 5 band, for hours in which  $\geq 50$  percent of  $\theta_{XB} < 30^\circ$ .



APPENDIX F

ASSOCIATION OF LOW-FREQUENCY WAVES WITH SUPRATHERMAL IONS  
IN THE UPSTREAM SOLAR WIND

# ASSOCIATION OF LOW-FREQUENCY WAVES WITH SUPRATHERMAL IONS IN THE UPSTREAM SOLAR WIND

G. Paschmann<sup>1</sup>, N. Sckopke<sup>1</sup>, S. J. Bame<sup>2</sup>, J. R. Asbridge<sup>2</sup>,  
J. T. Gosling<sup>3</sup>, C. T. Russell<sup>3</sup> and E. W. Greenstadt<sup>4</sup>

**Abstract.** Observations obtained upstream of the earth's bow shock with the LASL/MPI plasma instruments and the UCLA magnetometers on ISEE-1 and 2 have revealed a striking relationship between the presence of low-frequency fluctuations in solar wind density and field strength and the different types of distribution functions of upstream ions. Waves are absent when the ions have the beamlike distribution of the "reflected" ions. Large-amplitude waves are present only in conjunction with the "diffuse" ions, which are characterized by flat energy spectra and broad angular distributions. The waves are largely compressive, showing very good correlation between oscillations in magnetic field strength and plasma density.

## Introduction

Ions, apparently of bow shock origin, with energies several times the solar wind flow energy are known to exist in the region upstream of the earth's bow shock, generally on the dawn side (Asbridge *et al.*, 1968). It has been suggested that the low-frequency (0.01 to 0.05 Hz) magnetic waves observed in the same region might be caused by these ions as they stream through the solar wind plasma (Fairfield, 1969; Barnes 1970; Greenstadt *et al.*, 1970). A direct correlation between the presence of the waves and the upstream ions was reported by Scarf *et al.* (1970). Ions of considerably higher energies have also been observed in the upstream region. Lin *et al.* (1974) reported the nearly continuous presence of protons with energies above ~30 keV on field lines likely to be connected to the shock. Even at energies above ~100 keV, bursts of protons are quite common in the upstream region (West and Buck, 1976; Sarris *et al.*, 1976). Recently it was shown (Gosling *et al.*, 1978) that there actually are two distinctly different populations of upstream ions at energies between ~1 and ~40 keV, termed "reflected" and "diffuse" ions by these authors. The reflected ions are characterized by their narrow spectral and angular extent, i.e. they form a beam directed outward from the shock along interplanetary field lines. These ions are thus the type originally described by Asbridge *et al.* (1968). The diffuse ions, on the other hand, are characterized by rather flat energy spectra and broad angular distributions. Peak intensities are much smaller for the diffuse ions, although the total densities are nearly equal.

It is the purpose of this paper to show that the noted difference in upstream ion distributions is associated with a dramatic difference in the occurrence of the upstream low-frequency waves. In addition, the paper will demonstrate the good correlation between magnetic field and plasma density in the wave events. The observations were obtained with the LASL/MPI plasma experiments and the UCLA magnetometers on ISEE-1 and 2. Detailed descriptions of the instruments and data analysis techniques may be found elsewhere (Bame *et al.*, 1978; Paschmann *et al.*, 1978; Russell, 1978).

<sup>1</sup> Max-Planck-Institut für Physik und Astrophysik, Institut für extraterrestrische Physik, 8046 Garching, Germany

<sup>2</sup> University of California, Los Alamos Scientific Laboratory, Los Alamos, N.M. 87545

<sup>3</sup> Institute of Geophysics and Planetary Physics, University of California, Los Angeles, Ca. 90024

<sup>4</sup> TRW Defense and Space Systems Group, Redondo Beach, Ca. 90278

Copyright 1979 by the American Geophysical Union.

## Observations

Figure 1 shows a 24 minute interval of plasma and magnetic field data obtained on 8 December 1977. The satellites at this time were located near 18  $R_E$  geocentric distance and 300° ecliptic longitude, and moved inward, encountering the bow shock after 21:30 UT. The separation vector in GSE coordinates is (51, -349, 122) km with ISEE-2 closer to the earth. The magnetic field is shown in terms of its total strength,  $B$ . The plasma data are presented in terms of the density,  $N_E$ , of solar wind electrons and the density  $N_p$ , of suprathermal ions. The electron density,  $N_E$ , was computed from the two-dimensional distribution function obtained during one spacecraft revolution (~3 seconds). To avoid contamination by photoelectrons, only electrons with energies above approximately 10 eV were included. Since, in addition, spacecraft charging was neglected, absolute electron densities are probably accurate only within a factor of ~1.5.

The suprathermal ion densities,  $N_p$ , were obtained by integration over only those energy channels clearly above the solar wind protons and alphas. In the case of Figure 1, the integration extended from ~3.1 keV to ~40 keV for ISEE-1 and from ~2.6 keV to ~10 keV for ISEE-2. The difference in limits results from the fact that the two instruments were operated in different energy modes at this time.

Figure 1 shows that initially no suprathermal ions are present and that the solar wind is very quiet, with a density near 10  $\text{cm}^{-3}$ , a field strength near 5 $\gamma$ , and a bulk speed (not shown) of 300  $\text{km sec}^{-1}$ . Near 20:59 UT a low flux of reflected ions first appears, persisting until ~21:02 UT. (The seemingly higher densities seen on ISEE-2 are an artefact caused by the slightly lower integration limit on ISEE-2, as was noted above). The appearance of these reflected ions has no noticeable effect on  $N_E$  and  $B$ . At 21:02 UT there is a sudden onset of magnetic field and plasma density oscillations, coincident with an equally sudden increase in the suprathermal ion density. An inspection of the ion distribution functions (not shown) indicates that these ions are of the diffuse type. The wave amplitudes are very high, with both  $\Delta N_E/N_E$  and  $\Delta B/B$  being of order one. The transverse oscillations of the field (not shown) are even larger than the compressional. The electron temperature stayed nearly constant at  $1.8 \times 10^5$  K during the entire interval. Note the good correlation between the  $N_E$  and  $B$  oscillations and between the ISEE-1 and -2 records. The wave periods, in the spacecraft frame, are seen to be slightly less than one minute but with considerable variability. Detailed examination of the magnetic records shows that the phases observed by ISEE-2 are delayed by 0.3–1.0 sec relative to ISEE-1.

A detailed investigation of the waves is beyond the scope of this paper. It requires that the propagation velocity vector, frequency, and polarization be determined in the plasma frame of reference. While the plasma velocity is accurately known, the propagation direction, determined by minimum variance analysis of the magnetic data appears to be highly variable, and sometimes nearly at right angles to the spacecraft separation vector. Thus the observed phase delay between the two satellites cannot be converted to a reliable wave propagation speed by use of a simple model of plane phase fronts sweeping past the spacecraft. The wave polarization is also found to be complicated and variable.

In the data just discussed there was some suggestion that the presence of the waves was correlated with the diffuse ions, but not with the reflected ions. The brief duration and lower densities of the

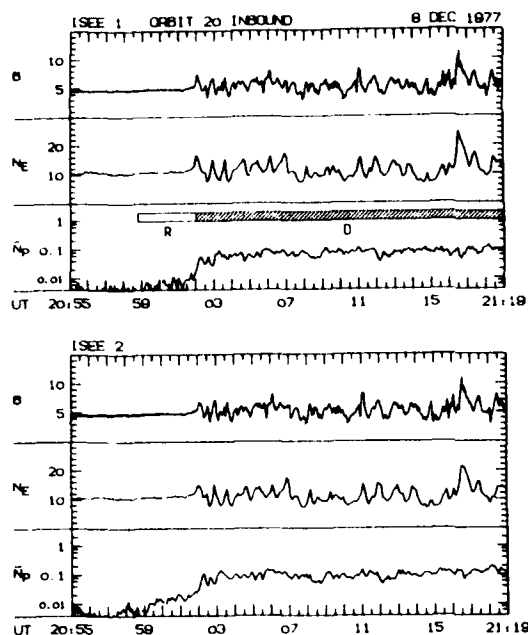


Fig. 1. Upstream wave event on 8 December 1977. The top three panels show the field strength  $B$  (in gamma), the solar wind electron density  $N_E$  (in  $\text{cm}^{-3}$ ) and the suprathermal ion densities  $N_p$  (in  $\text{cm}^{-3}$ ) as observed on ISEE-1. The lower three panels show  $B$ ,  $N_E$  and  $N_p$  from ISEE-2. Spacing for  $N_E$  and  $N_p$  is 3 seconds.  $B$  is sampled every 64 msec. The occurrence of reflected and diffuse ion populations are identified by the bars above the  $N_p$  plot. Spacecraft position was near  $18.0 R_E$  geocentric distance,  $306^\circ$  longitude and  $23.5^\circ$  latitude in ecliptic (GSE) coordinates.

reflected ions could, however, have accounted for the effect. The next example will demonstrate that the situation is indeed strikingly different for the two types of ions. Figure 2 shows ISEE-2 electron and suprathermal ion densities and magnetic field strength for one hour on 19 November 77. (An ion spectrogram for this interval is shown in Figure 2 of Gosling *et al.*, 1978). At the beginning the satellite was located at  $17.8 R_E$  and  $321^\circ$  longitude, moving inward and crossing the bowshock near 20:50 UT. The ion density has been computed for energies between  $\sim 2.5$  and  $\sim 10$  keV. Figure 2 shows that the low-frequency waves do not appear until about 19:01 UT,

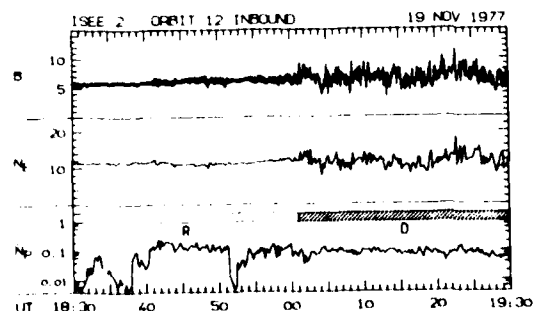


Fig. 2. Magnetic field strength, electron and suprathermal ion densities from ISEE-2 for a wave event on 19 November 1977. Spacing of plasma and magnetic field measurements is 12 and 0.25 seconds, respectively. Spacecraft position initially was  $17.8 R_E$  geocentric distance,  $320.5^\circ$  longitude and  $24.2^\circ$  latitude in GSE coordinates.

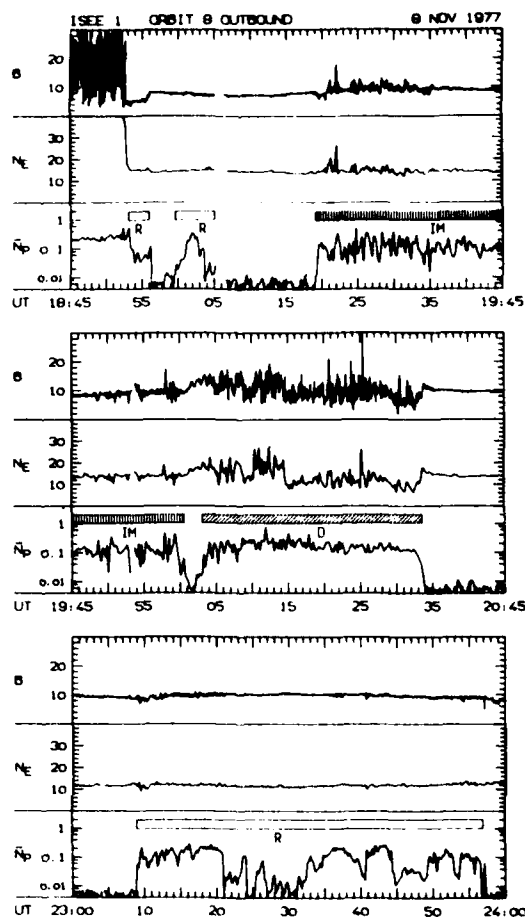


Fig. 3. Electron and suprathermal ion densities and magnetic field strength from ISEE-1 for three hours on 8 November 1977. Note the large time gap between the second and third intervals shown. The spacecraft crosses the bow shock near 18:53 UT, at  $16.1 R_E$  geocentric distance,  $299^\circ$  longitude and  $22.2^\circ$  latitude in GSE coordinates. At the end of the interval shown the spacecraft has proceeded to a distance of  $19.4 R_E$ . Again, occurrences of reflected and diffuse ion populations are indicated by the bars above the  $N_p$  plot. In addition, there is a period (between 19:20 and 20:00 UT) where ion distributions are characterized by intermediate widths in energy and angle, indicated by the bar denoted IM.

although suprathermal ions of substantial density are observed throughout most of this one-hour interval. Before wave onset, however, the ions were of the reflected type, whereas those observed afterwards were of the diffuse type. Note the presence of high-frequency ( $\geq 0.5$  Hz) fluctuations in field magnitude in conjunction with reflected ions for densities exceeding  $0.1 \text{ cm}^{-3}$ .

Further evidence for the intimate relationship between the presence of the waves and the nature of the ion distribution function is provided by Figure 3, which shows a total of three hours of ISEE-1 plasma and magnetic field data on 8 November 1977. An ion spectrogram for the same data is shown in Figure 1 of Gosling *et al.* (1978). Near 18:53 UT the bow shock is crossed, as evidenced by the large changes in electron density and average field strength. Note the large time jump between the second and third sections of the figure. The previously noted absence of waves in conjunction with the presence of upstream ions of the reflected type is clearly

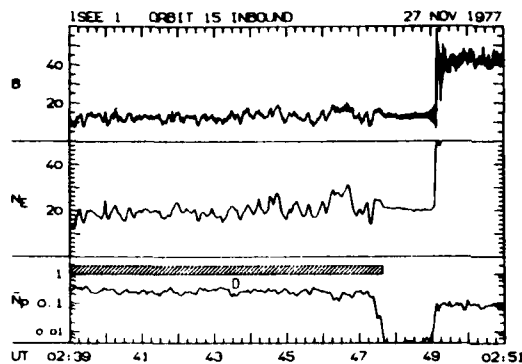


Fig. 4. Field strength, electron and suprathermal ion densities from ISEE-1 on 27 November 1977, showing abrupt termination of low-frequency waves and diffuse ions  $\sim 90$  seconds before bow-shock crossing (at 02:49 UT). At the beginning of the interval, the spacecraft was located at  $\sim 14.6 R_E$  geocentric distance,  $320^\circ$  longitude and  $23.4^\circ$  latitude in GSE coordinates.

evident during the long interval between  $\sim 23:10$  UT and  $\sim 23:57$  UT, and during two brief bursts near 18:55 and 19:02 UT. In contrast, large amplitude density and magnetic field fluctuations are seen between  $\sim 20:02$  and  $\sim 20:34$  UT, when ions of the diffuse type are present. In addition to these features which already emerged from the previous examples, Figure 3 contains a new feature. Between 19:19 UT and 20:00 UT the upstream ions have a distribution which is broader in energy and angle than normally observed for the reflected ions, but also considerably narrower than is typical for the diffuse ions. (See Figure 1 of Gosling et al., 1978.) During this interval of "intermediate" ion distributions, significant fluctuations in  $N_E$  and  $B$  are observed, although at much reduced amplitudes. Note that the density of suprathermal ions is nearly the same ( $\sim 0.1 \text{ cm}^{-3}$ ) under all conditions. To check whether the orientation of the IMF was the controlling factor on the appearance of these upstream particles and waves we calculated the angle between the IMF and the local expected shock normal. When there were no upstream waves the angle was  $58^\circ$  or greater. When reflected particles were present, it averaged about  $50^\circ$ . When intermediate particles were present, it averaged about  $40^\circ$  and when diffuse particles were present it averaged about  $30^\circ$ .

Finally Figure 4 shows an example of high-resolution data where the low-frequency waves (in  $N_E$  and  $B$ ) and the suprathermal ions (of the diffuse type) terminate just shortly ( $\sim 90$  seconds) before the bow shock is crossed ( $\sim 02:49$  UT). Again, as in the first example, the field and density fluctuations are in phase. The dominant period is  $\sim 20$  seconds. At the time when the low frequency waves disappear, the high-resolution magnetic field data show an onset of high-frequency waves, extending to the shock. The latter appear to be the whistler waves studied by Fairfield (1974). The noted change in character of the waves is associated with a change in the direction of the magnetic field. When the low frequency waves are present, the field makes an angle of about  $30^\circ$  to the expected shock normal. When the high frequency waves are present and the diffuse ions are absent the field makes an angle of  $60^\circ$  to the shock normal. In both cases the field direction is such that connection to the shock seems inevitable. Therefore it is unlikely that the sudden change in particle and field behavior could have resulted from disconnection from the bow shock.

#### Discussion

In the previous section we have demonstrated that the presence or absence of low-frequency waves in the upstream solar wind is intimately related to the type of suprathermal ion distribution. Large

amplitude waves were exclusively observed in conjunction with the broad distributions of the "diffuse" ion population, and not in conjunction with the narrow-beamed "reflected" population. This fact bears directly on the generation mechanism of the waves. Barnes (1970) has argued that the waves are magnetosonic waves caused by a cyclotron resonance instability of a fast ion beam travelling upstream through the solar wind. He predicts wave amplitudes which are proportional to beam density times its speed (in the solar wind frame). However, our observations indicate that fast ion beams of substantial density can propagate through the solar wind for extended periods (30 minutes and longer) without generating the waves. Quite obviously, if Barnes' mechanism is correct, there must be additional criteria for instability to occur. Nevertheless, once the waves are generated, they would strongly pitch-angle scatter the ions (Barnes, 1970), resulting in a more isotropic angular distribution. It is therefore tempting to think of the diffuse ions as the end result of the interaction between the original beam and the waves. The fact that the two populations are almost never observed simultaneously, yet have approximately the same densities, fits this picture well. A natural consequence would also be a correlation between wave amplitude and width of the angular distribution, in agreement with the "intermediate" case noted in the discussion of Figure 3. However, although the broad angular distributions of the diffuse ions might be explained this way, their flat energy spectra extending to  $> 40 \text{ keV}$  are not. Perhaps the electrostatic fluctuations reported by Scarf et al. (1970) to be associated with the low-frequency wave events can cause the energization. Of course, there might be no causal relationship between the two ion populations at all. Indeed, the correlation of the appearance of diffuse upstream ions and waves with the orientation of the field with respect to the local shock normal suggests that all upstream ions are accelerated at the shock, and that their different properties are associated with the nature of the shock structure at their point of origin. In this context it should also be pointed out that ions similar to the diffuse upstream type are observed downstream of the shock, showing a similar correlation with fluctuations in plasma properties (Asbridge et al., 1978).

No firm conclusion about the origin of the different population of upstream ions and the mechanism for generating the low-frequency waves appears possible at this time. Future work, for example a detailed comparison of the momentum and energy fluxes of the two upstream ion populations, should help to clarify whether a direct causal relationship exists. Studies of the geometry of the intersection of field lines with the bow shock and estimations of conditions at the projected source point of the ions are also necessary.

**Acknowledgments.** The authors wish to thank M. Halbig, J. Papamastorakis, E. Schopke, and E. Tech for programming support and data management. Helpful discussions with B. U. Ö. Sonnerup are gratefully acknowledged. Max-Planck-Institut portions of this work were supported by the Bundesministerium für Forschung und Technologie. Los Alamos portions of this work were conducted under the auspices of the U.S. Department of Energy with NASA support under S-50864A. Work at UCLA was supported under NASA contract NAS 5-20064 and at TRW under NASA contract NASW-3087.

#### References

- Asbridge, J. R., S. J. Bame and I. B. Strong, Outward flow of protons from the earth's bow shock, *J. Geophys. Res.*, **73**, 5777-5782, 1968.
- Asbridge, J. R., S. J. Bame, J. T. Gosling, G. Paschmann, and N. Schopke, Energetic plasma ions within the earth's magnetosheath, *Geophys. Res. Lett.*, **5**, 953-955, 1978.
- Bame, S. J., J. R. Asbridge, H. E. Felthaus, J. P. Glore, G. Paschmann, P. Hemmerich, K. Lehmann and H. Rosenbauer, ISEE-1 and ISEE-2 fast plasma experiment and the ISEE 1 solar wind

- experiment, *IEEE Trans. Geosci. Electronics*, GE-16, 216-220, 1978.
- Barnes, A., Theory of generation of bow-shock-associated waves in the upstream interplanetary medium, *Cosmic Elec.*, 1, 90-114, 1970.
- Fairfield, D. H., Bow shock associated waves observed in the far upstream interplanetary medium, *J. Geophys. Res.*, 74, 3541-3553, 1969.
- Fairfield, D. H., Whistler waves observed upstream from collisionless shocks, *J. Geophys. Res.*, 79, 1368-1378, 1974.
- Gosling, J. T., J. R. Asbridge, S. J. Bame, G. Paschmann and N. Sckopke, Observations of two distinct populations of bow shock ions in the upstream solar wind, *Geophys. Res. Lett.*, 5, 957-960, 1978.
- Greenstadt, E. W., I. M. Green, G. T. Inouye, D. S. Colburn, J. H. Binsack and E. F. Lyon, Dual satellite observations of earth's bow shock, *Cosmic Elec.*, 1, 279-296, 1970.
- Lin, R. P., C. I. Meng and K. A. Anderson, 30- to 100-keV protons upstream from the earth's bow shock, *J. Geophys. Res.*, 79, 489 to 498, 1974.
- Paschmann, H., N. Sckopke, G. Haerendel, J. Papamastorakis, S. J. Bame, J. R. Asbridge, J. T. Gosling, E. W. Hones, Jr. and E. R. Tech, ISEE plasma observations near the subsolar magnetopause, *Space Sci. Rev.*, in press, 1978.
- Russell, C. T., The ISEE 1 and 2 fluxgate magnetometers, *IEEE Trans. Geosci. Electronics*, GE-16, 239-242, 1978.
- Sarris, E. T., S. M. Krimigis, and T. P. Armstrong, Observations of magnetospheric bursts of high-energy protons and electrons at  $\sim 35 R_E$  with IMP-7, *J. Geophys. Res.*, 81, 2341-2355, 1976.
- Scarf, F. L., R. W. Fredricks, L. A. Franck, C. T. Russell, P. J. Coleman and M. Neugebauer, Direct correlations of large amplitude waves with suprathermal protons in the upstream solar wind, *J. Geophys. Res.*, 75, 7316-7322, 1970.
- West, H. I. and R. M. Buck, Observations of  $> 100$  keV protons in the earth's magnetosheath, *J. Geophys. Res.*, 81, 569-584, 1976.

(Received November 16, 1978;  
revised January 2, 1979;  
accepted January 23, 1979.)

APPENDIX G

MAGNETIC FIELD ORIENTATION AND SUPRATHERMAL ION  
STREAMS IN THE EARTH'S FORESHOCK

31219-6011-RU-00

MAGNETIC FIELD ORIENTATION AND SUPRATHERMAL ION  
STREAMS IN THE EARTH'S FORESHOCK

by

E. W. Greenstadt<sup>1</sup>, C. T. Russell<sup>2</sup>, and M. Hoppe<sup>2</sup>

<sup>1</sup>Space Sciences Department, TRW Defense & Space  
Systems Group, Redondo Beach, California 90278

<sup>2</sup>Institute of Geophysics & Planetary Physics,  
University of California, Los Angeles, Los Angeles,  
California 90024

May 1979

Space Sciences Department  
TRW Defense & Space Systems Group  
One Space Park  
Redondo Beach, California 90278

MAGNETIC FIELD ORIENTATION AND SUPRATHERMAL ION  
STREAMS IN THE EARTH'S FORESHOCK

by

E. W. Greenstadt, C. T. Russell, J. T. Gosling,  
M. Hoppe, and G. Paschmann

ABSTRACT

The different populations of backstreaming ions found earlier with ISEE instruments outside the earth's bow shock are organized by the orientation of the IMF to shock in the plane containing  $B_{SW}$  and the solar ecliptic X-axis (the B-X plane). The associations of ion classes with field geometry and shock structure are shown by means of computer-drawn three-dimensional sketches. Particles of several KeV, or about ten times the solar wind streaming energy, left the shock as "reflected" beams in a guiding center direction determined by  $B_{SW}$  and the interplanetary drift velocity. Their area of departure was the part of the shock where the transition from quasi-perpendicular to quasi-parallel structure began. Slightly farther toward the quasi-parallel portion of the shock, particles of lower energy escaped upstream, widening the ion spectra, exciting small magnetic waves, and forming a class of "intermediate" ions. Finally, in direct connection with the quasi-parallel structure, ions leaving the shock formed the "diffuse" group, containing a wide distribution of energies including high values well beyond any recorded in the other two classes. Sources of the various ion groups are postulated.



## INTRODUCTION

One of the striking early successes of the ISEE 1,2 mission has been the revelation that return ions, that is, ions streaming into the solar wind away from the bow shock, are comprised of separate classes having distinguishable energy and directional distributions (Gosling et al., 1978). Further, each of these classes of return ions, which are essentially all protons, is associated with its own level of upstream magnetic wave activity (Paschmann et al., 1979).

The general formation and variable location of the wave and particle foreshocks have been known to be determined by the relationship of the interplanetary magnetic field (the IMF, or  $B_{SW}$ ) to the bow shock. For an account of the pre-ISEE status of upstream wave and particle observations, the reader is referred to Greenstadt (1976) and Diodato et al. (1976). It was no surprise, therefore, that preliminary calculations indicated that the classes of ions were themselves associated with distinguishable local field-to-shock orientations, as represented by cone angle  $\theta_{Bn}$  between  $B_{SW}$  and the local normal (Paschmann et al., 1979; Gosling et al., 1979), and by the more sophisticated representations of Bonifazi et al. (1979). The purpose of this report is to supplement the rudimentary calculations of Paschmann et al. and Gosling et al. with a graphic description of the geometry of shock and field, to show that the geometry appears to govern the particle and wave classes, and to clarify the relationships between them and shock structure. Where the companion paper by Bonifazi et al. assumes the geometric relationship and parametrizes it in a general way, we attempt here to demonstrate the framework with specific particle pathways.

This report presents a series of schematic figures depicting the IMF-shock geometry for selected instants during the first two hours of ISEE particle data of 8 November 1977, published in Figure 3 of Paschmann et al., (1979). Two examples were selected for each of the four identified types of ion distribution: reflected, diffuse, intermediate, and none, according to the nomenclature of Paschmann et al. Similar figures corresponding to the various distributions in the other figures of Paschmann et al. have been examined; these corroborated the samples shown here.

The basis for the diagrams used herein is the motion of charged particles leaving the shock with guiding center velocities along  $B_{SW}$ , and subject to the electric field  $E_{SW} = -m/q(V_{SW} \times B_{SW})$ . The guiding center velocity  $V_{gc}$  of a proton can be represented as

$$V_{gc} = p_0 V_{SW} \hat{B}_{SW} + V_{SW} \sin \theta_{XB} \hat{D}, \quad (1)$$

where unit drift vector  $\hat{D} \equiv \hat{E}_{SW} \times \hat{V}_{SW}$ ;  $p_0 V_{SW}$  is the component of  $V_{gc}$  along  $B_{SW}$  written as a multiple  $p_0$  of the solar wind speed, and  $\theta_{XB}$  is the angle between  $X$  (i.e.,  $-V_{SW}$ ) and  $B_{SW}$ . For development of the reflected proton trajectory, see Benson et al. (1975). The result is that ions returned to the solar wind move in a plane containing  $B_{SW}$  and  $V_{SW}$  or, if we neglect aberration,  $B_{SW}$  and the solar-ecliptic  $X$ -axis, i.e., the  $B$ - $X$  plane. For observations at a given point on the trajectory of ISEE, we are therefore interested in the particular  $B$ - $X$  plane through the spacecraft location and in its curve of intersection with the bow shock. The shock was based on the symmetrized model

$$\rho^2 = Y^2 + Z^2 = .331 [(X - 75.25)^2 - 3686] \quad (2)$$

described by Greenstadt et al. (1975), and its location approximated in each case by scaling the subsolar point with the solar wind velocity  $V_{SW}$ , density  $N$ , and field magnitude measured by ISEE in the expression

$$R_o = 101 (1 + 1.1 \frac{M^2+3}{4M^2}) / (NV_{SW})^{1/6} \quad (3)$$

where  $R_o$  is the distance to the subsolar point of the bow shock and  $M$  is the magnetosonic Mach number (Formisano et al., 1973). The constant 101 was chosen to match the nominal model, and the  $\gamma$  in the formula of Formisano et al. was taken as 5/3. Values of  $V_{SW}$  and  $N$  were close to 275 Km/s and  $13 \text{ cm}^{-3}$  for all the cases discussed here.

#### DATA

The IMF  $B_{SW}$  and its three solar-ecliptic frame components that accompanied the varieties of upstream ions defined by Gosling et al. (1978) and Paschmann et al. (1979) for 8 November 1977 are plotted in Figure 1. The shaded columns labeled R, IM, and D duplicate the designations given by Paschmann et al. (1979, Figure 3), and signify reflected, intermediate, and diffuse ions, respectively. The qualities of these classes were described in the cited reports and can be seen best in Figure 1 of Gosling et al. (1978). Some characteristics of the classes will be recalled in later paragraphs. We assume that in the interval 1855 to 2045 UT the location of the shock did not change radically after it had been last seen at 1853, since, as already noted, both  $V_{SW}$  and  $N$  remained essentially constant during the interval, as did  $B_{SW}$  also.

We see in Figure 1 that each change in the type of particle observed was accompanied by some shift or drift in the average value of one or more components of the IMF, although the opposite was not necessarily true; that is,

not every shift in  $B_{SW}$  produced an alteration in particle class. It is best to keep in mind, however, that while the bars define valid generalization about the classes of ions measured, there were moderate variations in the actual spectra during the tenure of each class, requiring somewhat flexible definitions, and exhibiting occasional, but rare, transitory exchanges of category.

The lower case letters a to h in Figure 1 designate the eight times at which the field/particle geometry are displayed and analyzed in this report. They were chosen to be typical of each ion category. The number just below each letter gives the angle  $\theta_{Bn}$  between the IMF and the local normal of the model shock of equations (2) and (3) at that time.

#### PRESENTATION

Figure 2 illustrates the field geometry in a reflected particle beam and also defines the format in which the information of this report will be presented. At left is a three-dimensional sketch of the bow shock showing the orientation of the B-X plane through the observation point and its curve of intersection, C, with the shock. The shock is indicated in the figure by two outlines intersecting at the subsolar point, one in the ecliptic (X-Y) plane, the other in the vertical noon-midnight (X-Z) plane. A portion of the X-Y plane is shown to contrast with the tilted B-X plane above it. The point of observation at the time to which this particular sketch applies is denoted by an "O" (actually a small square computer symbol "□") situated on curve C, west of the X-Z plane.

The sketch at right was made by simply replotting the section of C containing the observation point on an enlarged scale, so it is seen, as if with a "zoom" lens, from the same viewpoint as at left. The enlarged figure shows the directions of  $\underline{B}$  and the guiding-center motion of reflected particles, P, through O, in the B-X plane, according to equation (1). The direction P was obtained by assuming that return protons passed outward through the observation point with velocity components (anti-) parallel to  $\underline{B}$ , equivalent to an observed energy of 3 keV. The dashed line represents a foreshock boundary defined as the forwardmost path possible for 3 keV particles leaving the shock along  $\underline{B}$ .

#### DIAGRAMS

Beam cases. The diagram shown in Figure 2 corresponds to case a, at 1855 UT, in Figure 1. The reflected beam appeared from the solar and eastern quadrants, principally the latter (Gosling et al., 1978). The beam energy ranged from about 1 keV to over 3 keV (op cit.), but an arrow describing 1 keV particles would actually pass inside the nominal shock, so protons of that energy should not have escaped upstream. It seems likely that the extremes of the recorded energy band corresponded to protons of nonzero pitch angle whose parallel components occupied a narrower energy range. That is, we imagine escaping protons having had a range of energies divided between parallel and perpendicular motion with respect to  $\underline{B}$ . Some particles at either extreme of the range of parallel energies would have had nonzero pitch angles and have been detected with total energies a little above the maximum or below the minimum that applied to the guiding centers. The value 3 keV

was therefore chosen as an approximate upper limit for guiding-center contributions to the measured beam. Protons of less energy would have followed paths closer to tangency and would have originated on the shock, sunward from the foot of the 3 KeV arrow.

A second case of a particle beam, case b at 1902 in Figure 1, is shown in Figure 3. At that time the B-X plane, left of Figure 3, had a greater tilt to the ecliptic than in case a, but the relationship of  $\underline{B}$ , P, and C were substantially the same, as seen in the detail at right. In this sketch the path of 2 KeV protons has also been depicted, together with its corresponding foreshock boundary. The peak energy of the beam was probably close to this value.

Null cases. Two cases from intervals in which no return particles were recorded are drawn in Figure 4. The cases are c and h, at 1913 and 2040 (Figure 1). Note that the B-X planes in these cases, and the distances of O from C and from the line of symmetry of C, were quite different even though the null observation was the same at both times. The details in Figure 4 show that in both cases the 3 KeV paths did not intersect the shock so that protons of even the highest parallel energies recorded in the beams earlier could not have reached the point of measurement. None did. The dashed tangent lines representing the foreshock boundary for 3 KeV particles demonstrate that the observations were outside that boundary at those times.

Diffuse cases. Two cases, f and g, of diffuse protons at 2010 and 2030 are conceptualized in Figure 5. Once again, the B-X planes and the global observation geometry associated with them were vastly different from one another. The local field geometry, however, which depended also on the X-component of  $\underline{B}$ , produced similar particle situations in the two cases. In

case f, paths of 1, 3, and 10 keV particles are shown, together with the 1 keV foreshock boundary; the diffuse spectrum ranged from about .6 keV to beyond the 10 keV limit of the Los Alamos particle record (Gosling et al., 1978). We picked a 1 keV lower limit as a round number, allowing for an unknown contribution from non-zero pitch angles. Higher energy particles would simply have streamed along lines closer to  $\mathbf{B}$  because of proportionately smaller contributions from the drift velocity. The 1 keV foreshock boundary would presumably have been near the closest tangent pathway; higher energy protons would have had larger foreshocks.

In the detail of case g, the viewing angle made it impractical to display more than the 1 keV particle path, which is already close to  $\mathbf{B}$ . Virtually the entire upstream region constituted the 1 keV foreshock.

Intermediate cases. Figure 6 exhibits two cases, d and e, at 1923 and 1950, from the section designated intermediate by Paschman et al. (1979). The IMF changed little during the intermediate section and the two images are substantially the same: the particles ranged from a few hundred eV to about 3 keV, and the details of Figure 6 show that the observation points were on or just inside the 1 keV foreshock boundaries.

## DISCUSSION

Reflected beams and mixed beams. During the interval described here, return particle beams contained energies from about 1 KeV to 3-4 KeV and entered the detector from the eastern and, to a lesser extent, the solar quadrants. "Intermediate" particles extended from a few hundred eV to about the same upper limit as the beams, 3-4 KeV, and entered the detector from the eastern, and in lesser intensities, the antisolar and solar quadrants.

The diagrams suggest an explanation: the shock stopped, trapped, and circulated (through its "foot") a subset of the solar wind protons which were accelerated by the interplanetary electric field to energies about 10 times the solar wind streaming energy. These protons slid westward along the shock surface until, in the region where the angle between the IMF and the surface expanded to about  $40^\circ$ , they were released, escaping upstream along  $\mathbf{B}$  with drift  $\mathbf{D}$ . (In terms of the conventional complementary angle of the shock normal,  $\theta_{Bn} \approx 50^\circ$ .) The escaping particles were not released exactly along  $\mathbf{B}$ , but with a moderate distribution of nonzero pitch angles. Some of these particles, or others trapped about where the first were released, escaped a little farther to the west, up to where the IMF made an additional  $10^\circ$  or so with the surface ( $\theta_{Bn} \approx 40^\circ$ ). In this extended region, protons of lower energies, i.e., lower guiding center velocities, and greater pitch angles could also escape. Thus the intermediate group appear to have been a beam that had spread to lower energies and wider angles of entry at the detector by virtue of relaxed containment geometry at the shock, or, more accurately, a mixture of beams from a larger area of the shock surface.

Diffuse ions. The diffuse ions ranged from a few hundred eV to energies beyond 10 keV. They entered the detector from all quadrants but with greatest intensity from the east. The diffuse ions therefore were a separable, if not independent phenomenon from the collimated, reflected particles at the forward edge of the proton foreshock. Strong geometrical support of this view is that the diffuse ion population included particles of high energies well above those found in the beams. Such particles could easily have escaped



the shock and reached the satellite with the beams, if they originated in the same place, but none was observed.

The angles, or range of angles,  $40^\circ \lesssim \theta_{Bn} \lesssim 50^\circ$  that appeared to separate the source of beam ions from that of diffuse ions are recognized as the same angles that separate quasi-perpendicular from quasi-parallel shock structure. Although the magnetic profile of the November 8 shock crossing at 1852:45, which has been displayed elsewhere (Russell and Greenstadt, 1978, Figures 15, 20), did not show the typical quasi-perpendicular step,  $\beta \approx 19$  was very high in this case and such a value of  $\beta$  has typically been associated with rapid, large amplitude fluctuations in the shock, even at large, nearly perpendicular  $\theta_{Bn}$  (Formisano et al., 1975). We therefore describe the crossing, with its connected reflection beam, as high- $\beta$ , quasi-perpendicular at  $\theta_{Bn} \approx 50^\circ$ .

True quasi-parallel structure has been tied closely to long period upstream waves (Greenstadt, 1976), which were not observed after the November 8 crossing, but were observed later in connection with smaller  $\theta_{Bn}$  and diffuse ions (Paschmann et al., 1979). We therefore associate the diffuse ions with quasi-parallel structure, although the latter structure could not be directly observed in these cases, the shock having already been left behind the spacecraft.

Ions and waves. The linking of diffuse ions, quasi-parallel structure, and upstream waves is supported by a simple calculation which at the same time relates the waves to the low, rather than the high, end of the backstreaming ion spectrum. The parameter  $p$  used in former studies to characterize the foreshock boundary (Greenstadt, 1972; Diodato et al., 1976) can be

found in terms of the guiding center energy of an observed return proton:

$$p = (E_r/E_{SW} - \sin^2 \theta_{XB})^{1/2} + \cos \theta_{XB}.$$

At 1923 (case d, Figure 6),  $p$  had the typical values listed in Table 1. In that case, the 1 keV foreshock boundary was tangent close to the subsolar point of curve C, where  $p \approx 1.6$  according to Diodato et al. (1976). This implies that the paths of particles a little below 1 keV were coincident with the boundary of the wave foreshock. Diodato et al. found in general that  $p$  averaged about 2 for the shock overall, a little less near the subsolar point, a little more toward the flanks. Calculations similar to the above were made for the other cases, with similar results. If we note that the intermediate cases, such as d, corresponded to the appearance of small wave activity (Gosling et al., 1979, Figure 10), we may infer that it was the 1 keV, or lower, contributions to the backstreaming ion populations that were closely associated with the familiar upstream wave activity outside the quasi-parallel shock. These contributions were marginally released upstream in cases of intermediate geometry and were a major part of the diffuse spectrum, where the waves were more pronounced.

We envision three models as potential explanations of the diffuse ions:

1. Origin in quasi-parallel structure. Since the q-parallel phenomena, including the diffuse ions, reign somewhere behind the foreshock boundary, the solar wind has already passed through beams of reflected ions and electrons before reaching the q-parallel region. These beams, made up of electrons and protons of diverse energies, are not necessarily co-located, implying the possible existence of charge separation potentials. Transit through the sunward foreshock beams may therefore in itself contribute to some scatter and acceleration of solar wind ions even before the large q-parallel waves are encountered. Then, typical large amplitude pulsations and upstream waves that

characterize the q-parallel shock could, through Fermi-mechanism or multiple acceleration by plasma wave bursts in wave gradients, energize a portion of the solar wind ions to tens of KeV; the pulsations themselves, and their associated upstream waves, would scatter the particles into a broad pitch angle distribution as they drift both upstream and downstream. Certainly, there is ample evidence that solar wind ion distributions are modified in the presence of the diffuse particles and their associated magnetic waves (Bonifazi et al., 1979).

2. Origins in quasi-parallel action on q-perpendicular, suprathermal ions. Some of the population of suprathermal ions up to  $10 E_{SW}$  created in the q-perpendicular shock and sojourning in its foot, of which the remainder escape and appear upstream as reflected beams, could slip further along the shock, or be convected downstream into the q-parallel structure where they could acquire additional energy through multiple accelerations and then be scattered upstream and downstream, essentially from the disturbed magnetosheath behind the parallel shock.

3. Origin in the magnetosphere. Through some magnetic pathway, ions of tens of keV in the magnetosphere, or at the magnetopause, could find their way into the magnetosheath where, in the region subtended by the q-parallel shock, their guiding centers could then be conveyed along the average field direction in the sheath (together with a drift) and into the upstream solar wind. As a result of strong scattering by q-parallel sheath pulsations they would appear as a population of diffuse suprathermal ions both in the sheath and in the foreshock.

Additional cases involving carefully selected spacecraft locations and analysis combining particle distributions with global and local field geometry will test these hypotheses.

## CONCLUSIONS

1. The quasi-perpendicular section of the bow shock accelerated solar wind ions up to about  $10 E_{SW}$  and released them into the upstream region about where  $\theta_{Bn} \approx 50^\circ$ , thus allowing ions with highest guiding center velocity to escape the shock.

2. Shock-accelerated ions appeared as a broader beam of lower energies and wider pitch angles from the section of the shock where  $40 \lesssim \theta_{Bn} \lesssim 50^\circ$ .

3. Diffuse ions were associated with the quasi-parallel section of the shock and included particles of energies  $> 10 E_{SW}$  not accelerated in, or more certainly not released from, the quasi-perpendicular section.

4. If we assume the concurrent existence of all specified upstream components observed only one-by-one in the data, the results are summarized by Figure 7 where, in a typical B-X plane the reflected beam (R), the mixed beam, or intermediate ions (IM), and the diffuse ions (D) are indicated by different shadings. Question marks designate areas where particle characteristics have not yet been recorded. For example, the amount and location, if any, of penetration by the boundary beam R of the foreshock into the diffuse ions is unknown. The field lines are shown as wavy in the foreshock outside the quasi-parallel region. The diffuse ions are known to penetrate the shock (Gosling et al., 1978), as depicted by their shading. It must be remembered that every plane parallel to the one illustrated would presumably exhibit the same configurations, forming together a three-dimensional form of which the sketch would be a single cross section. Finally, note that this empirical sketch is valid strictly where all the actual points of mea-

surements occurred near the nominal shock outline. The conceptual extrapolation to greater distances and other locations doesn't take into account the more subtle distinctions that might emerge from careful consideration of the differences between the three proposed explanations of the preceding DISCUSSION section or of Bonifazi et al. (1979). We believe new observations are too close to achievement to justify more detailed speculations at this time, and we hope to determine before long whether return ion scattering is proportional to distance from the nominal shock, from the foreshock boundary, or from the beam tangent point.

Table 1

Typical  $p$  Values for Intermediate Ion Energies at 1923.  $E_{SW} = 395$  eV,  
 $\theta_{XB} = 48^\circ$

$E_r$ (keV)	.6	1.0	2.0	3.0
$p$	1.5	2.0	2.7	3.3

## ACKNOWLEDGMENTS

Discussions with G. Moreno, C. Bonifazi, and D. Sentman were helpful.

This work was supported by NASW-3007, NAS5-20094, ...

## REFERENCES

- Benson, J., J. W. Freeman, H. K. Hills, and R. R. Vondrak, Bow shock protons in the Lunar environment, The Moon, 14, 19, 1975.
- Bonifazi, C., A. Egidi, G. Moreno, and S. Orsini, Backstreaming ions outside the earth's bow shock and their interactions with the solar wind, J. Geophys. Res., in press, 1979.
- Diodato, L., E. W. Greenstadt, G. Moreno, and V. Formisano, A statistical study of the upstream wave boundary outside the earth's bow shock, J. Geophys. Res., 81, 199, 1976.
- Formisano, V., P. C. Hedgecock, G. Moreno, F. Palmiotto, and J. Chao, Solar wind interaction with the earth's magnetic field. 2. The magnetohydrodynamic bow shock, J. Geophys. Res., 78, 3731, 1973.
- Gosling, J. T., J. R. Asbridge, S. J. Bame, G. Paschmann, and N. Sckopke, Observations of two distinct populations of bow shock ions in the upstream solar wind, Geophys. Res. Lett., 5, 957, 1978.
- Gosling, J. T., J. R. Asbridge, S. J. Bame, and W. C. Feldman, Ion acceleration at the earth's bow shock: a review of observations in the upstream region, Proc. Workshop on Particle Acceleration Mechanisms in Astrophys., January 1979.
- Greenstadt, E. W., Binary index for assessing local bow shock obliquity, J. Geophys. Res., 77, 5467, 1972.
- Greenstadt, E. W., Phenomenology of the earth's bow shock system. A summary description, Magnetospheric Particles & Fields, ed. B. M. McCormac, D. Reidel Publishing Co., Dordrecht, Holland, 13, 1976.

Greenstadt, E. W., C. T. Russell, F. L. Scarf, V. Formisano, and M. Neugebauer,  
Structure of the quasi-perpendicular, laminar bow shock, J. Geophys. Res.,  
80, 502, 1975.

Paschmann, G., N. Sckopke, S. J. Bame, J. R. Asbridge, J. T. Gosling, C. T.  
Russell, and E. W. Greenstadt, Association of low-frequency waves with  
suprathermal ions in the upstream solar wind, Geophys. Res. Lett., 6,  
209, 1979.

## FIGURE CAPTIONS

- Figure 1. The magnitude and components of the interplanetary magnetic field (IMF) during the upstream ion observations of Paschmann et al. (1979, Figure 3). Shaded sections cover intervals during which the three classes of return particle spectra, reflected, intermediate, and diffuse, were measured. The lower case letters mark times selected for the examples in the ensuing figures; angles  $\theta_{Bn}$  denote the orientations of  $\underline{B}$  to the local nominal shock normal at those times.
- Figure 2. The geometry of case a, corresponding to a beam of reflected ions. The three-dimensional diagram of the bow shock at left shows the B-X plane, its intersecting curve C, and the observation point O. Tic marks are at  $5 R_E$  intervals. The close-up at right of cross section C surrounding the observation point shows that the point was near the forwardmost origin of return-protons of 3 keV guiding center energy.
- Figure 3. The geometry of case b, for a reflected beam, showing both 2 keV and 3 keV boundaries relative to the observation point.
- Figure 4. The geometry of two cases, c and h, in which no return ions were detected. The observation points were outside the 3 keV boundaries.
- Figure 5. The geometry of two cases, f and g, when diffuse return ion distributions were recorded.
- Figure 6. The geometry of two cases, d and e, when intermediate return ion distributions were recorded. The observation points were within the respective 1 keV boundaries.



Figure 7. A representation of an inferred foreshock structure in the B-X plane. The cases (lettered circles) are indicated as if the structure, i.e., the IMF had been fixed and the observation point had moved around the shock.

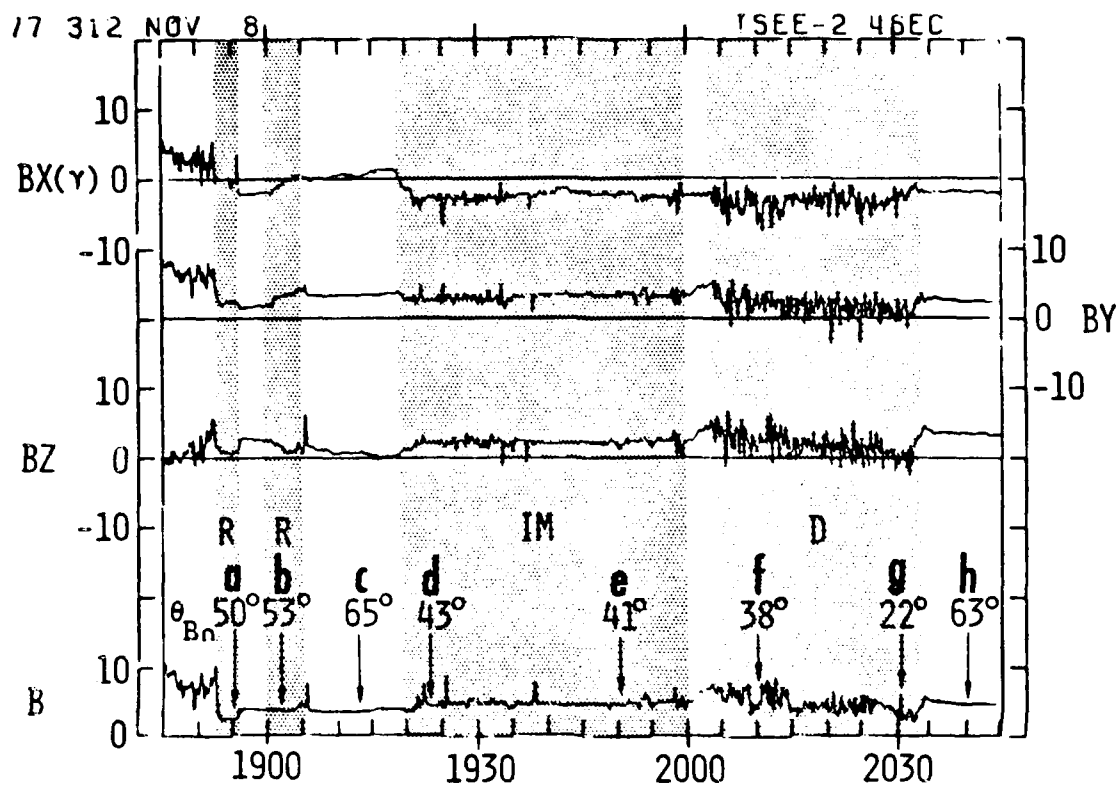


Figure 1. The magnitude and components of the interplanetary magnetic field (IMF) during the upstream ion observations of Paschmann et al. (1979, Figure 3). Shaded sections cover intervals during which the three classes of return particle spectra, reflected, intermediate, and diffuse, were measured. The lower case letters mark times selected for the examples in the ensuing figures; angles  $\theta_{Bn}$  denote the orientations of  $\underline{B}$  to the local nominal shock normal at those times.

AD-A092 369

TRW DEFENSE AND SPACE SYSTEMS GROUP REDONDO BEACH CA --ETC F/8 3/2  
A STUDY OF THE ASSOCIATION OF PC 3, 4 MICROPULSATIONS WITH INTE--ETC(U)  
NOV 77 E W GREENSTADT F49620-77-C-0018  
TRW-30435-6007-RU-00

UNCLASSIFIED

AFOSR-TR-80-1161

NL

2 2

2 2

2 2

2 2

2 2

2 2

2 2

2 2

2 2

2 2

2 2

2 2

2 2

2 2

2 2

2 2

2 2

2 2

2 2

2 2

2 2

2 2

2 2

2 2

2 2

2 2

2 2

2 2

2 2

2 2

2 2

2 2

2 2

2 2

2 2

2 2

2 2

2 2

2 2

2 2

2 2

2 2

2 2

2 2

2 2

2 2

2 2

2 2

2 2

2 2

2 2

2 2

2 2

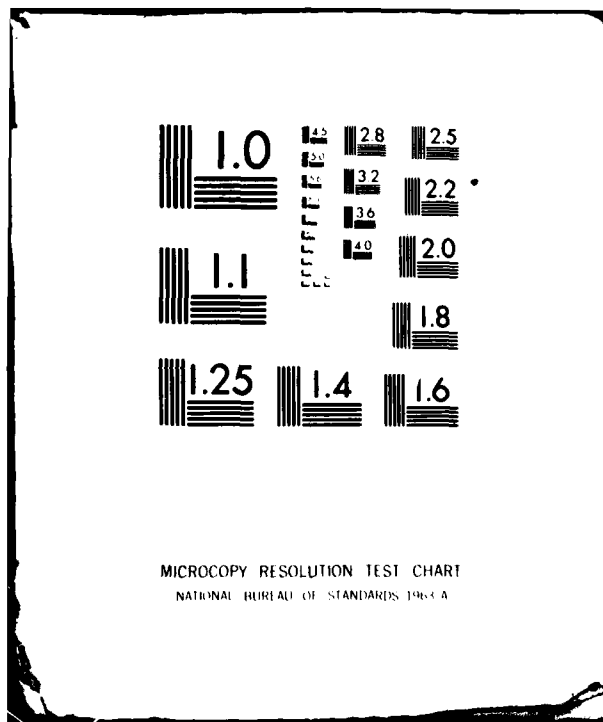
2 2

2 2

2 2

2 2

END  
DATE  
FILMED  
181  
DTIC



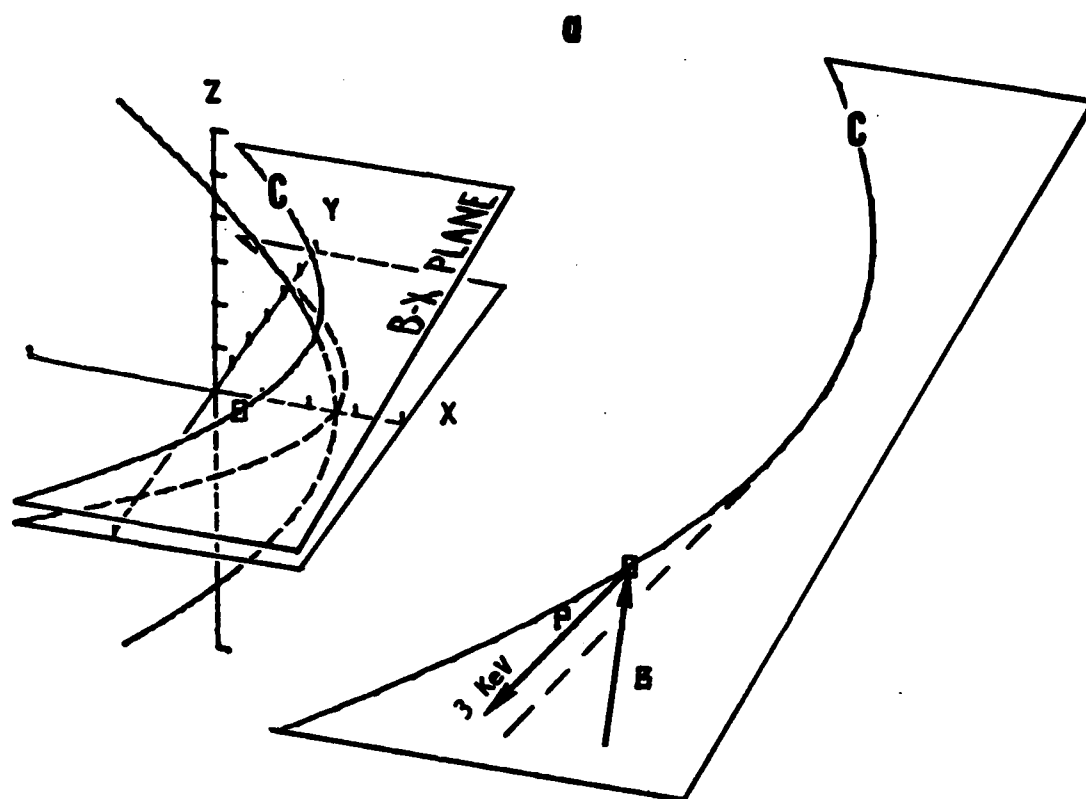


Figure 2. The geometry of case a, corresponding to a beam of reflected ions. The three-dimensional diagram of the bow shock at left shows the B-X plane, its intersecting curve C, and the observation point O. Tic marks are at  $5 R_E$  intervals. The close-up at right of cross section C surrounding the observation point shows that the point was near the forwardmost origin of return-protons of 3 keV guiding center energy.

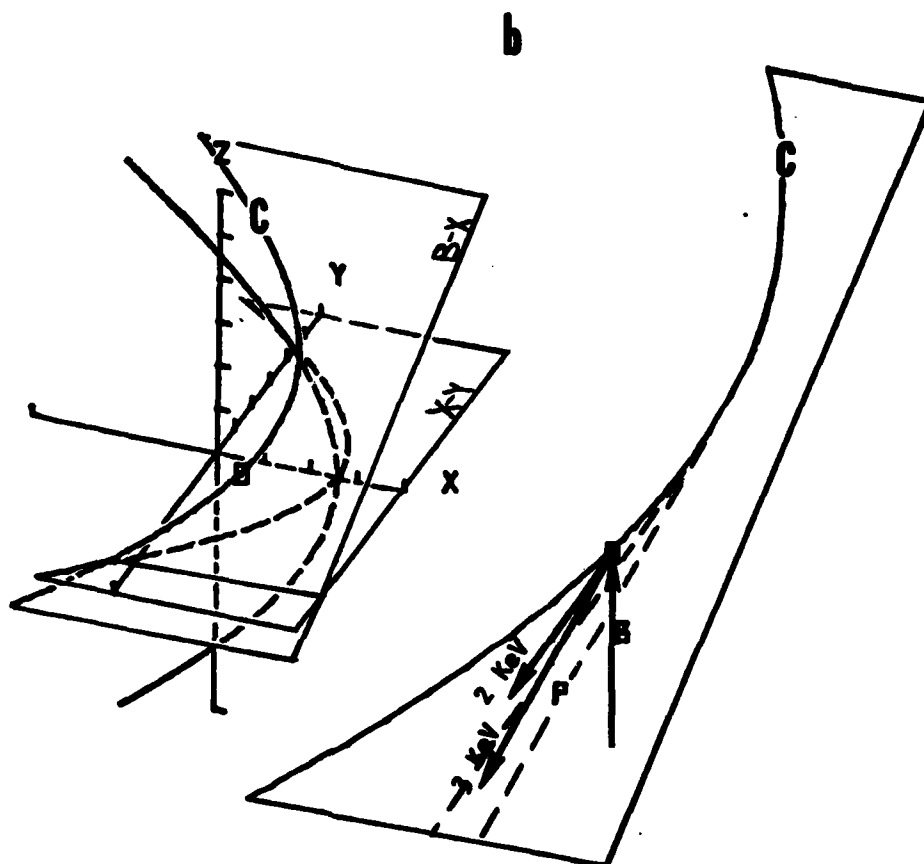


Figure 3. The geometry of case b, for a reflected beam, showing both 2 keV and 3 keV boundaries relative to the observation point.

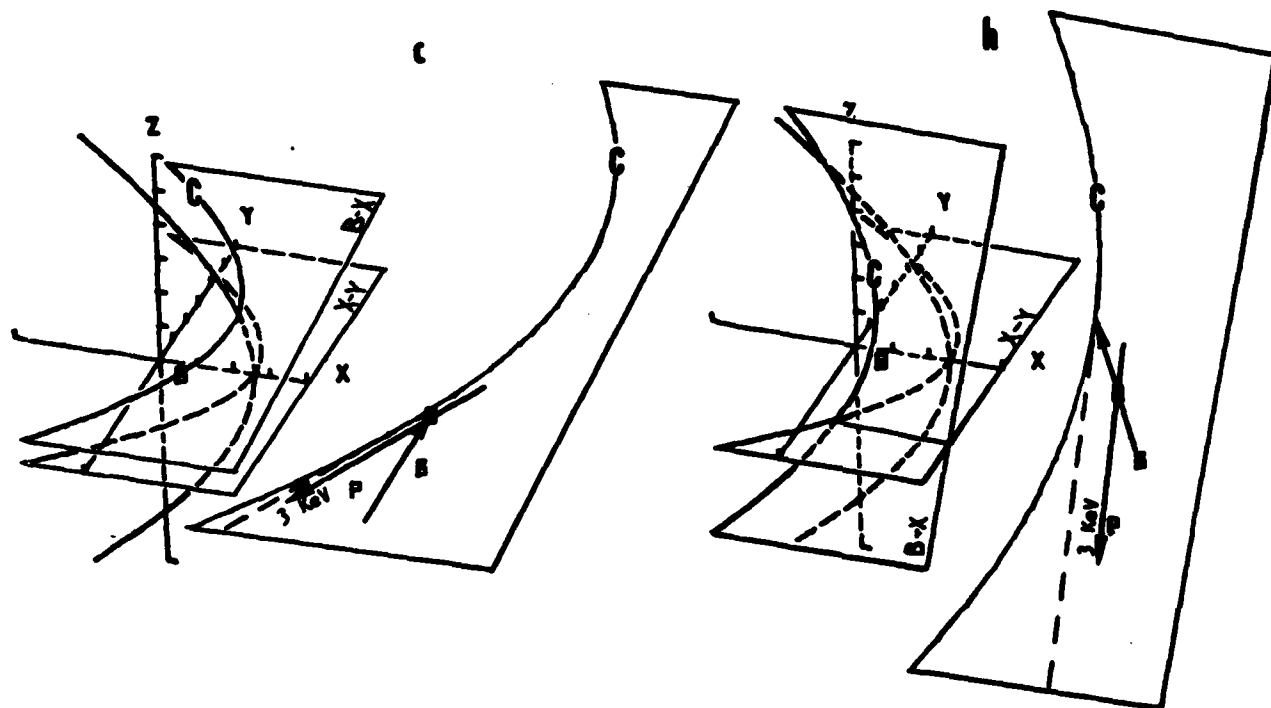


Figure 4. The geometry of two cases, c and h, in which no return ions were detected. The observation points were outside the 3 keV boundaries.

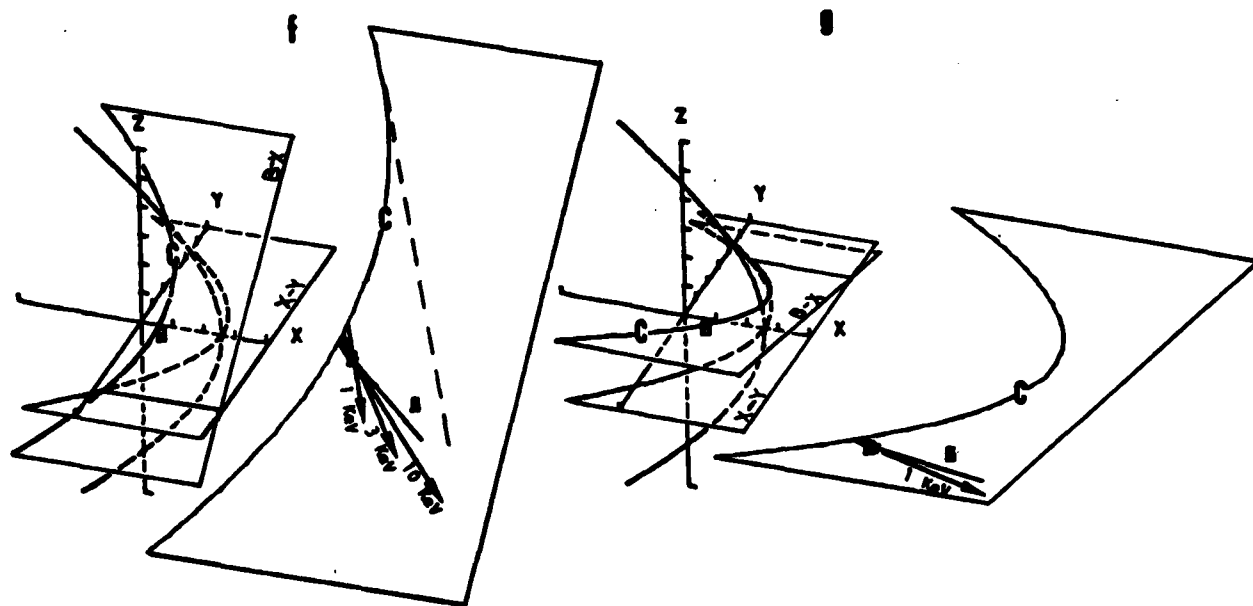


Figure 5. The geometry of two cases, f and g, when diffuse return ion distributions were recorded.



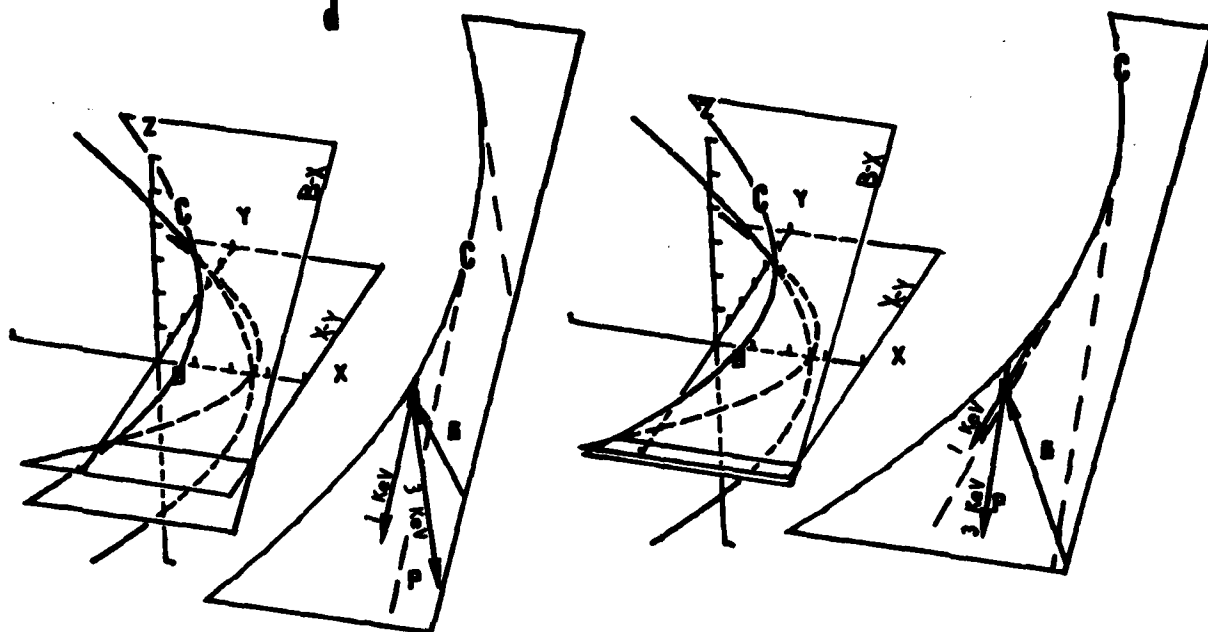


Figure 6. The geometry of two cases, d and e, when intermediate return ion distributions were recorded. The observation points were within the respective 1 keV boundaries.

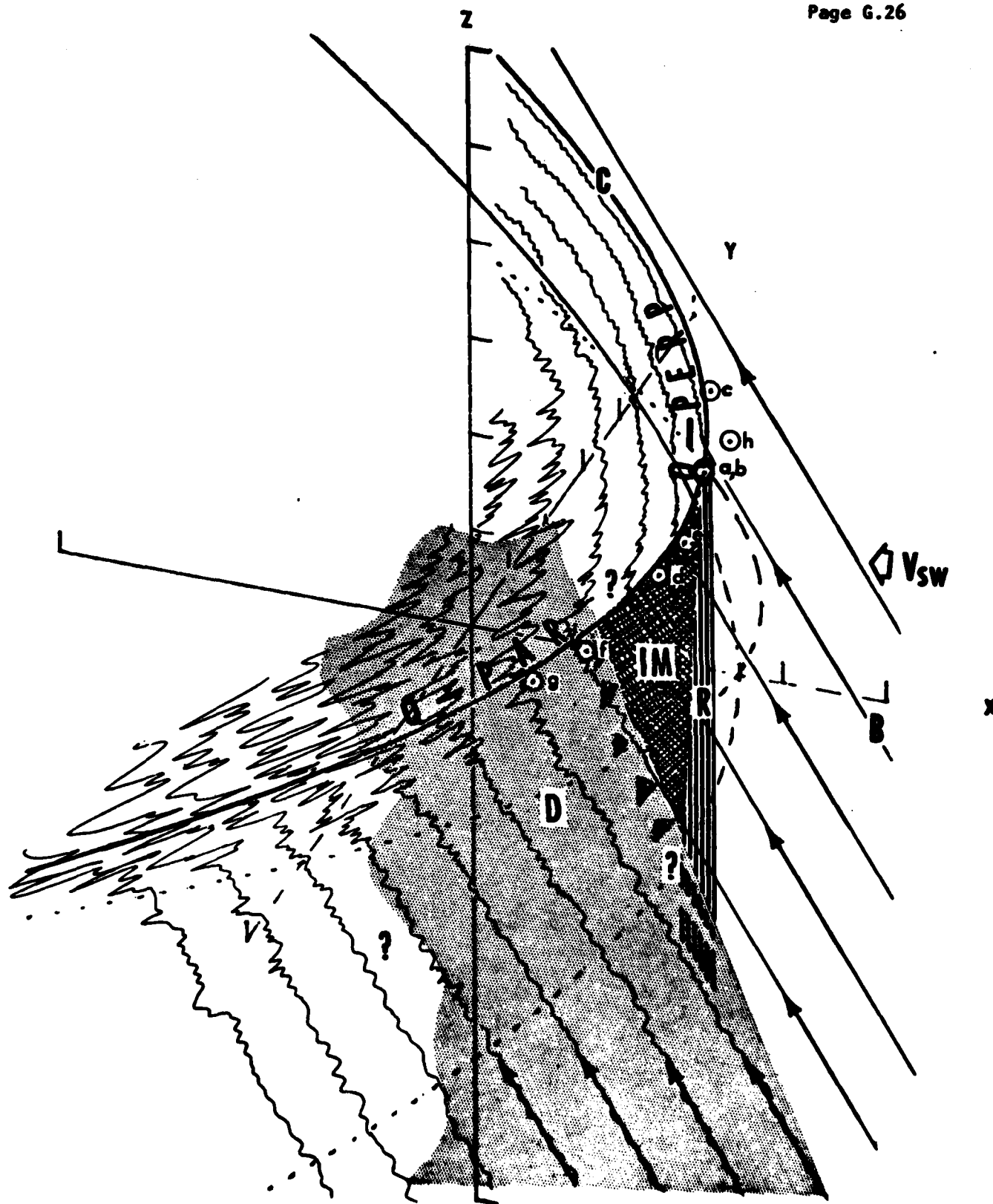


Figure 7. A representation of an inferred foreshock structure in the B-X plane. The cases (lettered circles) are indicated as if the structure, i.e., the IMF, had been fixed and the observation point had moved around the shock.

**APPENDIX H**

**CURRENT INVESTIGATION OF THE MID-PERIOD GEOMAGNETIC  
PULSATIONS AND POTENTIAL USE OF THE AFGL NETWORK**

# CURRENT INVESTIGATION OF THE MID-PERIOD GEOMAGNETIC PULSATIONS AND POTENTIAL USE OF THE AFGL NETWORK

E. W. Greenstadt

Space Sciences Department  
TRW Defense & Space Systems Group  
One Space Park  
Redondo Beach, California 90278

Medium-period geomagnetic pulsations are generated in the interaction between the solar wind and the magnetosphere, in the magnetosphere, or in both, and their characteristics are controlled by conditions in the solar wind, in the magnetosphere, or in both. Determination of what the correct relationships are between pulsations and the geomagnetic environment is currently under study by several groups, following older, pioneering work by Soviet investigators (Troitskaya et al., 197a; Gul'el'mi et al., 1973).

There is little doubt that some connection exists between the solar wind and pulsation activity at earth's surface. An example is shown in Figure 1. These

SOLAR WIND DEPENDENCE OF Pc3 OCCURRENCE

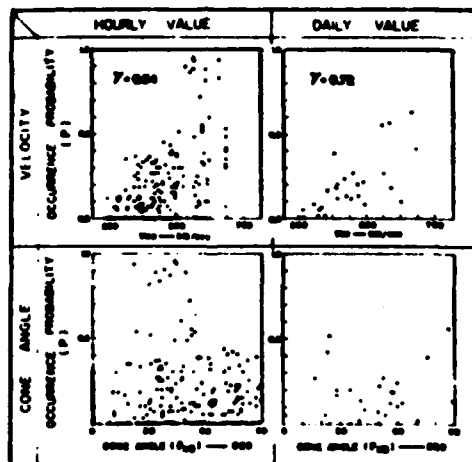


Figure 1

results by Saito et al. (1979) with hourly solar wind and pulsation data (left panels) virtually duplicate those by Greenstadt et al. (1979) and Wolfe et al., (1978). Pc 3 amplitude rises with  $V_{sw}$ , top left, and with decreasing cone angle  $\theta_{XB}$ , bottom left. The inverse correlation with  $\theta_{XB}$  clearly improves when  $\theta_{XB} \leq 50^\circ$ , but strong scatter has affected all studies. Cone angle  $\theta_{XB}$  is the angle between the IMF and the solar ecliptic X-axis. Part of the scatter may arise from the time scale of IMF orientation changes, which is generally much less than an hour. Hence the daily data in the right panels show little of interest.

There are two principal models for external stimulation of magnetospheric waves and pulsations, shown in the sketch at left of Figure 2. One model uses

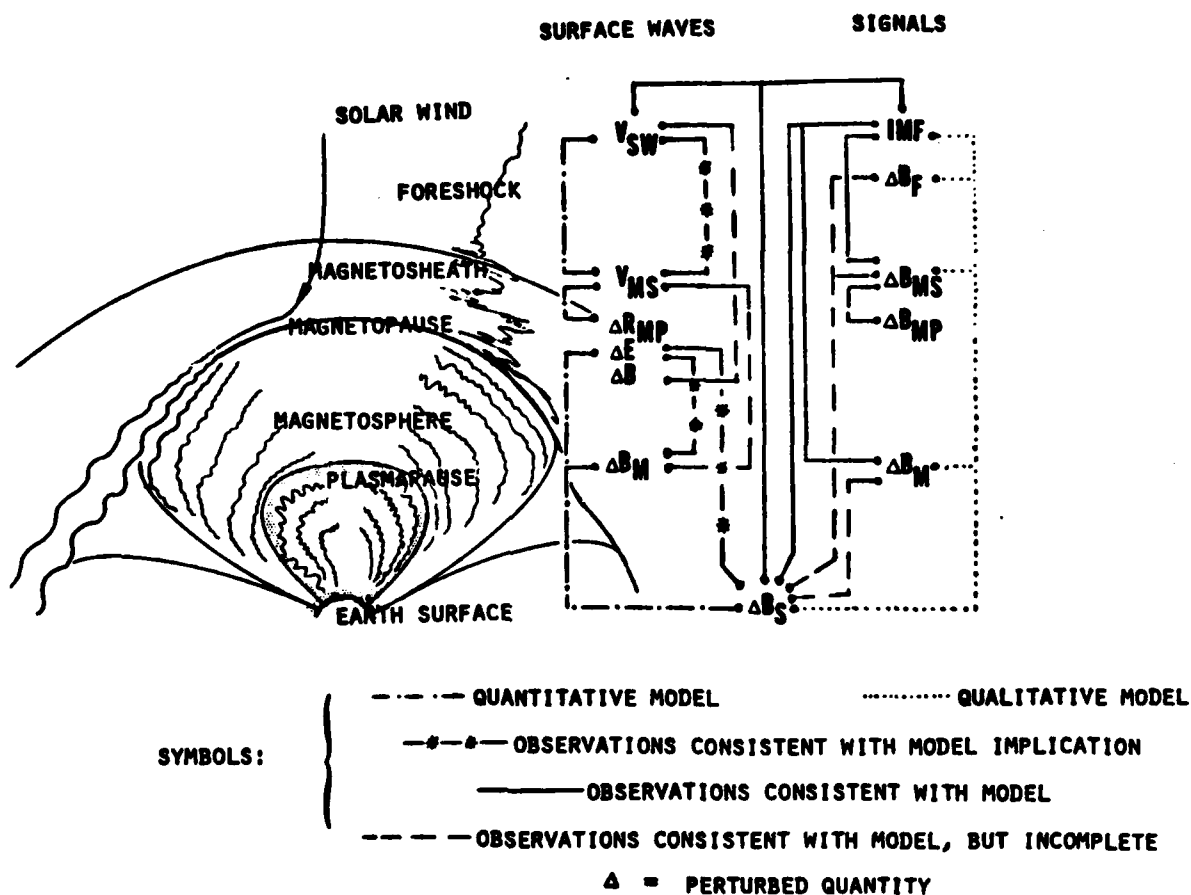


Figure 2

the solar wind velocity to drive magnetopause surface waves (Kelvin-Helmholtz); the other assumes that waves forming part of the quasi-parallel bow shock structure are transmitted into the magnetosphere. The diagram at right shows the various stages of physical participation each model requires and which ones have been linked by observation so far. A more complete account of the contributions to the connections in the center of the right-hand diagram of Figure 2 has been given by Greenstadt (1979).

The next stage of investigation of pulsation origin should include the following tasks:

1. Improvement of wave (K-H) model in noon-midnight meridian. Theoretical work on this model has concentrated on the equatorial plane, but there is

evidence that the noon-midnight boundary is an important source of magnetospheric waves.

2. Quantitative development of signal model. The signal model needs to be developed further to produce quantitative estimates that can be observationally tested.

3. Definition and refinement of surface-based "input level." Some means of conditioning and combining pulsation records from ground stations is needed that will characterize the global pulsation activity level as  $a_p$  does the global magnetic storm activity level.

4. Correlation of input level with solar wind parameters. The global pulsation measure, once defined, should be used to refine and improve the one-station correlations, such as those in Figure 1.

5. Tracing of signals through plasma regimes. Spacecraft observations should be used in an attempt to actually document the passage of specific signals from the solar wind or the magnetopause to the ground.

A statistical effort to link waves in the magnetosheath to pulsations via the same relationships already studied has been made recently. In Figure 3 we see that the correlation of signal amplitude with cone angle has been extended by Saito *et al.* (1979) to the magnetosheath, central panel, where signal power is highest for lowest  $\theta_{XB}$ . Signal power was also found to correlate inversely with angular distance  $\alpha$  from the subsolar line in the magnetosheath, right panel. Such statistical correlations need to be enlarged, and particular events in the sheath should be sought and studied.

$\theta_{XB}$  -  $\alpha$  - DEPEND. OF  $P_{MAX}$  IN THE MAGNETOSHEATH

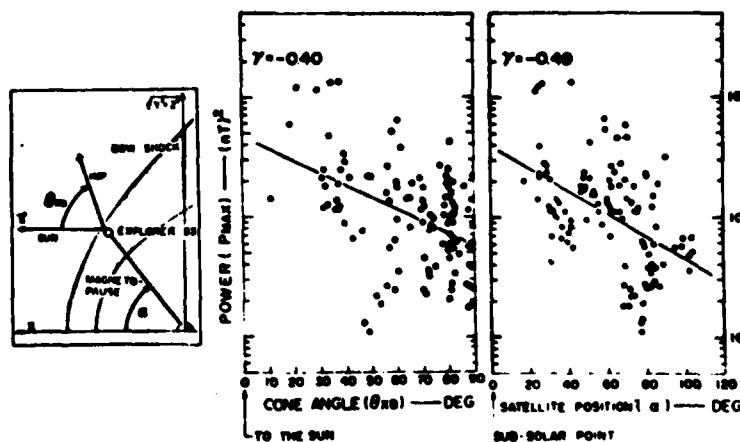


Figure 3

The Air Force's magnetometer system may be expected to make significant contributions to items 3, 4, and 5, above. One necessity for improved data on pulsation origin, both for statistical and individual-case approaches, is a set of ground stations insulated from the strongest sources of geomagnetic variability but responsive to wave signals. Some latitude may be much better than others, as illustrated in Figure 4. Pulsation period, which varies with geomagnetic latitude, at left, is also subject to dynamic variation caused by changing plasma density in the plasmatrough. This dynamic variability affects pulsation amplitudes through changing resonance periods and is probably responsible for much of the scatter in correlation diagrams. Diurnal contributions to the plasmatrough variation are seen in Figure 4 at right, where characteristic density enhancements are visible at certain local times. Both figures are from Orr (1979). The observatory symbols under the left figure

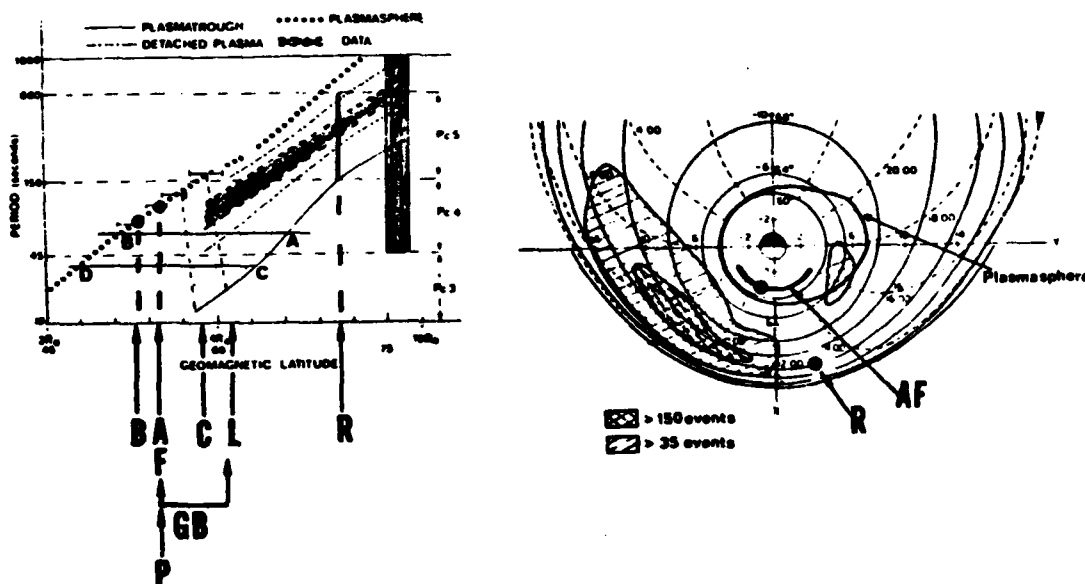


Figure 4

show the locations of the Air Force chain (AF) and most of the stations responsible for the solar wind parameter correlations. The stations, or station chains, are: Borok; Pittsburg, N. H.; Great Britain; Calgary; Leduc; Ft. Reliance. We may infer that the Air Force chain is advantageously situated for monitoring Pc 4 comparatively free of plasma trough variability. Ft. Reliance, or any station at about 70°, may also be a good site for monitoring Pc 5 in the afternoon.

The AFGL system should be equipped with the computing and communication hardware, software, and staff necessary to take advantage, through internal or external usage, of its unique potential.

# REFERENCES

- Greenstadt, E. W., The solar wind and magnetospheric waves, Magnetospheric Study 1979, Proc. Int'l Workshop on Selected Topics of Magnetospheric Physics, Tokyo, 160, Japanese IMS Committee, 1979
- Greenstadt, E. W., H. J. Singer, C. T. Russell, and J. V. Olson, IMF orientation, solar wind velocity, and Pc 3-4 signals: a joint distribution, J. Geophys. Res., in press, 1979.
- Gul'yel'mi, A. V., T. A. Plyasova-Bakunina, and R. V. Shchepetnov, Relation between the period of geomagnetic pulsations Pc 3, 4 and the parameters of the interplanetary medium at the earth's orbit, Geomag. & Aeron., 13, 331, 1973.
- Orr, D., Geomagnetic pulsations and their relationship to structure within the magnetosphere, Magnetospheric Study 1979, Proc. Int'l Workshop on Selected Topics of Magnetospheric Physics, Tokyo, 124, Japanese IMS Committee, 1979.
- Saito, T., K. Yumoto, T. Tamura, and T. Sakurai, Solar wind control of Pc 3, Magnetospheric Study 1979, Proc. Int'l Workshop on Selected Topics of Magnetospheric Physics, Tokyo, 155, Japanese IMS Committee, 1979.
- Troitskaya, V. A., A. V. Gul'el'mi, O. V. Bolshakova, E. T. Matveyeva, and R. V. Shchepetnov, Indices of geomagnetic pulsations, Planet. Space Sci., 20, 849, 1972.
- Wolfe, A., L. J. Lanzerotti, and C. G. MacLennan, Dependence of hydromagnetic energy spectra on interplanetary parameters (Abstract), EOS, 59, 1166, 1978.



**APPENDIX I**

**LETTERS TO DR. SAGALYN**

**TRW**

Page 1.1

79-4351.6-59  
Bldg R-1, Rm 1176  
19 April 1979

Dr. Rita Sagalyn, Chief  
Plasmas, Particles & Fields Branch  
AFGL  
Hanscom AFB, MA 01371

Dear Dr. Sagalyn:

Thank you for the opportunity to attend AFGL's geomagnetic workshop, 6-7 April. I thought the workshop informative, productive, and worthy of repetition. What more can be said?

Here are my answers to the items on your list of questions. Each reply is cast in the frame of my own project rather than in the full generality of the questions, which I presume are best answered in total by a panel or a composite of such individual responses.

To define my own project briefly, I am attempting to determine whether geomagnetic pulsations can be related to solar wind parameters with sufficient precision, i.e., reproducibility, to allow either phenomenon to serve as measure, or even predictor, of the other. The attempt involves study of both the physical processes that may be involved in connecting the solar wind to the ground and of "rule of thumb" methods of correlation that may permit utilization of some sort of index while understanding of physical processes is still incomplete.

There is a body of experimental and model investigation, many years old, that supports the existence of a connection between solar wind properties and Pc 3,4,5 properties, but the connection is, with rare exception, tenuous and unreliable because of the multivariate nature of the problem and associated methodological difficulties.

The approach I see is to assume that pulsation amplitude  $\delta B$  (at a point on the surface) is a function  $\beta$  of several variables:

$$\delta B = \beta(T, \theta_{XB}, V_{SW}, t_L, \Lambda_M, B_Z),$$

where  $T$ ,  $\theta_{XB}$ ,  $V_{SW}$ ,  $t_L$ ,  $\Lambda_M$ , and  $B_Z$  are the pulsation period, IMF cone angle, solar wind velocity, local time, magnetic latitude, and north-south IMF

Dr. Rita Sagalyn

79-4351.6-59  
19 April 1979  
Page 2

component, respectively. The period in turn is itself a function  $\tau$  of some of the same variables for possibly independent reasons:

$$T = \tau(t_L, \Lambda_M, B_Z, B_{SW}),$$

where  $B_{SW}$  is the IMF magnitude. I use  $B_Z$  merely as a shorthand external indicator of geomagnetic activity level. One task, for the present, is to find the means, methodologically, to hold as many variables constant as possible while searching for improved correlations among the remainder. The AFGL chain holds promise of yielding data stabilizing  $t_L$ ,  $\Lambda_M$ , and  $\tau(t_L, \Lambda_M, B_Z)$ , considerably simplifying the investigation.

Now the answers to your questionnaire:

1.a Two types, more precisely, two scales of information are needed. First, relatively brief, say, two-hour to two-day intervals of data corresponding to identified events or sequences of events are needed for the study of the physical transmission of waves through the magnetosphere to the ground. Second, relatively lengthy intervals, say several hours of data each day for several months, are needed to develop and test pulsation-based indices of magnetospheric and solar wind parameters. Within either scale, the information content consists of the time and amplitude, or power, of signals in selected frequency bands.

1.b The information can be made available from fluxgate or induction coil recordings as plots, films, tapes (or listings), depending on the application. Plots and tapes can be made available by mail; taped data can also be made available by telephone line between computers.

1.c.i. Mid-latitude networks, i.e., stations equatorward of the plasma-pause like AFGL's, are advantageously situated to escape some of the extremes in variability of pulsation characteristics that affect stations connected to the plasmatrough. The most outstanding example is periodicity: a station at, say  $60^\circ$  magnetic latitude may pick up a resonant response in the low end of the Pc 3 band, at a Pc 3 amplitude, one day and the low end of the Pc 5 band, at a Pc 5 amplitude, the next day because of changes in density in the plasmatrough. How can such measurements be compared? Badly.

Dr. Rita Sagalyn

79-4351.6-59  
19 April 1979  
Page 3

To first order, the plasmasphere above the AFGL chain tends to be more stable than the trough further north so that the stations ought to pick up signals or resonances, if any, concentrated in the Pc 4 band. That should help, because the amplitude in the one band, from day to day, may be more directly relatable to differences in the level of input perturbation, or signal, at the magnetopause, and less to local variations in the magnetosphere. We do not belittle the prospect of getting one variable out of the way in this business. Further, if this approach works, it may become possible to calibrate some of the more refractory, high latitude data so as to make them more usable.

1.c.i.i. Additional reduction in variability can be achieved at certain local times, so an E-W chain increases the probability that some station will be in the optimal location often enough to build up an acceptable population of cases. This probability becomes even higher if Eskdalemuir (U.K.), for example, is considered as an eastern extension of the AFGL network.

1.c.i.i.i. For the explicit purposes I am enunciating, a sampling interval of 20 seconds and a processing interval of five to ten minutes to obtain, for example, maximal amplitudes or spectral estimates, would be adequate. This is relatively undemanding and is well within the resolution of the AFGL system.

1.d Ground-satellite coordinated measurements are necessary both for studying cases and for statistical analysis. If the AFGL chain yields a decent result, then network-network coordination, particularly between the AFGL and other stations at about  $70^\circ$  would be desirable.

2. Pulsations can be monitored by visual inspection of filtered or unfiltered plots, by representations of filtered signals in terms of amplitude levels, power spectral densities, or dynamic spectra (in order of increasing cost, complexity, and information content). Such representations can be displayed as plots or recorded on tape for further processing and analysis.

Dr. Rita Sagalyn

79-4351.6-59  
19 April 1979  
Page 4

Some types of pulsations, Pi 2 for example, may be predictive of substorms or even, we may speculate, of geosynchronous satellite anomalies. Predictions of this sort are in their infancy and require investigation and development.

3.a As far as pulsations are concerned, the inadequacy of existing indices lies in the current lack of such indices. Years ago, Saito devised a pulsation index he called Kc 3, based on Pc 3 measurements at one observatory, which correlated well with solar wind velocity. This development was never followed up and never expanded into a worldwide index. The IMS network offers an opportunity and, I believe, an obligation to attempt such a project.

3.b New indices should be devised, but it will not be an easy task. It must begin as simply as possible with improved correlations that will lead to selection or establishment of stations most suitable for a worldwide monitor system. It's quite possible that the Air Force chain will serve as the core bases for recording data that can be fashioned into a worldwide index, or at least a mid-latitude index.

4.a.&b. For the particular investigation and application I have in mind, satellite-ground calibration, and the reverse, are intrinsic elements.

5. Yes and No. Existing methods are adequate, but the AFGL system does not appear at present to be set up to use them. First-order processing, i.e., spectral selection of data has not yet been developed for either internal or external use, and phone-line callup capability has not been established for external use. There did not appear to be a research plan at AFGL, whose unfolding would automatically result in the above facilities. For further detail, see commentary below.

6.a Current ground based plans seem to be mixed. Some recordings have already been terminated; some will be discontinued at the end of the IMS; some after MAGSAT; some as budgets dictate. Some stations are just now designing improvements for the future, signifying an intention to continue recording indefinitely.

Dr. Rita Sagalyn

Page 1.5

79-4351.6-59  
19 April 1979  
Page 5

6.b What is required is largely unknown for the simple reason that there is a sizeable phase lag between recording and analysis of IMS data. Serious inadequacies of IMS data collection, if they exist, may not become evident for a year or two. One of the major accomplishments of the IMS, in which the AFGL chain shares, is a great improvement in acquisition and recording technique, which now is ahead of the capacity of the analysis community to absorb the data. Although several significant results have already come out of the IMS, the bulk of advances in both quantity and quality will undoubtedly arise in the early 80's.

My view is that recordings should continue toward solar maximum until analysis shows which deletions or changes will be profitable. Consider the Air Force chain and pulsations as an example: recent work has shown the global nature of some selected pulsation events; that is, several stations, both meridionally spaced and conjugate to each other, observed similar manifestations at the same time. Some of the data were displayed during the workshop. The distance limits on such similarity have not been established. It may be (it may not) that the eight AFGL stations could be replaced by four with no serious loss of information content, but I don't think we'll know until well after the IMS is over (see below).

#### COMMENTARY

AFGL has installed an advanced system of geomagnetic data collection in which the acquisition points are advantageously located for at least some important geomagnetic investigations. Further, the data gathering and storage scheme creates a file of data of superior organization and accessibility. The file so created contains gargantuan amounts of information which can be extracted only by advanced techniques of data processing. Fortunately such techniques are available today, and at far less expense than they were even a very few years ago.

Dr. Rita Sagalyn

79-4351.6-59  
19 April 1979  
Page 6

I was surprised, and disappointed, to find that certain kinds of processing had not been planned as an integral part of the AFGL facility from the outset. One purpose of the system is to record and apply field oscillations, but the basic content of the recordings from which any analysis begins is a summary of what oscillations are present at a given time. Even if the spectral content is not stored separately, and I think it definitely should be, the capacity to comb any given set of tapes for spectral content should be a routine library function fundamental to virtually any exploitation of the pulsation records, whether internally or externally originated.

In a sense, the entire AFGL net may be regarded as a single geomagnetic instrument whose application requires an associated calibration. I offer two illustrations: suppose someone is interested in studying a selected storm or substorm or a set of them -- some IMS intervals, say. The disturbance fields would be obtained by subtracting  $S_q$ . But what is  $S_q$  for each of the AFGL observatories? Any individual wishing to examine a particular interval can hardly be expected to make a bulk analysis of the entire library to find  $S_q$  before he can begin work on a two-day storm. A set of  $S_q$  curves or tables should be regarded as a calibration that's part of the system description. Similarly, there is a diurnal variation in baseline pulsation level that can be used to indicate the best hours for selecting passband data and the level above which pulsation events can be said to have occurred. Curves and tables of such variations should be part of the system description.

#### RECOMMENDATIONS

It may be my misunderstanding, but I though I received conflicting evaluations of the resources available for data processing at AFGL. Personnel at the Saturday afternoon pulsations workshop indicated that the kind of data conditioning I have mentioned would be beyond those resources. I understood from conversation with you, however, that it might be possible to support some data manipulation. Naturally, I prefer your interpretation. I recommend an investment in data conditioning, processing, description, and communication, as follows:

Dr. Rita Sagalyn

Page 1.7

79-4351.6-59  
19 April 1979  
Page 7

1. Library routines, or microprocessor hardware, for digital filtering of the data with selectable passbands, start, and stop times should be developed and debugged, or bought, with the utmost dispatch.

2. A capability of recording filtered output on tape, printed listings, and plotted graphs should be acquired. I really see no reason AFGL shouldn't be accumulating, storing, and perhaps even mailing out, the same sort of f-t diagrams that Onagawa and Kakioka are providing. I am attaching a copy of a sample page from Onagawa.

3. Average, quiet-time characteristics of each station at all accessible frequencies should be discovered, recorded, listed, and printed as part of the system description.

4. A capability of telephone line coupling that would permit external computer access to any stored data set should be established.

In sum, there is hope and, I believe, expectation that the Air Force magnetometer net can be a productive element in geomagnetic research and application, but some definite steps need to be made now to turn promise into reality.

Sincerely,

Eugene W. Greenstadt  
Space Sciences Department  
TRW Defense & Space Systems Group

EWG:mjl

enc: as indicated





DEPARTMENT OF EARTH AND SPACE SCIENCES  
3806 GEOLOGY BUILDING  
LOS ANGELES, CALIFORNIA 90024

June 22, 1979

Dr. Rita Sagalyn  
Air Force Geophysics Laboratory  
Air Force Hanscom Field  
Sudbury, Massachusetts 01776

Dear Rita:

Thank you very much for the opportunity to participate in the Geomagnetic Field Workshop held at the Air Force Geophysics Laboratory. I think the meeting was quite worthwhile and I hope our suggestions will be of use to you.

My impression of the magnetometer network was very favorable. The network seems to be working well and the quality of the data returned is high. The mini-computer system supporting the network is quite satisfactory. The data presently being acquired, as well as that previously archived, should be of great value in a variety of research projects.

I must say that I am disappointed that the laboratory is not making greater use of the network data than it is. This is surprising in as much as the Air Force has need for the kind of information this network can provide. In fact, the Air Force is supporting the Space Environment Laboratory in Boulder to satisfy such needs.

I am not sufficiently familiar with the organization or goals of the AFGL to know the responsibilities of your group. However, I suspect you are obligated to study geophysical phenomena with the eventual goal of quantitatively predicting environmental parameters on a basis of a few, simply-monitored variables. An example of what I mean would be predicting the size of the auroral oval from polarcap magnetic variations. It does not appear that the laboratory is very deeply involved in such activities at the present time, since no one at AFGL seems to have published any papers on substorms in the last four years.

I choose this criteria for evaluation because it has recently become clear that the fundamental element of geomagnetic activity is the magnetospheric substorm. I believe most transient changes in the ionospheric or magnetospheric environment of interest to the Air Force can be related to substorms in some way. While I see

Dr. Rita Sagalyn

-2-

June 22, 1979

great interest at AFGL in magnetic indices and their relationship to ionospheric parameters, no person there appears to be specifically studying the physical processes involved in substorms. As a consequence, no one has been able to define uses for the data from the magnetometer network.

To define possible uses for the network and its data I must try to answer the first question in your list of discussion topics, i.e., what are some of the important unsolved problems of magnetospheric physics. In my opinion, these include:

- 1) What causes the onset of a substorm expansion phase?
- 2) What controls where the substorm will occur, how big it will be, how long it will last?
- 3) What determines the properties of particles energized and injected by the substorm?
- 4) What are the mechanisms for redistributing injected particles?
- 5) What are the loss mechanisms for these particles?
- 6) How is the energy released by the substorm dissipated in the ionosphere?
- 7) What effects does this energy deposition have on the ionosphere?

As you know, many of us working on the subject of substorms have speculative answers to most of these questions, but based on inadequate data. You also know these models are quite controversial and are certainly far from being quantitative.

With regard to your second question of what information is needed to solve these problems, I suggest the following:

- 1) Better monitoring instruments with higher time and space resolution.
- 2) Better distribution of instruments such as ground networks and multiple satellites.
- 3) Better data acquisition techniques.
- 4) Better archiving and retrieval systems.
- 5) More support of researchers studying these problems.

As a specific example, I believe great progress could be made on the question of substorm onset mechanisms if we had an auroral imaging device producing high resolution pictures of the aurora at a rate of one per minute. Using solar wind, magnetospheric and ground network data obtained simultaneously, the auroral pictures would help immensely in deciding which models to use in interpreting our ground data.

To answer your questions of what contributions the AFGL chain of magnetometers can make to substorm studies, we must first ask in what ways is the chain unique. These include:

Dr. Rita Sagalyn

-3-

June 22, 1979

- 1) One of the few constant magnetic latitude chains in the world.
- 2) Identical instrumentation at all stations.
- 3) Instruments have high sensitivity and low noise.
- 4) Data is acquired at very high time resolution.
- 5) Exceedingly accurate relative timing at all stations.
- 6) Data are acquired and stored in real time.
- 7) There is an extensive historical data file.

Geomagnetic phenomena which can be studied with your data are those which produce strong magnetic perturbations at sub-auroral latitudes. These include substorm field aligned currents and pulsation phenomena associated with the plasmopause such as Pi 2 pulsations.

Both of these subjects are currently of great interest to magnetospheric physicists and appear to be closely related topics. The onset or the expansion phase of a magnetospheric substorm is characterized by a number of events including a short burst of Pi 2 pulsations and the formation of a wedge of field aligned current diverting a portion of the near earth tail current through the auroral oval. There is some evidence that the Pi 2 burst is the initial transient associated with the resonant properties of the circuit carrying this field aligned current.

Since the cause of the substorm expansion onset is not presently known, it is important to identify the processes which occur near the region of onset, at the time of onset. Pi 2 pulsations can be used in such studies because they define expansion onset times precisely. The AFGL network with its high sensitivity, low noise, high time resolution, accurate timing, and location just equatorward of the plasmopause is ideally suited for observations of Pi 2 pulsations. One important application of the network data would be to create a list of substorm expansion onsets for use in substorm research projects.

It is equally important to know where an onset occurs and how it subsequently develops. Information regarding this question can be obtained from the east-west magnetic variations (D component) measured along a constant magnetic latitude chain. The center of the sheet of field aligned current entering the ionosphere in the morning sector is near the longitude of maximum negative deviation in D, the center of the outward current near the longitude of maximum positive deviation in D, and the center of the current systems where the D perturbation is zero. The AFGL network is ideally located for determining such parameters when North America passes through the midnight sector.

The preceding comments partially answer one of your major questions, how can magnetic field data be used to monitor magnetic activity, pulsations, etc.

My preceding comments are also relevant to your question regarding possible new indices. Since the AFGL is of limited extent in

June 22, 1979

local time, it is not possible to generate planetary indices. However, the data can be used to generate indices during fixed intervals of universal time. For example, an important contribution the network data could make would be to produce pulsation indices for various types of magnetospheric wave activity. Specifically, a Pi 2 index of substorm activity could be generated by band pass filtering out the 60 second period band. An indirect monitor of solar wind characteristics could be generated by band pass filtering the Pc 3 band.

The final question I would like to touch on is that of data dispersal. I must say that it is here that the AFGL seems to be having the most difficulty. Until very recently, few persons outside AFGL had ever seen the data. Further, to my knowledge, very little had been done with it inside AFGL. The reason for these problems seems to be psychological. The individuals who have set up the system consider themselves scientists not support staff. Also it appears that the pressure on these individuals to utilize the data has not been sufficient, or that they have been otherwise occupied. Thus, while it is possible to acquire small amounts of data in graphical form, a request to study a major portion of the digital data would not be easy to satisfy.

The cheapest and easiest way for AFGL to disperse the data would be to duplicate the entire data file as it is and send it to the World Data Center in Boulder. Alternatively, AFGL can act as a data center filling requests as they come in; however, this requires staff specifically dedicated to this function. Still another alternative would be to provide a dial-up computer link so outside users could access the on-line data files. This method is limited by the amount of data kept on line, by the data transmission rates, and by the costs of dial-up link. It would also require software development to make possible the access by other computers.

Any of the above methods is unlikely to result in extensive use of the data file because of the costs involved in using the data. To obtain such use, AFGL will have to support the cost of research on the data base. Possible methods include:

- 1) Reassignment of current AFGL staff.
- 2) Addition of new AFGL research staff.
- 3) Visiting scientist positions.
- 4) Summer research positions.
- 5) Consulting arrangements.
- 6) Grants to universities or research organizations.

If the data are to be analyzed at AFGL, additional support must be put into the mini-computer facility in the form of dedicated programmers and additional hardware and software. Without this, AFGL's staff or visitors will not be able to access the data. In addition,

Dr. Rita Sagalyn

-5-

June 22, 1979

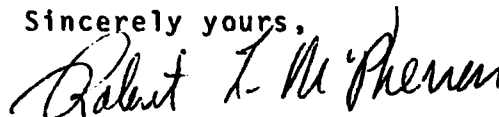
institutional arrangements must be made whereby those interested in the data can influence program development. For example, in my opinion, a major problem with the existing data processing scheme is that suitable averages and indices are not generated by the data acquisition and archiving program at the time the data are acquired. Since I pointed out the need for this four years ago while we were building the instruments at UCLA and it was not implemented by those responsible, I doubt they would accept this suggestion today.

An attractive alternative is for the AFGL to sponsor research and development grants in outside organizations. For example, the algorithms, programs, etc. required to analyze AFGL data elsewhere could be implemented at AFGL by existing staff members provided proper documentation of these was generated by the grantees.

It seems likely that current research areas in geomagnetism will eventually become matters of continuous importance to both military and civilian agencies. When this happens, continual monitoring of magnetic activity with magnetometer networks like AFGL, and also real time processing and display of data from these networks, will be essential. I believe one important goal of AFGL research activities should be to incorporate various research tools into the real time data acquisition system so that their value in monitoring can be demonstrated.

I hope these comments and suggestions will be of some use to you. I would be glad to discuss any of these topics with you or your laboratory in greater detail. Let me know if I can be of further help.

Sincerely yours,



Robert L. McPherron  
Professor of Space Science

RLM:jm

